Author:
Covey, Anna

Title:

How can we use modern deglaciated rivers to predict the effects of Patagonian Ice Field shrinkage?

Using non-glaciated rivers as an analogue for future change

How can we use modern deglaciated rivers to predict the effects of Patagonian Ice Field shrinkage?

USING NON-GLACIATED RIVERS AS AN ANALOGUE FOR FUTURE CHANGE

ANNA COVEY

A dissertation submitted to the University of Bristol in accordance with the requirements for award of the degree of MSc by Research in the Faculty of Science

School of Geographical Sciences

February 2020

Word count: 32,955

Abstract

A reduction in precipitation and in a warming climate over recent years has caused many glaciers in Chilean Patagonia to retreat (Rivera et al., 2002; Rivera 2004; Bown, 2004; Masiokas et al., 2008). This changing precipitation also affects the discharge and water quality of many hydrological systems in South America (IPCC, 2014). However, despite these profound changes, little is known about meltwater, sediment, and solute export from remote glaciers in South America.

This study focused on two Patagonian river catchments (glaciated and de-glaciated). The glaciated Rio Huemules drained meltwater originating from the Steffen glacier, the most southerly glacier in the Northern Patagonian Icefield. The de-glaciated Rio Lloncochaigua was 580km further north. The catchments were 670 and 107 km^2 respectively, and were chosen due to similarities in climate and bedrock lithology as well as being remote enough to avoid anthropogenic contamination. Data reported in this thesis were collected over 5 field seasons (2016- 2019).

Conductivity, temperature, depth, and turbidity were monitored in situ in both river catchments (Keller DTX-22, Turner Cyclops-7 and RBR*Tu* sensors). Meteorological data were obtained from local weather stations. To enable the conversion of turbidity to suspended sediment (SS), manual samples of SS were also collected. Discharge records were generated for both study catchments following conversion of sensor depth to discharge, calibrated using Rhodamine dye tracing. Mean discharge was twice as high in the glaciated catchment (Rio Huemules: 106 m^3s^{-1}, σ: 156; Rio Lloncochaigua: 44.7 m^3s^{-1}, σ: 23.9). The water yield of the Rio Huemules (4.73m) was also higher than in the Lloncochaigua (0.885m), as glacial melt supplements rainfall collected within a larger catchment area. This melt created a steady discharge, on top of which the rainfall events had little effect. Discharge seasonality was also explored in both catchments, with the glaciated catchment typically showing peak flows in summer (1.6 times the winter background) whereas the non-glaciated catchment was almost unchanging.

Additionally, fluxes and yields of suspended sediment concentration from both rivers were studied. Annual sediment flux was five hundred times larger and the yield was almost ninety times larger in the Rio Huemules, reflecting the greater capacity of the glacier to erode its substrate.

Dedication and acknowledgements

I owe huge thanks to all my friends and colleagues who've supported me throughout the epic journey which this project turned into.

Firstly, thank you to my supervisor, Jemma, who trusted me to disappear off on my own to Chile with vast amounts of expensive field gear. Thank you for allowing me to spend so much time in a place where I was so happy.

Thanks to Jon for allowing me to join my first field season, for patiently teaching me all I needed to know, for being the source of all data and for introducing me to Huinay. Thanks to Adam and Jeni for helping me prepare for my solo field season, and to Alejandro for driving me from Puerto Montt to Huinay and helping me get settled into life in Chile.

An enormous thank you to everyone in Huinay Scientific Research Station, Pueblo Huinay and the Fiordo Comau community. I will never be able to repay your kindness for adopting me into your lives with open arms, for teaching me Spanish and sharing your culture with such enthusiasm. Thanks for all the asados, fogatas, mesas, riendo and mate, and for making me feel so welcome. Special mention to Vreni and Fossi for being so accommodating, to Aris for introducing me to everyone, to the boat captains Eduardo and Carlos for their assistance in the Vodudahue, to Lizzy for being the best room-mate I could have asked for, to Nano for always looking out for me, to Meche, Karen, Carolina and Tamara for keeping me so well-fed, to Jhon and Marcus for the laughs and to Boris and Sole whose house was always open, whose kettle was always brewing and whose ears were always listening. Thanks also to everyone who's kept in touch with me on my return to the UK, for allowing me to stay a tiny bit connected with you all.

Back in the UK, I'm indebted to all my fantastic friends who supported me through a period of post-Chile culture-shock and temporary homelessness. To Claire, Emily, Tamsin, Alex, Owen and Tian, thank you so so much for allowing me to occupy your floors/ sofas/ spare rooms for sometimes extended periods of time and often at short notice. Thanks also, to Chris for stepping in as second supervisor and helping me to piece this thesis together, and to Helena for always being a caring, friendly face. I'm also beyond grateful to everyone who's listened to my grumbles and worries.

Finally, thank you so much to my wonderful family who waved their daughter/ sister off to the other side of the world, who put up with the subsequent intermittent communication and who took me phoning home to say I wouldn't be home for a further 4 months like absolute champions.

Author’s Declaration

I declare that the work in this dissertation was carried out in accordance with the requirements of the University's *Regulations and Code of Practice for Research Degree Programmes* and that it has not been submitted for any other academic award. Except where indicated by specific reference in the text, the work is the candidate's own work. Work done in collaboration with, or with the assistance of, others, is indicated as such. Any views expressed in the dissertation are those of the author.

SIGNED: .... DATE:..........................

Table of Contents

List of figures and tables

Figure 20: The relationship between sediment yields and annual mean discharge from a range of glaciated and non-glaciated catchments throughout Chile. The two field sites for this study are outlined in red. All data, apart from the Rio Huemules and Rio Lloncochaigua, were sourced from Pepin et al., 2010.

Figure 21: A storm hysteresis plot for Rio Huemules, 2nd- 5th February 2017.

Figure 22: A storm hysteresis plot for the Rio Lloncochaigua, showing a mid-winter storm from 2nd-11th August 2018.

Figure 23: A hysteresis plot for a summer storm in the Rio Lloncochaigua catchment from 21st- 22nd November 2018.

Figure 24: The Rio Lloncochaigua catchment in winter.

1.0 Introduction

1.1 Overview

With an expected increase in global temperature of 2 °C (IPCC, 2014), a projected decrease in precipitation in Patagonia over the next 100 years (Vera et al., 2006), and an associated reduction in glacial cover, up to 85% of glacial rivers worldwide are hypothesized to transition to de-glaciated systems by 2100 (IPCC, 2014). This may be exacerbated in South America due to changes in wider patterns of atmospheric circulation associated with the Southern Annular Mode, a scale recording the pressure differences between 40^{o}S and 65^{o}S (Garread, 2013) and the the El Niño cycle, which is already known to affect glacier mass balances (Coudrain et al., 2005). This warming climate, coupled with reduced precipitation, has already led to the retreat of many glaciers in Chilean Patagonia (Rivera et al., 2002; Rivera 2004; Bown, 2004; Masiokas et al., 2008), with changing precipitation also affecting the discharge, and water quality of many hydrological systems in South America (IPCC, 2014).

Despite these profound changes, little is known about meltwater, sediment, and solute export from remote glaciers in South America. The largest masses of glacial ice are found in Chile, associated with the Northern and Southern Patagonian Ice Fields. These icefields constitute the largest mass of ice in the Southern Hemisphere outside of Antarctica. Meltwater from these glaciers feed numerous rivers which were harnessed to generate 43.5% and 24.0% of Chile's national energy supply in summer and winter (November and June respectively) of 2018 (Generadoras de Chile. 2019. *Boletines Mercado Electrico* [Online] [Accessed 25 August 2019] Available from: http://generadoras.cl/documentos/boletines), before discharging into intricate fjord systems down the coast of Southern Chile. Within these fjord systems lies the seventh largest salmon fishing industry in the world (The Economist. 2010. *Net profits.* [Online] [Accessed 25 August 2019] Available from: https://www.economist.com/the-americas/2012/08/11/net-profits), an important source of jobs for local people and supporting the national economy GDP by 1.2 % (The world bank. 2019. *Agriculture, forestry, and fishing, value added (% of GDP) – Chile* [online] [Accessed 12th January 2020] available from:

https://data.worldbank.org/indicator/NV.AGR.TOTL.ZS?end=2018&locations=CL&start=2018&view=bar). To add to this, the rivers are important for the local ecosystems in Patagonian fjords, as they transport nutrients from bedrock and suspended sediment to the fjords (Masiokas et al., 2008). The glacial meltwater exporting high concentrations of sediment into fjords limits light (Gonzales et al., 2011). As a result, little marine life has been observed within many continental fjords (Carney et al., 1999), as well as south of the Taitao Peninsula (Thatje & Mutschke, 1999; Haussermann, 2006) and around Puerto Natales (Haussermann, 2006); all areas heavily influenced by glacial meltwater-fed rivers. However, closer to the mouth of the fjord, away from the meltwater-fed rivers, where suspended sediment concentrations are lower, higher levels of primary productivity are observed (1-3g C m^{-2} day^{-1}), resulting in the export of high quantities of carbon to the benthic sediments (0.2-0.6g C m^{-2} day^{-1}; Iriarte et al., 2010). This means that the fjords are acting as a major CO_2 sink, a balance which could be easily upset by changes in riverine exports of water, sediment and solutes.

Shrinkage of the Patagonian Ice Fields, a highly erosive environment due to subglacial rock crushing below warm-based glaciers, has been accelerating in recent years (Davies and Glasser, 2017), leading to a shift from glacier melt fed river regimes to rainfed river regimes. The £3.7 billion Chilean fishing industry is reliant on terrestrially-derived nutrients, concentrations of which have been shown to be higher in glaciated catchments (Hodson et al., 2005), therefore it is vital to understand the effects of glacier meltwater discharging into fjord and coastal ecosystems in order to better predict and prepare for their reduction.

Despite the clear importance of meltwater, sediment, and solute export from glacial rivers (Apollonio, 1973; Dunbar, 1973; Hood et al., 2009; Cape et al., 2019), worldwide studies of this subject covering an entire hydrological year or longer are rare, this is particularly evident in the southern hemisphere (Jansson et al., 2003). Even with recent rapid economic development in Chile, led by the salmon farming industry which depends so much on the nutrients within the fjord (Forsterra et al., 2005), oceanographic research in the Patagonian Fjords into which these rivers drain mostly concentrates on the northern fjords (Pickard, 1971; Silva et al., 2001; D´avila et al., 2002; Guzm´an and Silva, 2002; Valle-Levinson et al., 2002; Valle-Levinson et al., 2007; Prado-Fiedler and Salcedo-Castro, 2008; Sievers, 2008; Calvete and Sobarzo, 2011; Castillo et al., 2012), with a few recent studies in the south (Pantoja et al., 2011).

The hydrological impacts of the different water inputs (rainfall and melt) to glaciated and de-glaciated catchments is expected to differ, and better understanding the links between rainfall, river discharge and suspended sediment will allow better prediction of the changes which will occur in the rivers and fjords with these changes in precipitation. With this in mind, this thesis aims to answer four key questions:

1. How and why do the quantities and seasonality of precipitation vary between the glaciated and de-glaciated catchments?
2. How and why does the relationship between the differing sources of water feeding the rivers and their discharge vary seasonally in glaciated and non-glaciated catchments, and how are these seasonal variations comparable between the two study sites?
3. How does the discharge seasonality affect the delivery of suspended sediment in glaciated and de-glaciated catchments?
4. What are the implications of these differences in water and sediment delivery in a deglaciating Patagonia?

These four questions will be addressed by studying two different river systems in Chilean Patagonia: the Rio Huemules and the Rio Lloncochaigua. The Rio Huemules is a glaciated catchment, with water supplied by melting of the Steffen glacier. The Rio Lloncochaigua is a non-glaciated catchment, located to the north of the Patagonian ice sheets. The Rio Lloncochaigua’s more northerly location means it is non-glaciated, and allows it to be used as an analogue for how the Rio Huemules and the associated fjord ecosystems may change in the upcoming century. Results from this research project will then be compared with similar global systems in order to contribute towards greater international knowledge of how glacial retreat will alter glacial river systems.

1.2 Assessing the role of glacial cover on hydrological regimes

Glacial cover within drainage basins has been observed to impact seasonal hydrological regimes (Meier and Tangborn, 1961; Meier, 1969; Krimmel and Tangborn, 1974; Fountain and Tangborn, 1985; Rothlisberger and Lang, 1987). Research during the 1990's attempted to quantify this seasonal variation, resulting in the development of the 'glacier compensation effect' (Fountain and Tangbourn, 1985). Early work on the glacier compensation effect concluded that in winter conditions, where low temperatures and high precipitation occur, glaciers will act as a water store, and drainage basins with higher glacial cover will have lower river discharge as more of the precipitation is stored as ice (Meier and Tangborn, 1961; Meier, 1969; Krimmel and Tangborn, 1974; Fountain and Tangborn, 1985; Rothlisberger and Lang, 1987). The storage of water as ice is a well-known phenomenon, with people reproducing glacial water stores in icehouses to later melt for drinking water since 1780 BC (Dalley et al, 2002). In summer, where higher temperatures and lower rates of precipitation prevail, glaciers release water through glacial melt, thus drainage basins with a high glacial cover will show an elevated river discharge. Many communities worldwide have built civilizations near rivers draining glaciated catchments to take advantage of the more reliable summer discharge, when there is less precipitation available for irrigation and sanitation.

Table 1: A comparison of seasonal hydrological conditions in rivers draining glaciated and non-glaciated drainage basins.

	Summer hydrological conditions	Winter hydrological conditions
River fed by rainfall (Non-glaciated catchment)	Low rainfall leads to low river levels.	Higher rainfall leads to a high base river flow with additional storm peaks.
River fed from seasonal snowpack	Rivers peak in late spring- early summer as the ambient temperature warms, leading to the melting of the snowpack (Denner et al, 1999; Villanueva et al).	Rivers typically show low flow levels, despite increased precipitation, as much of this precipitation is falling as snow and thus is not moving into the river network.
River fed by glacial melt (glaciated catchment)	Rivers are highest in mid- late summer when low albedo ice surface are exposed, leading to more melt, coupled with the opening of subglacial and englacial storage to create a highly efficient drainage system (Lang, 1987; Chen and Ohmura, 1990b; Denner et al, 1999; Jansson et al, 2003).	Cold winter temperatures freeze most glaciers to their bases thus cutting off the water supply to the river. In some cases, these highly seasonal rivers dry up completely.

Table 1 demonstrates the different seasonal discharge patterns observed in glaciated and non-glaciated rivers, as well as rivers fed by seasonal snowpacks. The difference in seasonal flows is stark, with glaciated rivers showing peak discharges in late summer and non-glaciated rivers exactly the opposite, with peak flows occurring in winter when many glacial rivers run dry. Glaciated drainage basins demonstrate peak discharge later in the year than rivers whose water is sourced from seasonal snowpacks. This is because peak melt conditions (warmer temperatures, clear skies without cloud cover, and low ice albedo ice surfaces leading to increased absorption of energy) aren't reached until late summer. By this time, the seasonal snowpacks have already melted away, however the glaciers are much larger and can, therefore, continue to melt with increasing intensity, thus raising discharge.

The examples presented in Table 1 represent the absolute end-members of a sliding scale from rivers whose water is sourced solely from glacial melt to rivers with no glacial cover in any of the drainage basin. In complex systems, water can drain from a variety of sources, and will vary in percent glacial cover. Research by Fountain and Tangborn (1985) demonstrated that in North American drainage basins, an increase of glacial cover within a drainage basin of between 5 and 15 % delayed the period of highest river discharge by up to a month. Doubling the glacial cover from 50- 100 % was found to delay peak discharge by just two weeks (Fountain and Tangborn, 1985).

Further work in quantifying the glacier compensation effect showed that seasonality, measured as the ratio of summer discharge to total discharge, increases in glacial catchments with increased glacial cover within the drainage basin (Lang, 1987; Jansson et al, 2003). This is supported further by the work of Ostrem (1973) who observed that glaciated Scandinavian drainage basins released 85% of their total annual discharge between June and August; and further work conducted by Escher-Vetter and Reinwarth (1994) in Vernagtferner basin, Austria of which 81% is glaciated, observed that 90 % of the total annual discharge was released between June and October, northern hemisphere summer.

1.2.1 The effects of glacial water storage and subglacial hydrology on hydrological regimes

When precipitation is added to a glacial system at a greater rate than the drainage system can transport it or if it is added as snow, the water will be stored (Jansson et al., 2003). The relationship between rainfall/melt and discharge in glaciated systems is dependent on englacial and subglacial water storage, as this dictates the water retention time prior to the water being released downstream (Lawson 1993; Denner et al., 1999).

Rain falling directly onto ice drains immediately (Behrens et al., 1982; kohler, 1995; Nienow et al., 1996; Jansson et al., 2003), though early geophysical studies discovered porous year-old snow lying on top of impermeable glacial ice in many catchments: perfect conditions to form an aquifer in which to store rainwater (Sharp, 1951; Behrens et al., 1976; Lang et al., 1977; Schommer, 1977; Oerter and Moser, 1982; Oerter et al., 1982; Fountain, 1989; Schneider, 1999). Despite this potential storage capacity, further research estimated that only about 40% of this storage space can be used, due to low permeability of the overlying snow (Fountain, 1989; Jansson et al., 2003). This means that the firn, year old partially recrystallized snow, only contains enough storage space for 10% of annual precipitation. Storage of water in firn aquifers until they are full enough to drain can delay movement of precipitation by several days or weeks (Jansson et al., 2003). Later research into water storage in the glacial environment discovered englacial (within crevasses, englacial pockets and the englacial drainage network) and subglacial (in subglacial cavities, the subglacial drainage network, and in subglacial aquifers in the till of the glacier bed) storage (Jansson et al., 2003).

Denner (1999) compared the effects of large rainfall events on an Alaskan glacier at different times in the melt season, demonstrating that large rainfall events have a different effect on glaciers at contrasting times of the year. The study showed that 28 mm of precipitation falling in midwinter lead to little change in the river level at all, as much as this fell as snowfall, and any rain falling on the glacier would be trapped and stored by the inefficient discharge network. By comparison, 56 mm of precipitation in summer lead to an eight-fold increase in river discharge, as the precipitation could make its way quickly through the network of moulins, crevasses and subglacial drainage to reach the river.

1.3 Hydrological drivers of suspended sediment in glaciated and de-glaciated catchments

Suspended sediment often accounts for up to 99% of the sediment flux for a river, the remaining 1% being attributed to bedload (Meade et al., 1990). In glaciated environments, the generation of subglacial sediment reflects a range of erosional processes at the glacier bed. Loosely consolidated sediment completely saturated with meltwater loses some of its structural integrity, and is thus more prone to erosion. Glacial movement over these poorly consolidated sediments leads to sediment deformation (Hart, 1995). In catchments where the glacier is moving over a well consolidated bedrock, such as an igneous or metamorphic bedrock, material is eroded by subglacial rock crushing (McGee, 1984), abrasion (erosion of rocks by the abrasive power of sediment attached to the base of the glacier) and plucking (freezing of the glacier onto the rock base then ripping sections out as the glacier moves on) (Hart, 1995). This eroded material is then washed out of the glacial environment by subglacial water flow. Fine sediments transported in non-glacial rivers can come from a wide range of sources. Erosion of the river bed or bank is linked to the force of the water moving within the river channel. As well as a base erosion rate, erosion can be increased during specific bank erosion events (Bull, 1997). These bank erosion events occur during periods of bad weather when the river experiences elevations in discharge, and the bank is weakened by prolonged water through-flow. Bank erosion events can occur on small scales within the river, as well as on a catchment scale, such as movement events like landslides or debris flows. Anthropogenic overuse of the riverbanks, for example by farming, foresting or mining can increase the sediment input into the river channel by weakening the soil structure (Mao et al., 2016).

Understanding the drivers and delivery mechanisms of suspended sediment in rivers is important, as sediment has been found to transport high loads of labile nutrients (Kumar et al., 1995) and also contaminants (Santiago et al., 1994). This affects the water quality for the communities who may drink it, as well as the flora and fauna making up the local ecosystem (Mao et al., 2016). High loading of sediment transported to the fjord ecosystem by glacial rivers causes a high stress environment for benthic marine organisms, blocking out light, as well as the deposition covering organisms which live on horizontal surfaces (Lemaire et al., 2002; Loucaide et al., 2008). Both high light and DSi concentrations are required by diatoms living in the fjords of Patagonia for optimal frustule formation (Lemaire et al., 2002; Loucaide et al., 2008). High sediment loads, blocking light, inhibits uptake of DSi (Loucaide et al., 2008).

The relationship between suspended sediment and discharge has also been extensively studied in non-glacial rivers (Müller and Förstner, 1968; Lefrançois et al., 2007; Ayes Rivera et al., 2019). Fan et al. (2013) noted a "store and release" system in a non-glacial catchment, with sediment building up in dryer seasons then being washed out in rainier seasons when the river had more energy (Mao et al., 2016). Kelly et al. (2018) noted that concentrations of sediment can also vary with variations in discharge associated with storm events, with the largest storms having the greatest energy potential for carrying large quantities of suspended sediment.

Early field campaigns (Collins, 1979; Denner et al., 1999), studying suspended sediment concentrations in glacial river catchments concluded that the suspended sediment concentration within a river was a result of sediment availability within the catchment, as is true in non-glaciated rivers. Results demonstrated that however high the discharge was, it could only transport a concentration of suspended sediment proportional to the sediment available in the catchment. This is supported by Jiang et al., (2010) who observed suspended sediment concentrations to be greater during the rising limb of a storm than the equivalent discharge on the falling limb. This was attributed to washing out of the easily eroded sediment. Therefore, by the time the river fell, most of the sediment of a size-fraction movable by a river at that discharge had already been removed.

Further work on the relationships between discharge and suspended sediment concentrations throughout the glacial melt season of Estereo Morales, in the Chilean Andes, conducted by Mao et al., (2016) demonstrated that suspended sediment concentrations decrease as the season progressed, demonstrating an exhaustion of sediment supply. Data presented from a de-glaciated catchment in north-eastern USA by Kelly et al., (2018) was in agreement, reporting that subsequent storms flush out less sediment than the first, relative to discharge, indicating that the suspended sediment concentration is external to the river bed, and thus is being exhausted over time.

Another factor controlling the suspended sediment concentration measured in rivers is the energy in the river discharge. The idea was first discussed by Willis and Richards, 1996, who tried to establish the links between suspended sediment concentration and discharge in a glacial river. Previously, increased concentrations were believed to be due to increased erosion of the sediment source, however this paper suggested that they were in fact linked to changes in subglacial conditions, for example opening or connecting of subglacial meltwater channels. This idea was expanded by Hasnain (1996), who studied the importance of subglacial pathways and the volumes of water able to flow through them. The paper also noted the difference between cold-based glaciers, which have lower suspended sediment concentrations, and warmer-based glaciers which have open pathways through which water can flow and transport sediment (Hasnain, 1996).

Later studies on other glacial rivers used hysteresis analysis to better examine the relationship between suspended sediment and river discharge, and to infer the availability of sediment within river catchments (Mao et al., 2019; Misset et al., 2019) which may represent a combination of factors. Hysteresis analysis involves plotting the relationship between river discharge against the suspended sediment concentration for a hydrograph showing a peak in discharge, typically following a storm or period of elevated glacial melt. The relationship between suspended sediment concentration and the river discharge is usually different on the rising and falling limbs of the hydrograph, therefore the hysteresis plot usually takes on an oval form with peak suspended sediment concentration occurring either before or after peak discharge. The rising limb of the hydrograph may be accompanied by simultaneously increasing suspended sediment concentrations, if the water and sediment are originating from the same place, which will result in a clockwise hysteresis plot. Mao et al. (2016) observed a non-glaciated drainage basin in which the river hydrographic regime was dominated by snowmelt. During the spring, they observed that increased discharge due to the snowmelt washed out sediment which had been stored on the river bed during winter resulting in clockwise hysteresis. As the season progressed, this sediment stored on the riverbed was depleted, and later storms mobilised sediment on the valley sides which was no longer protected by the covering of snow, resulting in anticlockwise hysteresis plots as there was a delay between rising discharge and rising suspended sediment concentrations (Mao et al., 2016).

Continuous or near continuous datasets of suspended sediment concentrations are rare (Horowitz, 2003). At present, there is only very limited field evidence of hysteric analysis in glacial rivers, primarily in the Alps (e.g. Mao et al., 2014, who used hysteresis plots to study how sediment availability changes throughout the year), the Himalayas (e.g. Andermann et al., 2012, who used hysteresis plots to measure periods of groundwater storage), and in Greenland (field campaigns by Hindshaw et al., 2014 recorded a strong correlation between diurnal changes in suspended sediment concentration and diurnal changes in discharge). There is currently no use of hysteresis analysis in South American glacial rivers (Mao et al., 2016).

1.4 The role of glacial cover in suspended sediment delivery

The erosion of bedrock by glaciers has been studied for centuries (Gastaldi, 1873; Bonney, 1893; Russell, 1898). The rate at which bedrock is eroded is known to influence the flux of sediment-bound nutrients exported in river discharge (Murray et al., 1993; Murray et al., 2000; Latimer and Filippelli, 2001; Hartmann and Moosdorf, 2011). Despite these high nutrient conditions, early biological expeditions reported little marine life within many Patagonian continental fjords (Carney et al., 1999), as well as south of the Taitao Peninsula (Thatje & Mutschke, 1999; Haussermann, 2006) and around Puerto Natales (Haussermann, 2006); all areas heavily influenced by glacial meltwater rivers. Later studies (Pizarro et al., 2000; Pizarro et al., 2005; Prado-Fiedler 2009, Gonzalez et al., 2011) linked this to the suspended sediment blocking out the light, which is used by organisms for photosynthesis.

An early study into suspended sediment yields in Icelandic glaciated basins recorded a suspended sediment yield five times higher in the glaciated Hoffellsjokull river than a non-glacial river in the near area (Embleton and King, 1975). This was suggested to be due to increased erosion in the glaciated catchment. Work by Jansson (1988) studying 1,358 drainage basins with areas ranging from 350 to 100,000 km^2 also supported this hypothesis, as did further research by Ferguson (1984), Warburton (1990), and Harbor and Warburton (1992), which suggested remobilization of sediments in front of the glaciers may also play an important part in increasing suspended sediment yield in the river. Hasnain (1996) looked into the future of suspended sediment fluxes, concluding that even following glacial retreat and deglaciation, glaciers will continue to contribute to increasing weatherability of soil, by leaving a poorly consolidated moraine (Hasnain, 1996). More recent studies used downstream ecosystem productivity to infer glacial sediment inputs into a river catchment (Filippelli, 2002; Hodson et al., 2005; Lydersen et al., 2014).

Early research into glacier movement observed an important link between glacial flow and erosion (Perutz, 1947). Bezinge et al. (1989) suggested that most movement of suspended sediment from glaciers into meltwater rivers occurred during extreme rain events, which typically occurred during winter. These two opposing ideas about the factors affecting suspended sediment delivery both suggest a seasonality to suspended sediment concentrations - higher flows (and thus more erosion and a higher suspended sediment flux) would lead to highest suspended sediment concentrations in summer, whereas winter storms would flush out more sediment in winter.

Field measurements in the Alaknanda basin, Garhwal Himalaya, by Hasnain and Chauhan (1993) revealed that the concentrations of suspended sediment drained from this glacier were highest near to the glacier tongue and decreased further downstream. The paper concluded that 70% of the suspended sediment flux was temporarily stored in the river catchment throughout the summer months and released in monsoon season. Further work on the seasonality of suspended sediment fluxes by Salcedo-Castro et al. (2015) found a strong correlation between air temperature and suspended sediment concentration in the fjord. This was explained by the increasing air temperatures increasing glacial melt and therefore the speed at which the glacier erodes the bedrock beneath it. The paper concluded that sediment deposition in glacial fjords is directly related to the glaciers melting cycles (Salcedo-Castro et al., 2015).

1.5 Summary

The above differences in hydrological regimes and suspended sediment fluxes in glaciated and de-glaciated river catchments are important because they affect the timing, quantity and rate of water and sediment supplied to downstream populations and ecosystems (Denner et al., 1999). Yet despite this, projects comparing glacial and non-glacial rivers are rare, especially in Patagonia. In this thesis, data will be collected and analysed from two river catchments with different levels of glaciation to enable current research to be extended to Patagonian rivers and glaciers.

4.1. Research questions and hypotheses

1. How and why do the quantities and seasonality of precipitation vary between the glaciated and de-glaciated catchments?

Due to the different latitude, catchment elevations and mean ambient temperatures, the increased winter precipitation expected in both catchments will differ, with the Rio Lloncochaigua experiencing a higher volume of precipitation, mostly falling as rainfall, and the Rio Huemules experiencing less overall precipitation, mostly as snowfall.

2. How and why does the relationship between the differing sources of water feeding the rivers and their discharge vary seasonally in glaciated and non-glaciated catchments, and how are these seasonal variations comparable between the two study sites?

Significant contrasts in the proportions and timing of precipitation reaching each river (e.g. snow and ice melt in glaciated catchments, rain in non-glaciated catchments) and the contrasts in catchment characteristics (e.g. steepness of slope, forest cover, glacier cover) will lead to a higher discharge in the Rio Huemules, especially during the summer months, whereas in the Rio Lloncochaigua a dependence on rainfall will lead to a lower overall discharge which peaks in winter.

3. How does the discharge seasonality affect the delivery of suspended sediment in glaciated and de-glaciated catchments?

Compared to the Rio Lloncochaigua catchment, where the suspended sediment concentration will be a function of sediment availability and discharge energy (shown by larger, clockwise, open hysteresis loops following winter storms), the Rio Huemules will show higher, more constant suspended sediment concentrations and a flux varying proportionally to the discharge, due to the erosive action of the glacier and the "filtering" effect of the lake (shown by smaller, very tight hysteresis loops observed during diurnal melt cycles in summer), however the presence of this lake will lead to the measurement of lower suspended sediment concentrations in this catchment than other glaciated catchments.

4. What are the implications of these differences in water and sediment delivery in a deglaciating Patagonia?

The results presented in this thesis will enable a better understanding of the effects of deglaciation in this currently unstudied region. Although hypotheses cannot be tested for the future, deglaciation is expected to lead to a transition from conditions observed in the currently glaciated Rio Huemules to the non-glaciated Rio Lloncochaigua. Precipitation will enter the river faster due to a reduction in glacial storage, leading to a much flashier hydrological regime. In addition, sediment delivery to the rivers will be greatly reduced following the disappearance of the highly erosive glacier, and will follow different seasonal patterns as are currently observed in the Rio Lloncochaigua.

1.0 Study sites

The coast of Chile can be divided by breaks in benthic marine species composition, giving rise to two biogeographic zones: the warm northern zone (6-30 °S) and the cold southern fjord zone (40 to 56 degrees south; Brattstrom and Johanssen, 1983; Lancellotti and Vasquez, 1999; Santelices and Menses, 2000; Camus 2001; Vidal et al., 2008). Differences in species composition within the two zones has been hypothesized to be a result of historical and current biogeochemical processes such as increased dissolved silica exported during glaciations (Hurd, 1977; Anderson, 2005) creating differences in oceanographic conditions (Brattstrom and Johanssen, 1983; Lancellotti and Vasquez, 1999; Santelices and Menses, 2000; Camus 2001; Vidal et al., 2008; Macaya et al., 2010). At 42°S the glacial fjord system starts, stretching south for over 1,500 km, resulting in a greatly expanded variety of ecosystems (Forsterra et al., 2005; Haussermann, 2006). These fjord regions, carved out by glaciations, show more species diversity than the northern coast (Fernandez et al., 2000), a result of the wide variety of habitats (Ward et al., 1999; Antezana, 1999; Valdovinos et al., 2003; Haussermann and Forsterra, 2005). Within the fjord regions, the highest marine biodiversity was reported by Haussermann (2006) to be in the most northern parts where warmer water, with reduced suspended sediment input dominates.

Glaciers in the Patagonian Andes cover an area of approximately 20,000 km^2 (Masiokas et al., 2003). In the northern regions of Patagonia, warmer temperatures result in the dominance of smaller glaciers, predominantly found at higher altitudes. However, further south, cooler temperatures enable the formation of glaciers at lower altitudes (Masiokas et al., 2003). Between 35°S and 45°S, there are 300 km^2 of glaciers (Lliboutry, 1998), most of which are west of the Andes. Because they are so small, they are very sensitive to changes in temperature and precipitation (Masiokas et al., 2003). Between 46°S and 51°S sit the Northern and Southern Patagonian ice fields (4,200 km^2 and 13,000 km^2 respectively; Masiokas et al., 2003). Both the North and South Patagonian Ice Fields have been impacted by warming ambient temperatures (Rosenbluth et al., 1997; Rasmussen et al., 2007), and most Patagonian glaciers have retreated since the 1950's (Lopez et al., 2010) as the Northern and Southern Patagonian ice fields shrink (Holmlund and Fuenzalida, 1995; Rigot et al., 2003; Aniya, 2007).

Two river catchments were selected for study (Figures 1- 4): the Rio Huemules (glaciated; site A), and the Rio Lloncochaigua (de-glaciated; site B). These study sites were chosen to enable a comparative assessment of the delivery of suspended sediment between a glacial and non-glacial catchment within a similar geoclimatic region. The Rio Huemules catchment drains meltwater originating from the Steffen glacier, the largest glacier draining the southern margin of the Northern Patagonian Ice Field, before feeding into the Baker fjord (Warren and Sugden, 1993). The sampling site was situated at 47°32'45''S, 73°41'00''W, and is accessed via the village of Tortel. The de-glaciated Rio Lloncochaigua is situated 580 km further north draining into the Comau fjord. The sampling site was located at 42°21'43''S, 72°24'12''W, which is accessed from the Huinay Scientific Research station. This thesis includes data collected by the author and others (see section 9.1) from sampling campaigns over 5 field seasons (Rio Huemules: summer 2016, summer/winter 2017; Rio Lloncochaigua: summer 2017, summer/winter 2018 and summer 2019).

Figure 1: An image showing the Rio Huemules, and its catchment. Photo courtesy of J. Wadham.

Figure 2: An image showing the Rio Lloncochaigua and its catchment.

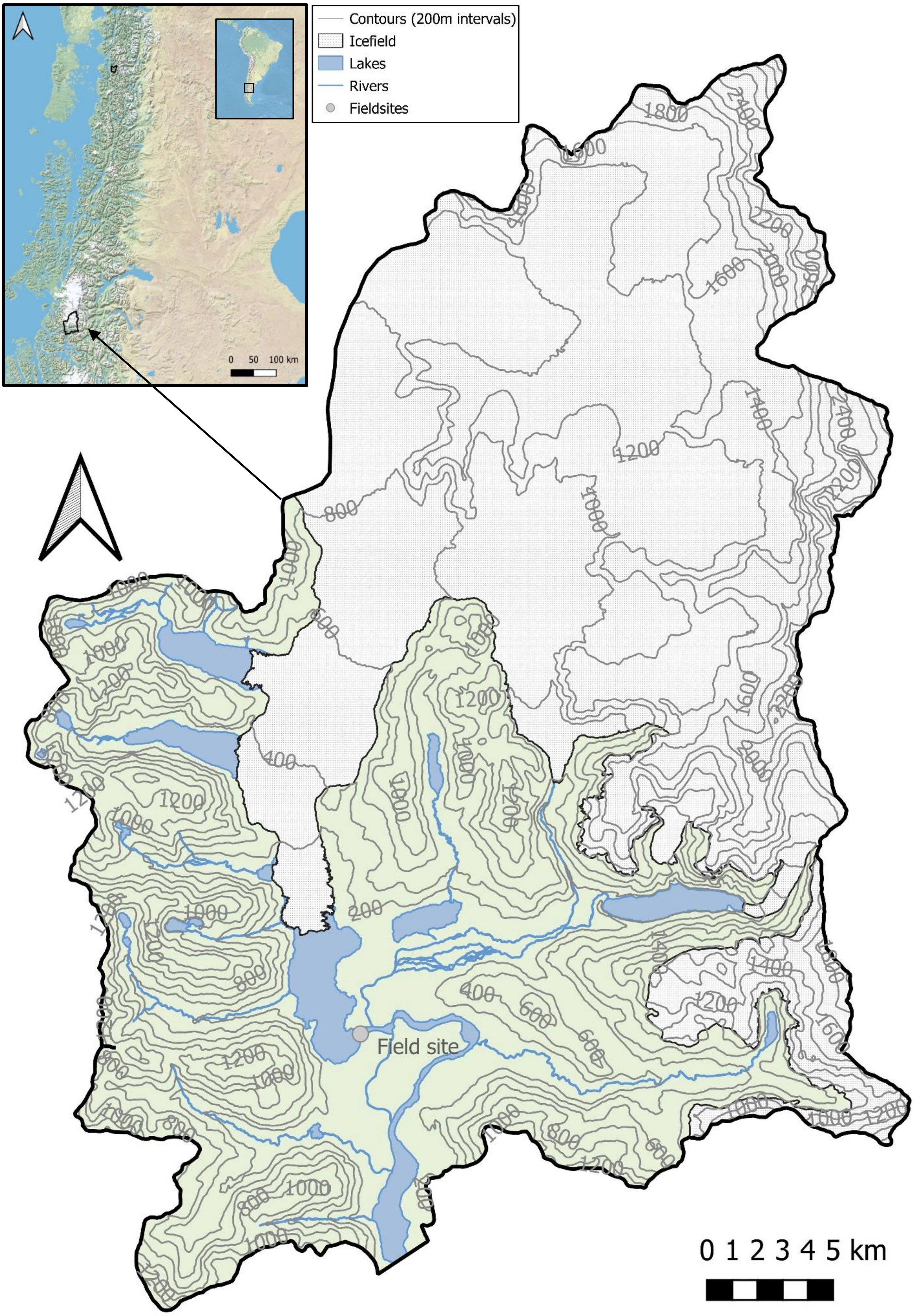

Figure 3: A map of the Rio Huemules catchment.

Figure 4: A map of the Rio Lloncochaigua catchment.

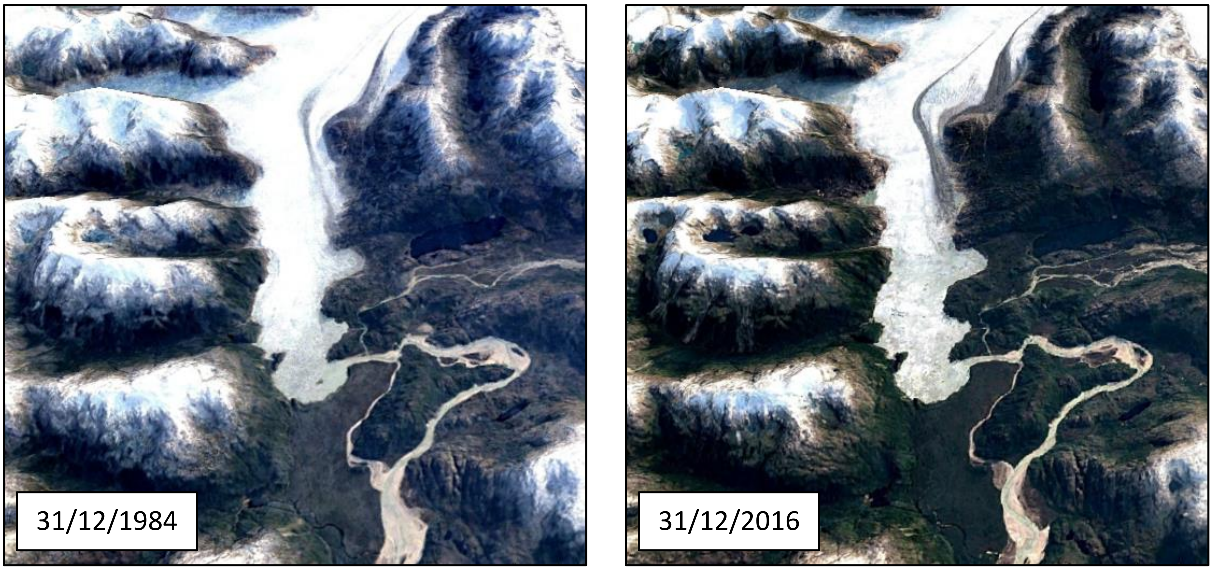

Figure 5: Two images of the Steffen glacier and Rio Huemules showing glacial retreat over the 32 years previous to this study.

Figure 5 shows two Landsat images of the Steffen glacier and the Rio Huemules in 1984 and 2016. During these 32 years, the glacier can be seen to have retreated 2.3km, however since then, the glacier appears to have stabilised. The Huinay valley in the Rio Lloncochaigua catchment was last glaciated during the Quaternary (Dasilva, 1995; Weis and Melzer, 2012), so is a useful analogue to use to predict changes which may occur in the Rio Huemules (amongst others) during deglaciation of the Steffen glacier over the next 100 years as part of Patagonian Ice Field shrinkage (Rivera et al., 2007).

Precipitation in this region is high and extremely variable with rainfall totals of up to 6,700 mm/year, with some northern areas receiving six times more precipitation than other areas in central and southern Patagonia (Pickard 1971; Castilla et al., 1993; Forsterra et al., 2005). Research conducted by Aravena et al. (2009) found rainfall to decrease with increasing latitude. For example, mean June rainfall (midwinter) is 225 mm in Puerto Montt (41^{o}S), but falls to 20 mm in Punta Arenas in the far south of Chile (52^{o}S; Aravena et al., 2009). This is due to the Antarctic Oscillation, otherwise known as the Southern Annular Mode or SAM, which causes pressure differences between 40˚S and 65˚S which change during autumn and spring (Stammerjohn et al., 2008). These in turn lead to zonal wind variations (Silvestri and Vera, 2003), and therefore fluctuations in rainfall as the strong westerly winds are forced upwards by the Andes mountains (Garreaud et al., 2013) to form what has been called one of the most dramatic precipitation gradients on earth (Smith and Evans, 2007; Carrasco et al., 2002).

In recent years, however, these zonal winds which encircle Antarctica have been shifting south and strengthening (Garreaud et al., 2013) due to changes in atmospheric greenhouse gas composition in the ozone layer (Kushner et al., 2001; Thompson and Solomon, 2002; Gillett and Thompson, 2003). This resulted in a significant decrease in precipitation falling in southern Chile between 1960 and 2000 (Haylock et al., 2005), which was mainly observed as a reduction of winter rainfall. Although this study is too short to monitor such long-term trends, it is important to note that in the glaciated Rio Huemules catchment, the Steffen glacier is acting as a water store, and therefore releasing meltwater which fell as precipitation in the past when precipitation rates were higher. Therefore, the volumes of water available for release from this system will be higher than the volumes of water being added to the system by current precipitation levels.

As illustrated in Figures 3 and 4 and Table 2, the Rio Huemules drains an area six times larger than that of the Rio Lloncochaigua. The Rio Huemules catchment has a flatter topography and is almost entirely glaciated. This contrasts with the Rio Lloncochaigua which is mostly forested, with very steep valley sides, thin moorland soils and some small patches of open grassland in the valley bottom which is used to graze cattle and sheep. Both have similar climates and overlay impermeable intrusive volcanic rocks, allowing meaningful comparisons to be made about weathering and nutrient release, whilst also being remote enough to avoid anthropogenic contamination. Inter-seasonal vegetation changes to interception are minimal due to a high proportion of coniferous trees in the drainage basins.

Table 2: A comparison of drainage basin characteristics

	Catchment area (km^2)	**Latitude**	**Land cover classification**
Field site A (Rio Huemules)	670	47°32’45’’S	Glaciated (71 %)
Field site B (Rio Lloncochaigua)	107	42°21’43’’S	Glaciated (1.2 %). Forested slopes with grassy valley.

3.0 Methods

3.1 Metrological data

Rainfall data were collected using HOBO RX3000 weather stations situated in the two study catchments. The gauges were situated in exposed locations to avoid shelter from structures with all wind directions, thus avoiding wind directional bias (Stow and Dirks, 1998). In the Rio Lloncochaigua catchment, data were obtained from two HOBO rain gauges associated with the Huinay research station, situated on the valley side and also on the coast (42°22'S, 72°24'W). These data were generated and maintained by IFOP and the Huinay Scientific Research station. No weather stations were situated in the Rio Humules catchment. The nearest weather station was situated in Tortel, 29 km away (47°47'S, 73°31'W). Data here was maintained and collected by the Direccion General de Agua (DGA), and is freely available online to download (https://snia.mop.gob.cl/BNAConsultas/reportes).

In both cases, precipitation was collected via a funnel into a tipping bucket rain gauge, this was then measured automatically at 10-minute intervals. A study by Stow and Dirks (1998) showed that measuring rainfall at 15 second intervals was best, to allow enough time for enough rain to be collected to allow accurate measurement by the sensors, but also to create a high-resolution dataset with clearer short, sharp showers, however rainfall data were collected every ten minutes at the two sites. This allowed easier comparison between different parameters measured on these and other sensors at the same time, as well as intermediate weather measurements.

3.2 Discharge data

Keller DTX-22 Conductivity, Temperature, Depth sensors (CTD's) were installed within the two river catchments, measuring electrical conductivity, water temperature and pressure.

As shown in Figure 6, the CTD's were installed on wire cables which hung submerged in the water within protective plastic tubes. These tubes had holes drilled into them to allow ease of water flow to the sensor, and also served to keep the CTD's at a constant height in the water, and to protect the sensors from damage. Figure 7 shows the location of the CTD sensor in the Rio Lloncochiagua in low and high flow conditions observed in summer and winter.

Figure 6- The CTD mounted in its protective tube

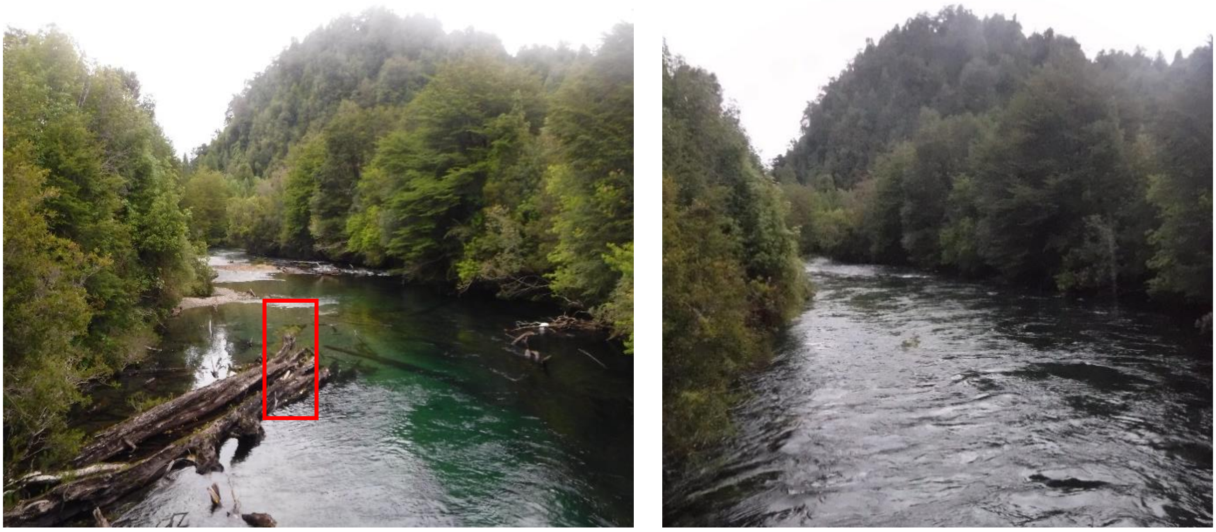

Figure 7- Two photos showing the location of the sensors in the Rio Lloncochaigua, which were taken in summer (mid-January) and winter (mid-July) respectively. The red box shows the sensor location; however, the sensor can't be seen on this photo.

In order to use this CTD depth data (measured as pressure in mbar) to derive river discharge, a method was required to first correct the pressure data for fluctuations in atmospheric pressure, then convert this pressure data into discharge, expressed in $m^3 s^{-1}$.

River discharge can be measured using physical, chemical and remote methods. Although remote sensing methods (using optical, near-infrared, passive and active microwave imaging sensors to measure river width, and radar and laser altimetry to measure the surface elevation of the river; then manipulating and ground-truthing to create a rating curve) have seen increased popularity in the past ten years, this method was discounted due to the CTD sensor already being installed in the study locations to collect EC and water temperature data. They are also challenging to apply in small streams and forested watersheds.

Physical methods by manual gauging (multiplying the channel area by river velocity to calculate discharge) are popular within the hydrology community, as they can be used without specialist equipment and can therefore produce cheap results. However, they require accurate measurement of the cross-sectional channel area, and velocity measurements in multiple locations across the channel, to account for lateral changes in flow speeds. This was deemed prohibitively dangerous for use in this study due to the extremely isolated river locations (10 and 8 hours from the nearest hospital at Rio Huemules and Lloncochaigua respectively) where extra precautions must be taken to ensure safety. In addition to this, the high sediment concentrations expected in the glacial river has been noted to affect the use of flow meters to calculate velocity (Tazioli, 2011). Studies in Italian streams by Tazioli (2011) compared the discharge data produced by current meters with that measured using a chemical dye (rhodamine). The results showed current meters to operate only in a small window of river conditions: losing accuracy in small (shallow water, low flow velocity) streams and underestimating discharge by nearly 30% in high flow conditions. The conclusion of the paper recommended the use of artificial tracers, via dilution gauging of flow, for more than two measurements when creating the rating curve (Tazioli, 2011). For this study, fluorescent dye tracers were chosen over radioactive tracers, as they would not contaminate the river for future studies or downstream stakeholders.

Rhodamine, the chosen dye, has a strong fluorescence, is easily diffused, is chemically stable and is non-damaging towards ecosystems and does not appear to present a carcinogenic or mutagenic hazard, nor is it acutely toxic (Sabatini and Austin, 1991; Panini et al., 1999; Vasudevan, 2001; Close et al, 2002; Dierberg and Debusk, 2005; Tazioli, 2011). Only a small amount of rhodamine dye is necessary for an accurate measurement of discharge (Tazioli, 2011), as rhodamine can be detected in the field as low as 1 ppb (Vasudevan, 2001). Repeat tests by Tazioli (2011) produced results with 5% error. However, rhodamine has been shown to decay under high light conditions (Vasudevan, 2001) and some absorption into suspended sediment, stream bed gravel, alluvium sediment and organic matter has been demonstrated in conditions with high concentrations of rhodamine (Sabatini and Austin, 1991; Vasudevan, 2001; Tazioli, 2011). Despite these factors, rhodamine dye dilution gauging was selected as the most appropriate method to generate robust discharge data for the study sites in this study.

A fluorometer (Turner Cyclops 7F) connected to a data logger (Turner DataBank) was used to monitor rhodamine fluorescence intensity, which is proportional to its concentration. To ensure lateral mixing and to keep the equipment above the maximum water level, the fluorometer was positioned in the centre of the channel by attachment to a metal pole. Between 100 and 250 ml of rhodamine dye ($C_{29}H_{29}N_2O_5Na_2Cl$) was then added into the river 1.54 km upstream. Longitudinal mixing was calculated using procedures developed by the International Organisation for standardisation (method number: ISO 9555-4:1992). A typical rhodamine dye trace can be seen in Figure 8.

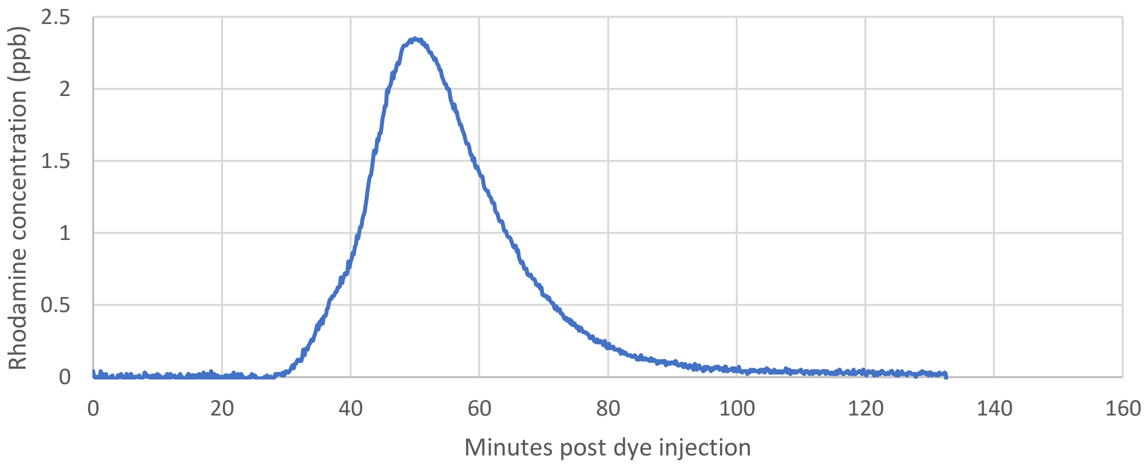

Figure 8- A typical rhodamine dye trace for the Rio Lloncochaigua.

Discharge was then calculated using equation 1. Where Q = calculated discharge and peak area describes the area under the dye trace peak.

$$Q = \frac{(\text{Dye volume x 0.000001) x (Dye concentration (\%) / 100)}}{(\text{Peak area x 0.000000001})} \qquad \text{Eqn. 1}$$

The atmospheric pressure was measured in both locations by HOBO HWS Bariometric Pressure sensors which were situated alongside the rain gauges, and used to correct instream pressure values. The water pressure-discharge relationship observed in Figure 9 was then used to generate a long-term discharge from each corresponding site using Equation 2.

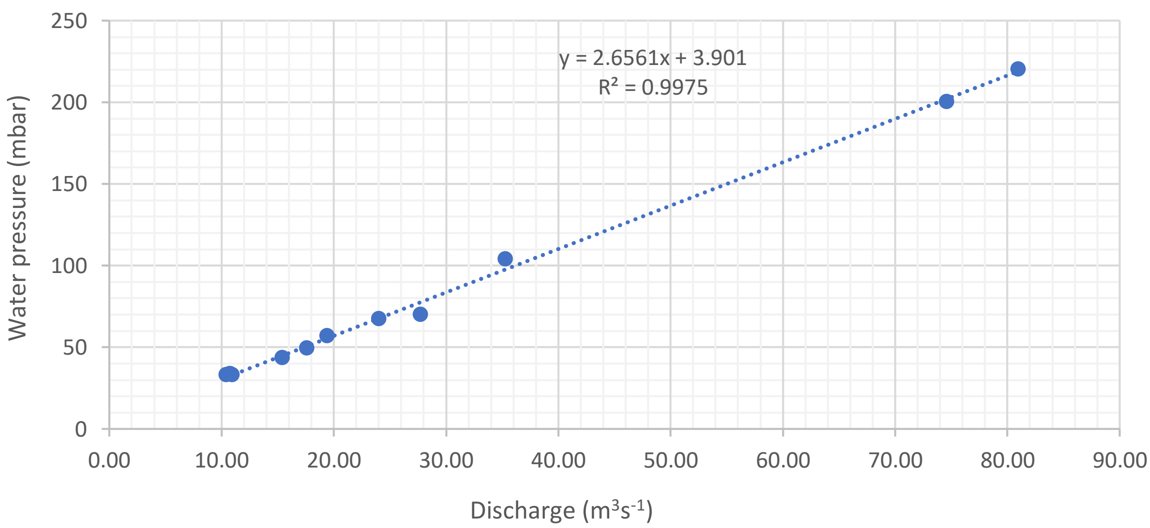

Figure 9- The rating curve used to convert pressure data to stage in the Rio Lloncochaigua

$$Q = \frac{CTD\ pressure - 3.901}{2.6561} \qquad \text{Eqn. 2}$$

3.3 Suspended sediment concentration

There are over 20 different methods which can be used to monitor suspended sediment concentrations (Horowitz, A.J., 2003). There have been many attempts to create models which enable the suspended sediment concentration to be calculated using the discharge volume (Campbell and Bauder, 1940; Walling, 1978; Syvitski et al., 1987; Jansson, 1996; Mossa, 1996; Asselman, 1999, 2000; Syvitski and Morehead, 1999; Syvitski et al., 2000; Morehead et al., 2003), however this tends to under report sediment levels at high concentrations and over predict concentrations at low concentrations.

In this study, turbidity sensors were installed in both rivers (a Turner Cyclops-7 turbidity sensor in the Rio Huemules, and a Turner Cyclops-7 turbidity sensor in early Rio Lloncochaigua field trips (installed in the river 28th January to 16th February 2018), then an RBR*Tu* turbidity sensor in the final field season (installed in the river from 27th July 2018 until 1st April 2019)) collecting data at 10-minute time intervals. Turbidity meters have also been used in conjunction with regression analysis via both manual and automatic sample collections for over 30 years (Walling, 1977; Horowitz, 1995). The equipment required to determine suspended sediment concentrations (turbidity sensors and automatic samplers to collect the water) is relatively cheap to obtain, however require specialist installation, calibration, and upkeep, which can be expensive (Horowitz, 2003).

Water samples were taken from the rivers as often as possible during the field seasons. This was consistently daily in the Rio Huemules and varied between daily and weekly in the Rio Lloncochiagua (depending on the time taken to process the previous sample). 47 samples were collected in the Rio Huemules, and 55 in the Rio Lloncochaigua[1] in a range of hydrological conditions in order to get a good calibration (sample size recommended by Horowitz, 1995; Christensen, 2001).

[1] Unfortunately, 50 of these samples were destroyed in a small fire in the oven during the drying process.

Following sample collection, the water was then filtered through a pre-weighed 0.45µm cellulose nitrate membrane filter paper (whatman, 7184-004). In the first summer field season at Huinay, 2L was filtered, however lab analysis revealed that this didn't allow the collection of sufficient sediment to form a strong calibration of the Cyclops-7 sensor (R^2: 0.31). Thus, on returning for the second field season, up to 8L of water was filtered per paper to enable collection of more sediment. This took time, however, and sampling dropped to every 4 days and on occasions weekly if the sample was taking longer to process. The samples collected in the glaciated field site contained much higher suspended sediment concentrations, therefore only 500 ml was filtered before adequate sediment sample was obtained.

On returning from fieldwork, the filters were dried overnight in the oven to remove any moisture, before being re-weighed and the empty filter weight subtracted to calculate sediment weight. The Rio Huemules sediment weights were plotted against the turbidity sensor data, and a regression analysis carried out (Figure 10) to produce Equation 3 which could be used to convert the rest of the Rio Huemules turbidity data (measured in VDC) into suspended sediment concentrations (g L^{-1}). For this data, the 95% confidence interval for the measured suspended sediment concentration lies between 0.831 and 0.956 g L^{-1}. For the turbidity readings, the 95% confidence interval is between 147 and 152 VDC.

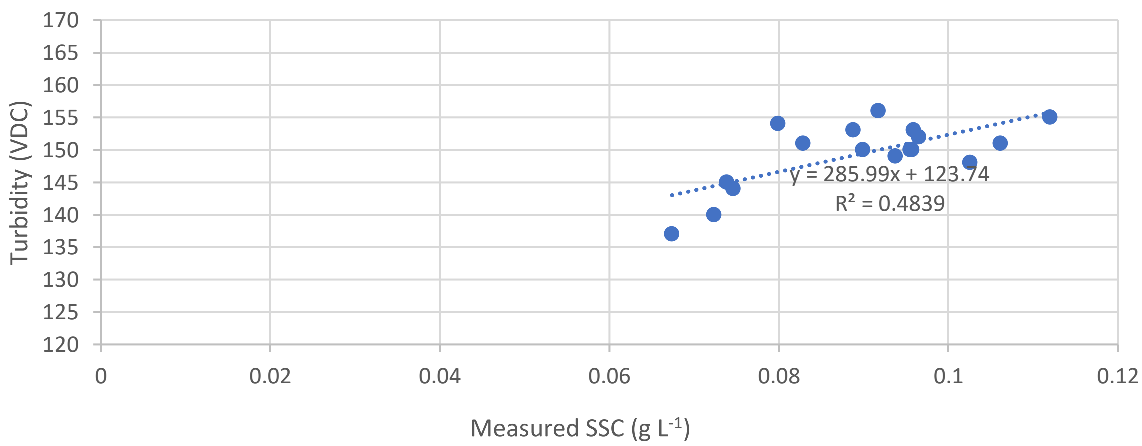

Figure 10. The regression analysis used to convert turbidity readings from the Turner Cyclops-7 sensor to suspended sediment concentration, using samples collected during fieldwork in the Rio Huemules.

$$Suspended\ sediment\ concentration = \frac{Turbidity - 123.74}{285.99} \quad \text{Eqn. 3}$$

As mentioned above, the volumes of water filtered from the Rio Lloncochaigua during the early field season didn't allow the collection of sufficient sediment to form a strong calibration of the Cyclops-7 sensor (R^2: 0.31). Although the Rio Huemules calibration was also obtained using the same Turner Cyclops-7 sensor, a different gain setting to the Cyclops-7 installed in the Rio Lloncochaigua was used, therefore it wasn't possible to use this Rio Huemules calibration for the Rio Lloncochaigua Cyclops-7 sensor. To add to this, the Cyclops-7 sensors recorded data in voltage, rather than NTU, so as this record was for a much shorter time period than the RBR*Tu* and there was no way to convert this to a unit comparable with other data presented, these data were abandoned.

For the RBR sensor, the loss of the majority of the suspended sediment filter papers unfortunately lead to a calibration of the sensor which was deemed to be too weak for use in the thesis (R^2: 0.08). The use of the Cyclops-7 sensor data to form a combined calibration was explored but unsuccessful, and no manufacturer calibration was available for the RBR sensor, thus, the data was left in NTU units for presentation in this thesis. Periods of time where the sensor was clearly malfunctioning have been removed, and thus data is presented from 27th July- 27th November 2018 as a time-series and used for analysis of hysteresis patterns (with discharge).

The 7 suspended sediment samples measured during fieldwork in January- February 2018, and the 5 remaining suspended sediment samples from the July 2018- April 2019 field season (collected between 4th December 2018 and 28th February 2019), covering a range of hydrological conditions from 17.4- 55.4 $m^3 s^{-1}$, were averaged to calculate a mean suspended sediment concentration (0.00062, σ: 0.00037 units?). The mean river discharge from the times at which the suspended sediment concentration was measured was similar to the total annual mean discharge (mean discharge during times of suspended sediment sample collection: 39.1 $m^3 s^{-1}$, σ: 11.1; annual mean discharge: 27.1 $m^3 s^{-1}$, σ: 23.9). Additionally, all discharge data (excluding the peaks of the largest storms) were within the same range as the suspended sediment samples, therefore it was assumed that although the data for this mean suspended sediment concentration was collected solely during the summer, it could also be applied in winter. This mean SSC concentration was multiplied by the total annual and seasonal cumulative discharge values to calculate suspended sediment flux and yield estimates. The range of suspended sediment concentrations measured, and their corresponding river discharge values can be seen in Table 3.

Table 3: The suspended sediment samples used to calculate yield and flux values, and the river discharge at the time of sampling.

Sample collection date	**Measured suspended sediment conc. (g L^{-1})**	**River discharge (m^3 s^{-1})**
07/02/2018 10:00	0.00060	46.3
09/02/2018 10:00	0.00077	55.4
10/02/2018 10:00	0.00046	50.3
12/02/2018 10:00	0.00028	40.4
13/02/2018 10:00	0.00020	39.0
14/02/2018 10:00	0.00033	38.8
15/02/2018 10:00	0.00013	38.0
04/12/2018 10:20	0.00131	30.7
16/12/2018 10:00	0.00061	47.5
28/12/2018 10:50	0.00110	26.1
12/02/2019 09:56	0.00094	*No data- sensor error*
28/02/2019 09:54	0.00071	17.4
Mean (σ)	0.00062 (σ: 0.00037)	39.1 (σ: 11.1)
Annual mean (σ)	*n/a*	27.1 (σ: 23.9)

4.0 Results

4.1 How do rainfall inputs and ambient temperature conditions differ in the two study sites?

Figures 11 and 12 depict the temporal variation in daily rainfall amounts in the Rio Lloncochaigua and Rio Huemules over the two study periods, from 7th September 2017 until 9th April 2019 in the Lloncochaigua catchment and 28th August 2016 until 28th July 2017 in Rio Huemules. These data support the first hypothesis, showing that mean rainfall was higher in the Rio Lloncochaigua catchment, with a greater range, frequently reaching over 50 mm per day (mean: 11.5 mm, σ: 0.158, max: 203.8 mm). In the Rio Huemules, rainfall rarely reached over 40mm per day (mean: 7.0 mm, σ: 10.685, max: 62.2 mm).

In order to study the seasonal differences in precipitation, the year was arbitrarily divided up into two seasons. This was done by dividing the 365 days of the year into two parts, then arranging those parts so that the middle days hung on both the summer and winter equinoxes. This meant that "summer" was defined as the period between 21st September and 20th March, and "winter" was from 21st March until 20th September. Although the reality of the annual climate patterns is much more complicated, this simple division meant that the two seasons had the same number of days, making the inter-seasonal analysis fairer.

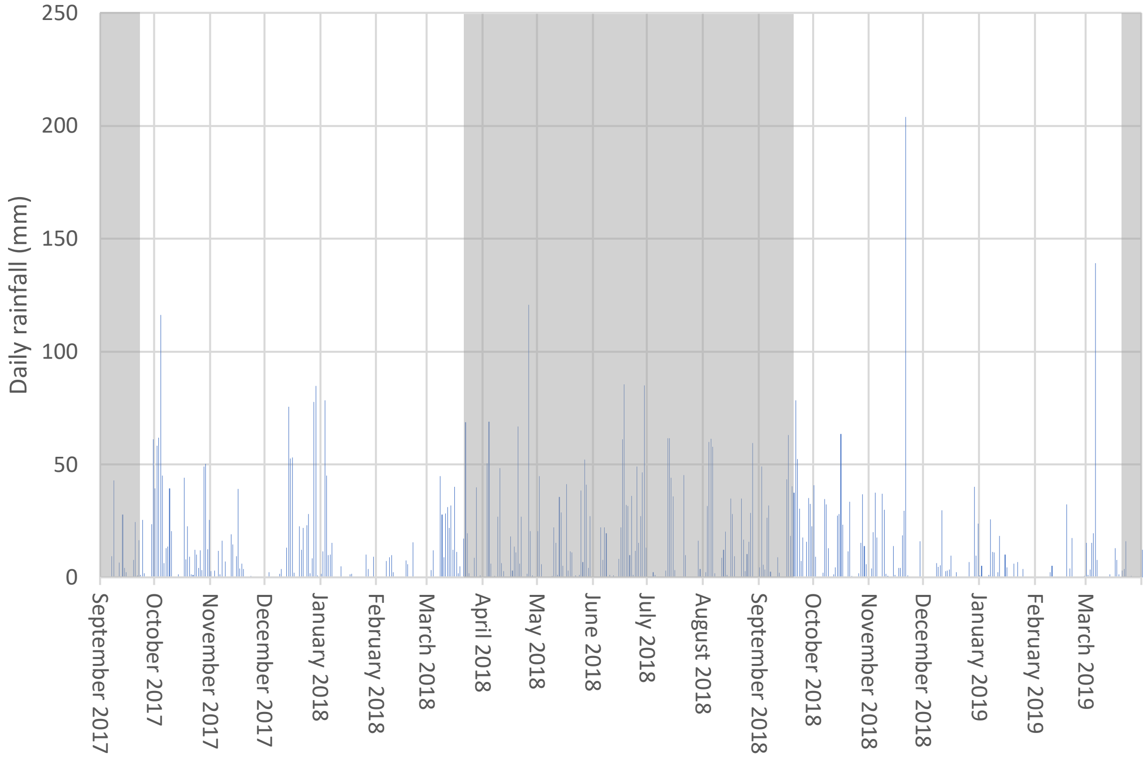

Figure 11- Total daily rainfall for the study period within the Rio Lloncochaigua catchment. Shading indicates winter months.

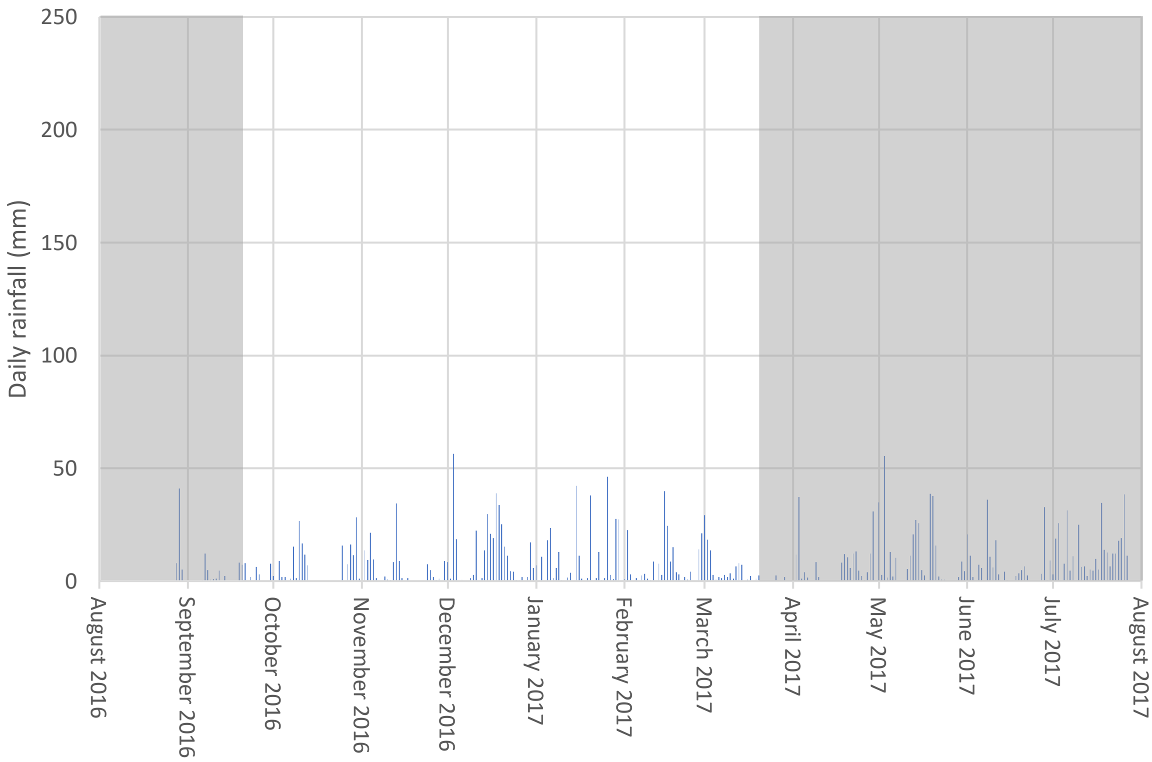

Figure 12- Total daily rainfall for the study period within the Rio Huemules catchment. Shading indicates winter months.

Table 4- A summary of rainfall data measured in the two catchments.

		Rio Huemules	**Rio Lloncochaigua**
Summer (21st September- 20th March)	Minimum daily rainfall (mm)	0	0
	Maximum daily rainfall (mm)	46.2	203.8
	Mean daily rainfall (mm)	6.4	10.1
	σ	10.604	0.223
	Rainy days as a % of total	77 %	61 %
	Total summer rainfall (mm)	1089	1975
Winter (21st March- 20th September)	Minimum daily rainfall (mm)	0	0
	Maximum daily rainfall (mm)	62.2	120.6
	Mean daily rainfall (mm)	7.6	15.3
	σ	11.0836	0.143
	Rainy days as a % of total	79 %	77 %
	Total winter rainfall (mm)	1380	2813
Whole year	Minimum daily rainfall (mm)	0	0
	Maximum daily rainfall (mm)	62.2	203.8
	Mean daily rainfall (mm)	7.0	11.5
	σ	10.685	0.158
	Rainy days as a % of total	78 %	69 %
	Total annual rainfall (mm)	2469	4788

As was set out in in hypothesis 1, peak precipitation falls in the winter months in both of the study areas (June to August). The seasonal patterns in precipitation in the Rio Huemules (summer mean daily rainfall: 6.4 mm, σ: 10.604; winter mean daily rainfall: 7.6 mm, σ: 11.08 see Table 4) are important, as concurrent seasonal temperatures (shown in Figure 13) in different parts of the river basin governs whether the bulk of annual precipitation is stored frozen or discharged immediately. Much of this winter precipitation will fall as snow in the accumulation zone, in the higher reaches of the catchment, and therefore only precipitation falling as rain on the lower ablation zone will have an immediate effect on the flood hydrograph. During summer there is less precipitation (summer mean daily rainfall: 6.4 mm, σ: 10.604; winter mean daily rainfall: 7.6 mm, σ: 11.08 see Table 4), though warmer temperatures (summer mean temperature: 10.8˚C, σ: 1.181; winter mean temperature: 5.4 ˚C, σ: 1.773) mean that a higher proportion of this will fall as rain.

Seasonal trends in precipitation are clearer in the Rio Lloncochaigua catchment. In the glaciated Rio Huemules, rainfall occurs on 77% of summer days, and 79% of winter days, (Table 4), however in the Rio Lloncochaigua catchment, summers are typically punctuated with large rainstorms events which are often larger than the more persistent winter rain. Rainfall occurs on 61% of summer days and 77% of winter days. Like the Rio Huemules, some precipitation falling in the winter months fell as seasonal snow in the mountainous parts of the catchment. This leads to a dampening of the storm in the hydrograph, as this precipitation doesn't reach the river until the spring melt.

Figure 13 depicts the mean monthly air temperatures observed in the two river catchments. Of the summer months, February is typically the warmest with temperatures rising to 15°C in the non-glaciated Rio Lloncochaigua catchment and 12°C in the Rio Huemules catchment. Note that the seasons discussed here are the austral seasons, therefore are the opposite months to their northern-hemisphere equivalents. From then, temperatures fall until June in the Rio Huemules and July in the Rio Lloncochaigua, which are the coldest months at 3°C and 5°C respectively. During the first half of the year, the Lloncochaigua catchment is 2.6°C warmer on average than the Rio Huemules. However, the mean temperature continues to fall for a month longer, bringing the two temperatures closer together and for the rest of the year the mean temperature difference is just 1.2°C, σ: 1.1°C.

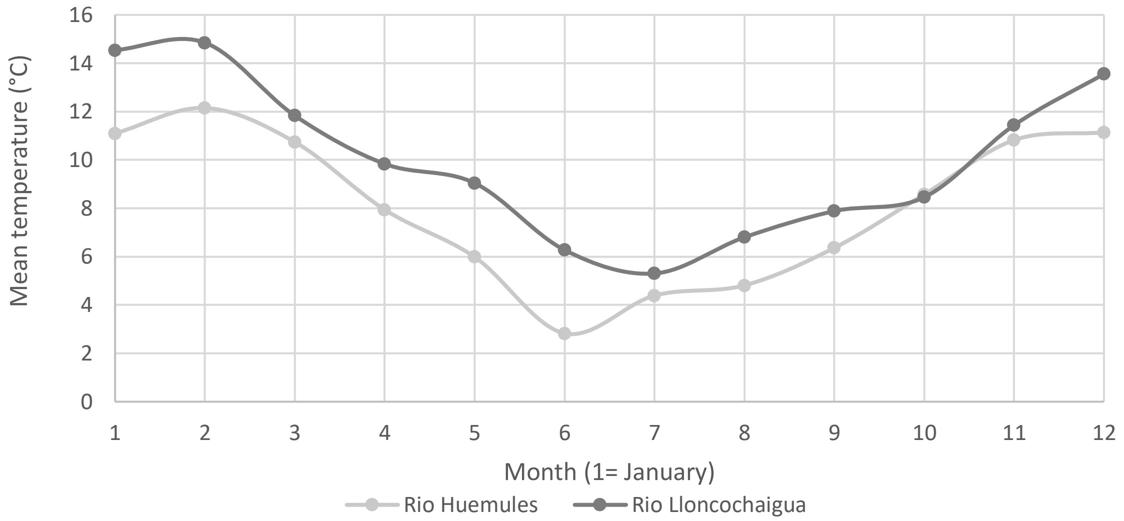

Figure 13- Mean monthly ambient temperatures in the two catchments, measured in 2016.

Table 5- A summary of temperature data measured in the two catchments.

		Rio Huemules	**Rio Lloncochaigua**
Summer (21st September-20th March)	Minimum temperature (°C)	8.6	8.5
	Maximum temperature (°C)	12.2	14.8
	Mean temperature (°C)	10.8	12.4
	σ	1.181	3.986
Winter (21st March-20th September)	Minimum temperature (°C)	2.8	5.3
	Maximum temperature (°C)	7.9	13.7
	Mean temperature (°C)	5.4	7.5
	σ	1.773	3.635
Whole year	Minimum temperature (°C)	2.8	5.3
	Maximum temperature (°C)	12.2	14.8
	Mean temperature (°C)	8.1	10.0
	σ	3.150	4.682

4.2 How does glacial cover within a catchment affect the hydrological regime?

4.2.1 Long-term data sets

Mean discharge in the river at the glaciated Rio Huemules site shown in Figure 15 is almost four times higher than the discharge measured in the de-glaciated Lloncochaigua site (106 $m^3 s^{-1}$, σ: 156, in comparison to 27.1 $m^3 s^{-1}$, σ: 23.9). Apart from a GLOF event on 28th March 2017, when discharge peaked at 2610 $m^3 s^{-1}$, maximum recorded discharge in the glaciated Rio Huemules was 484 $m^3 s^{-1}$ on 4th May 2017, as opposed to 113 $m^3 s^{-1}$ in the Lloncochaigua on 18th June 2018. The Lloncochaigua discharge record (Figure 14) shows higher values during April- May (autumn), and the lowest monthly discharge during February (summer), matching studies by Villanueva et al. (2016) in similar Andean catchments in Bariloche, Argentina.

Note that due to the different field season dates, and different maximum discharge values, both the x and y axis in Figures 14 and 15 are different scales.

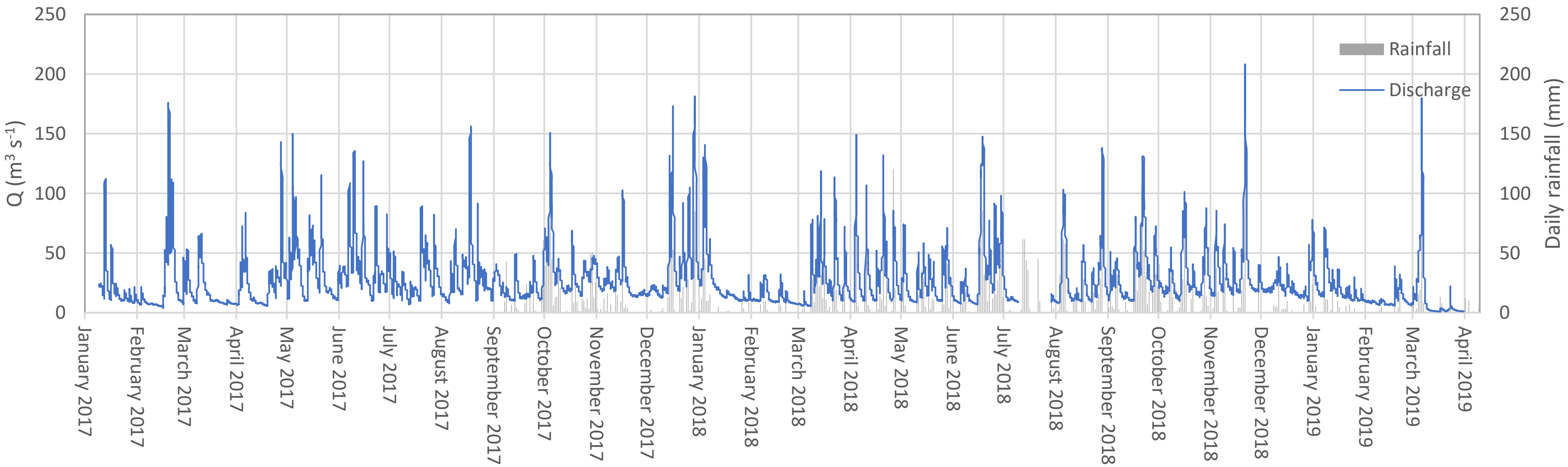

Figure 14- Temporal variations in discharge in the non-glaciated Rio Lloncochaigua throughout the study period, 9th January 2017- 9th April 2019.

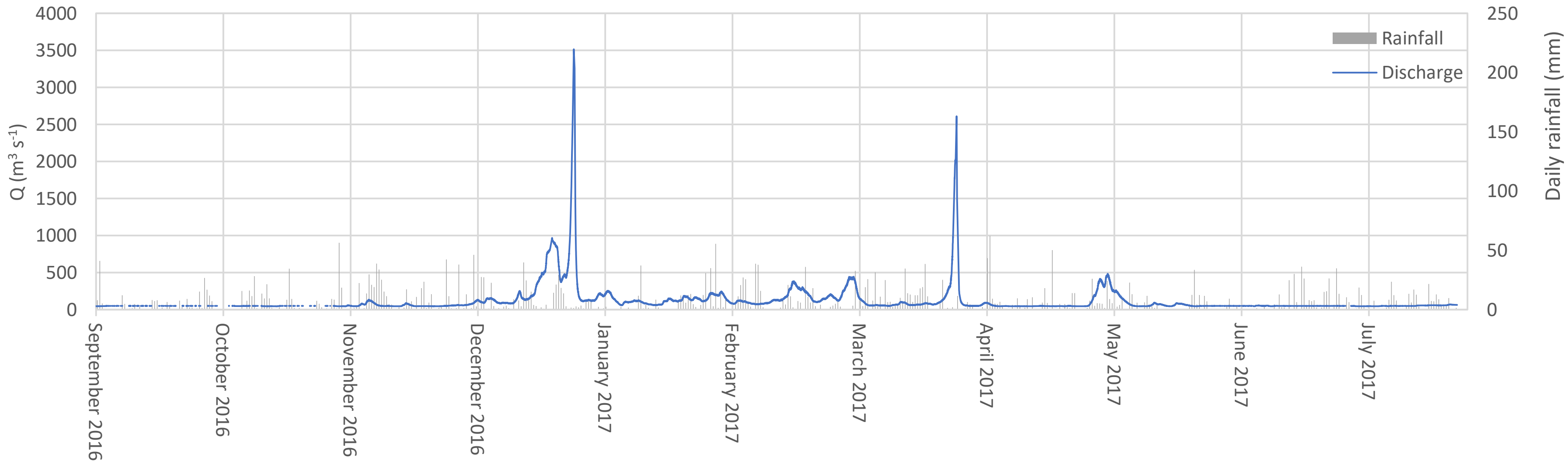

Figure 15- Temporal variations in discharge in the glaciated Rio Huemules throughout the study period, 28th August 2016- 29th July 2017.

During December, a large outburst flood event occurs, as can be seen in Figure 15. These outburst events occur due to release of water previously contained by a dam within or in front of the glacier, which gives way. Research has shown these to be an increasing hazard in recent years, due to warmer climate increasing their frequency (Dussaillant et al., 2010; Pena and Escobar, 1983a; Tanaka, 1980; Harrison, 2006).

Table 6 shows the differences in total river discharges in summer (21st September to 20th March) and winter (21st March to 20th September) in the two catchments. Summer discharge in the Rio Huemules is one and a half times higher than the winter observations (142.914 $m^3 s^{-1}$ in summer, as opposed to 88.884 $m^3 s^{-1}$). This agreed with previous expectations. However, there is much less seasonal variation in the non-glaciated Rio Lloncochaigua, and neither summer nor winter typically discharges more water than the other.

Table 6- A summary of stage data measured in the two catchments.

		Rio Huemules	Rio Lloncochaigua
Summer (21st September- 20th March)	Minimum discharge ($m^3 s^{-1}$)	50.5	3.79
	Maximum discharge ($m^3 s^{-1}$)	444	181
	Mean discharge ($m^3 s^{-1}$)	143	25.1
	σ	83.9	25.5
	Total cumulative discharge (km^3)	2.14	0.415
Winter (21st March- 20th September)	Minimum discharge ($m^3 s^{-1}$)	45.4	5.62
	Maximum discharge ($m^3 s^{-1}$)	2610	156
	Mean discharge ($m^3 s^{-1}$)	88.9	29.2
	σ	179	22.5
	Total cumulative discharge (km^3)	1.027	0.440
Whole year	Minimum discharge ($m^3 s^{-1}$)	45.4	3.79
	Maximum discharge ($m^3 s^{-1}$)	2610	181
	Mean discharge ($m^3 s^{-1}$)	106	27.1
	σ	157	23.9
	Total cumulative discharge (km^3)	3.17	0.947
	Specific discharge (m)	4.73	0.885

Figure 16 shows the mean discharge plotted against the mean daily rainfall in the Rio Lloncochaigua. Despite precipitation data varying by a factor of 10, (2 - 22 mm per day), the discharge doesn't reflect this: only varying by a factor of 3 (varying between 23 and 62 $m^3 s^{-1}$). This is also reflected in the seasonal means: during summer, the mean discharge was 45 $m^3 s^{-1}$ (σ: 25.467) with a mean daily rainfall of 9 mm (σ: 0.223), yet despite an increase of mean precipitation to 15 mm (σ: 0.143), winter mean discharge only increases to 47 $m^3 s^{-1}$ (σ: 22.471).

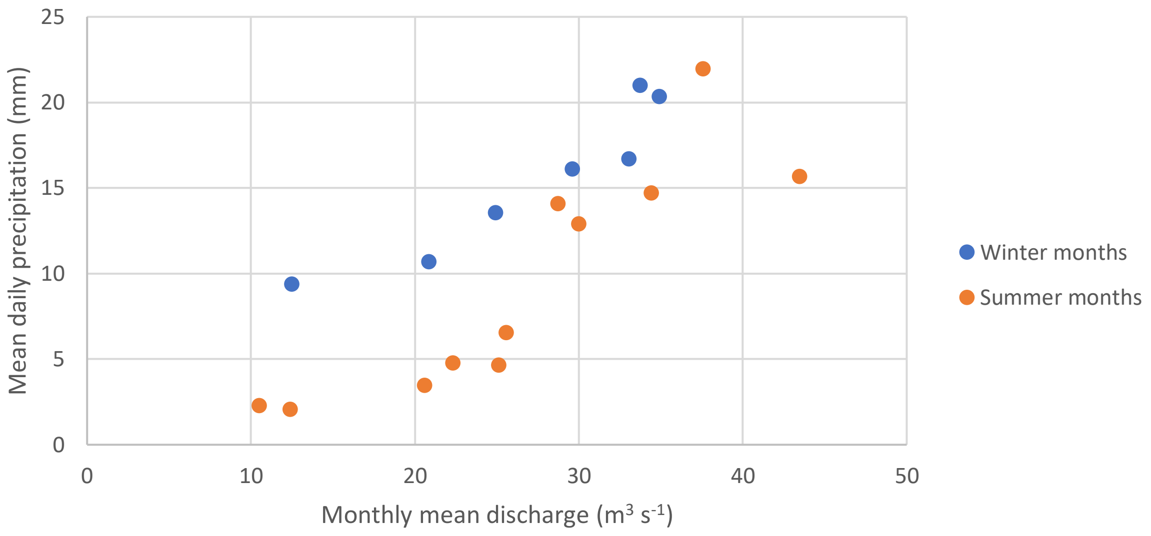

Figure 16- The relationship between mean daily precipitation and discharge, in summer and winter, in the de-glaciated Rio Lloncochaigua catchment.

Figure 17 compares the annual mean discharge in the Rios Huemules and Lloncochaigua to other Chilean rivers (data sourced from Pepin et al., 2010). Multiple records from the same river represent data from different hydrological stations along the length of the river, however as the data is ordered by the latitude of the hydrological station (with the northernmost stations on the left-hand side of the graph), multiple records from the same river are not organized upstream-downstream or vice versa.

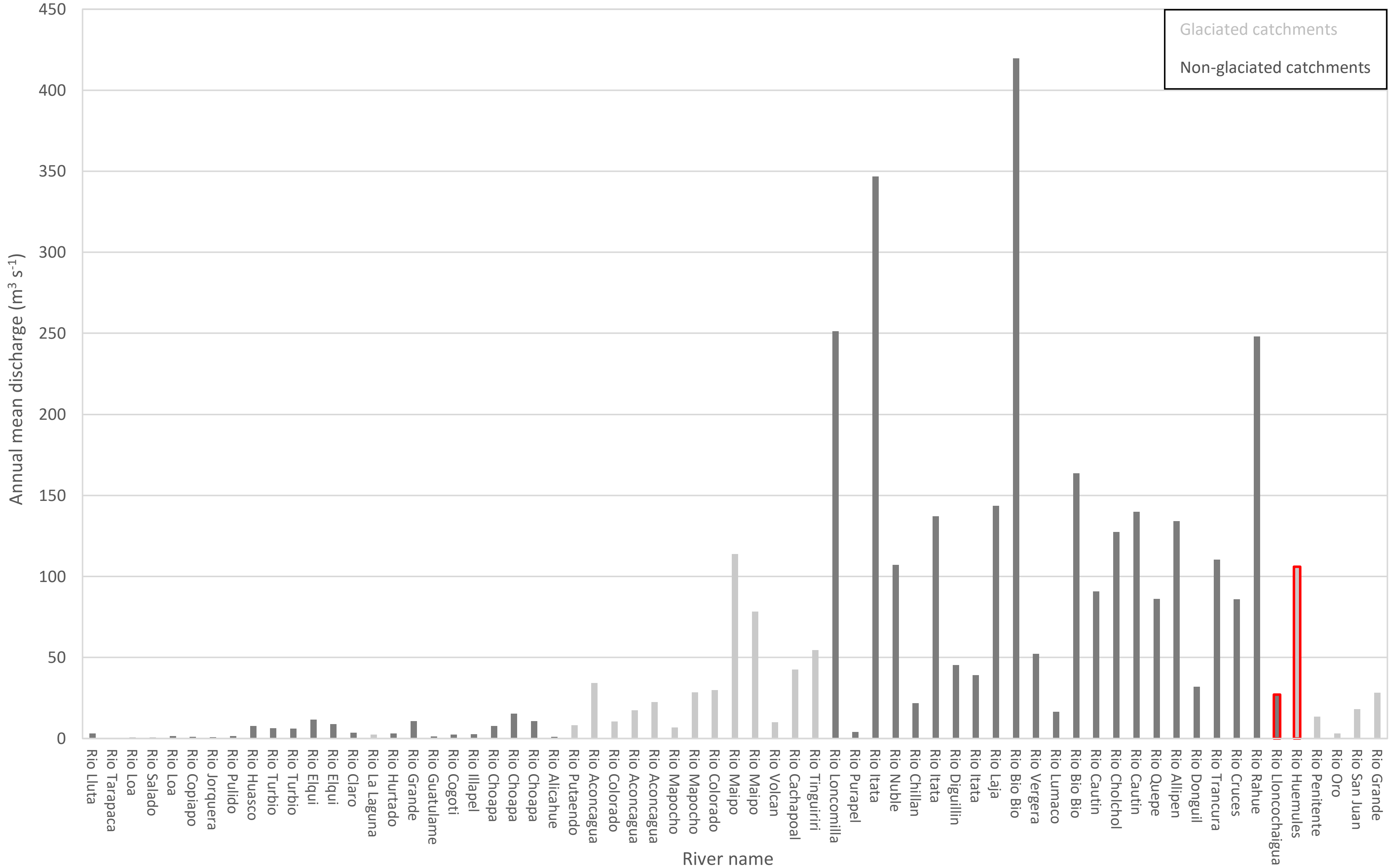

Figure 17- A comparison of annual mean discharge in Chilean rivers (L-R: N-S). All data presented (excluding the Rio Huemules and Rio Lloncochaigua, outlined) sourced from Pepin et al. (2010).

4.2.2 Do daily patterns in river discharge observed in glaciated and de-glaciated catchments differ, and are different proportions of daily patterns observed in different seasons in glaciated and de-glaciated catchments?

Daily patterns in river discharge can be observed in both catchments. In order to better present these patterns, and quantify the frequency of observance of the various patterns, a new method of analysis was created. Patterns were observed over daily (defined as the period of time covering a full 24 hours from midnight to midnight) time periods, as this is a short (thus allowing the collection of a large number of datapoints per season), natural cycle. Many parameters (for example daylight and air temperature) also change on a daily cycle, and therefore matching the analysis period with these cycles allowed their influence to be studied- this is more pertinent in the Rio Huemules. It is recognised that had the day been defined as mid-day to mid-day, the results would be different, however midnight to midnight was chosen as the universally-accepted definition of a day. The discharge for each day was plotted as a simple line graph, then manual observation allowed the pattern observed to be arbitrarily grouped into the six types displayed in tables 7 and 8. It is noted that this manual observation introduces user bias, affecting the end results.

Tables 7 and 8 show the clearest examples from the dataset of the six major patterns identified in the variations in daily discharge in the Rio Huemules and Lloncochaigua. Time, along the x-axis, goes from midnight to midnight of the following day, thus covering a 24-hour period. The different patterns are each given a name and colour, which is used in future analysis.

Table 7- The six forms of daily discharge patterns observed in the glaciated Rio Huemules catchment. The X axis' show time of day, from midnight to midnight, and the form names and colours are referred back to throughout the thesis.

Increasing diurnal

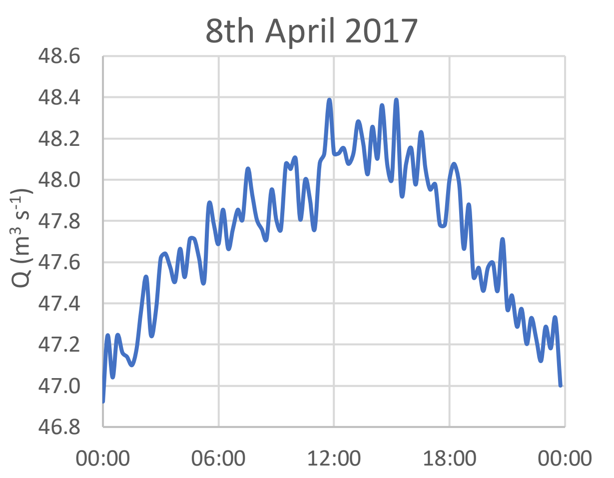

Consistent

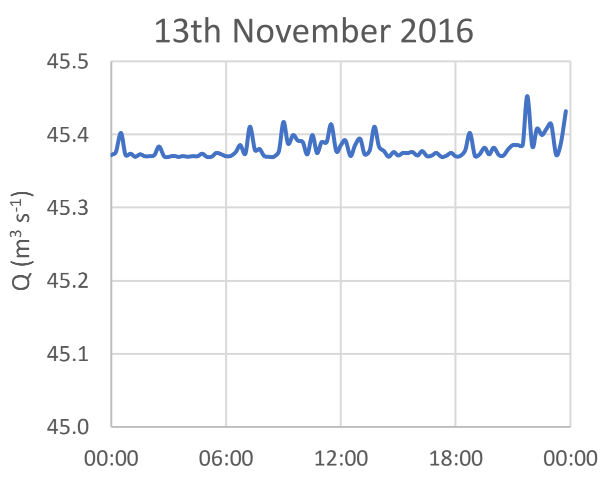

Daily rise

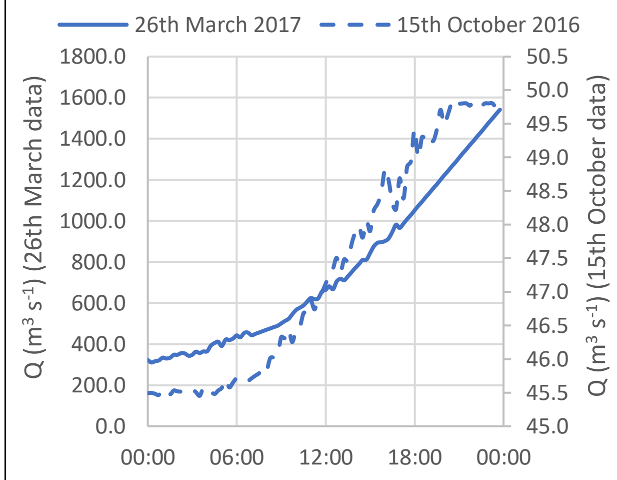

Daily fall

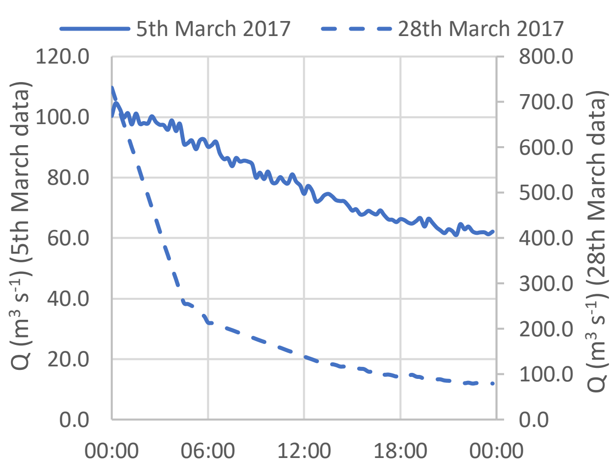

Irregular

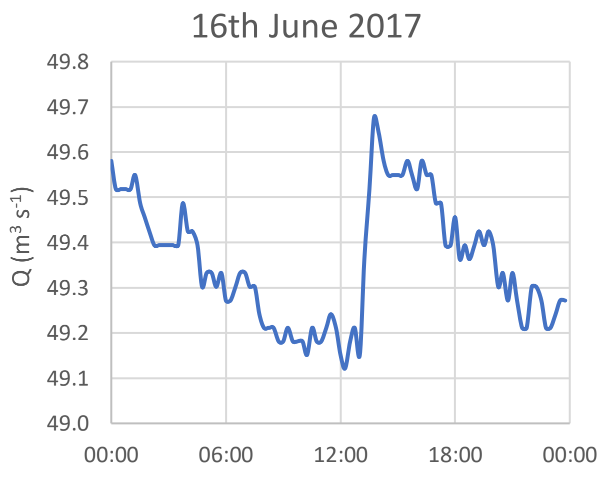

Decreasing diurnal

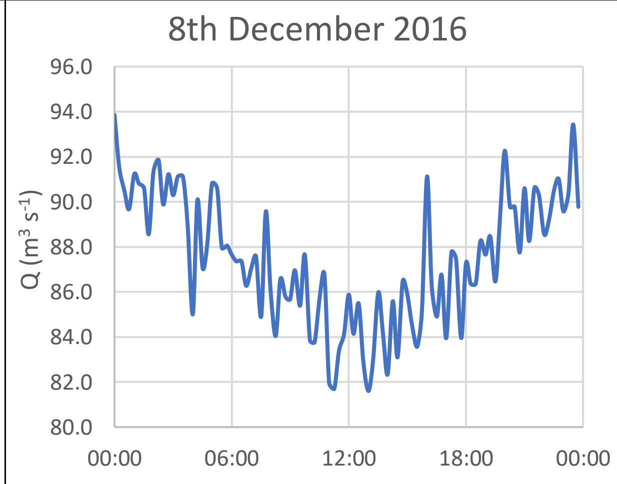

Table 8- The six forms of daily discharge patterns observed in the non-glaciated Rio Lloncochaigua.

<table>
<tr><th>Increasing diurnal</th><th>Consistent</th><th>Daily rise</th></tr>
<tr><td>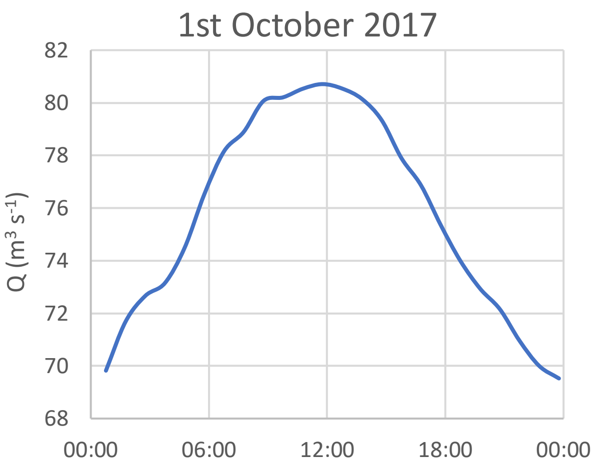
</td><td>No consistent days observed in this catchment.</td><td>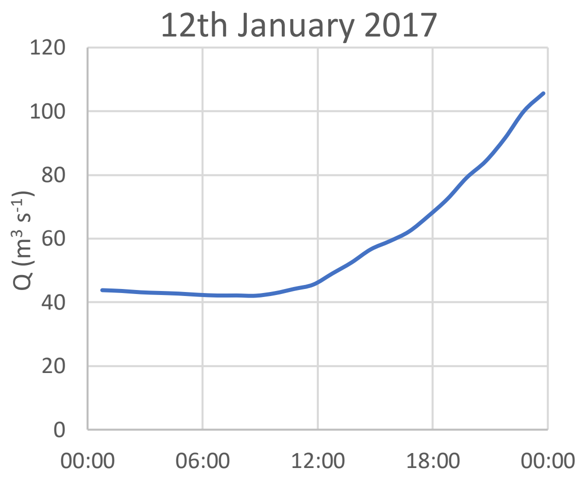
</td></tr>
<tr><th>Daily fall</th><th>Irregular</th><th>Decreasing diurnal</th></tr>
<tr><td>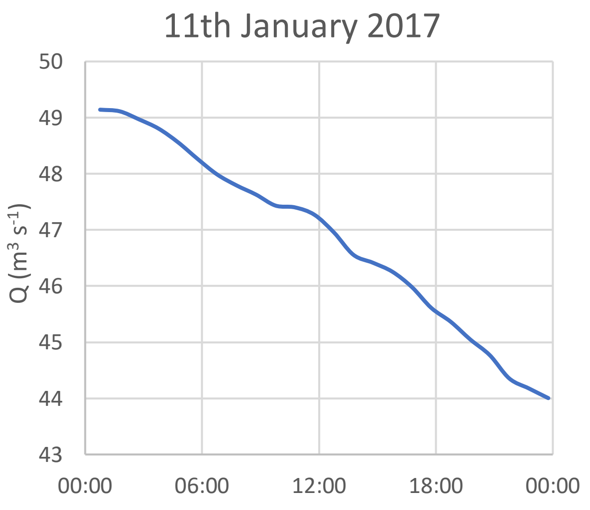
</td><td>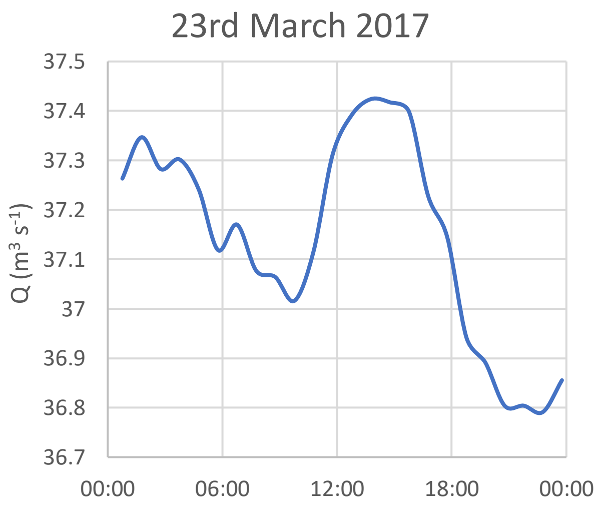
</td><td>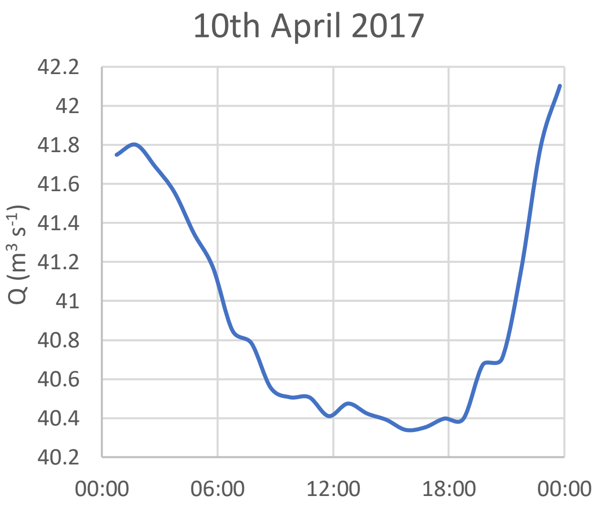
</td></tr>
</table>

Table 9- A collection of pie charts displaying the different proportions of different daily flow patterns in the glaciated Rio Huemules and non-glaciated Rio Lloncochaigua through the different seasons within the study period. A: days showing increasing diurnal patterns, B: consistent days, C: days with daily rise patterns, D: days with daily fall patterns, E: Irregular days, F: days with decreasing diurnal patterns.

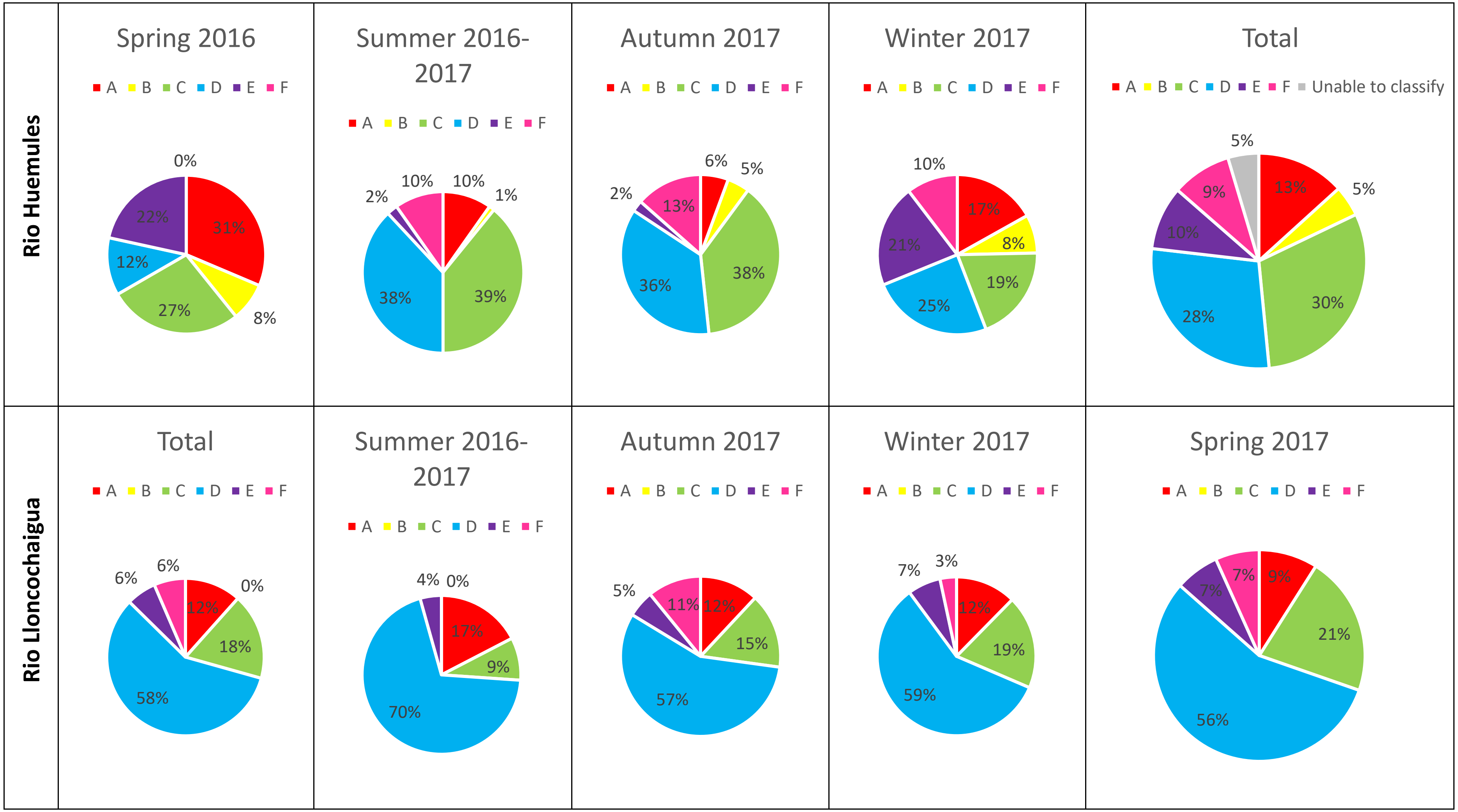

Increasing Diurnal days show a rise and fall in the hydrograph form via a regular diurnal pattern. In order for a day to be classified as this type, it must have roughly equal time where the river is rising and falling, and the river must end the day roughly equal to the discharge at which it begun.

Consistent days show very little variation in discharge throughout the day. There are very few of these days in the dataset within either catchment, with many being attributed to errors in the sensor record.

During *Daily Rise* days, the river level is rising through the entire 24-hour period. For the purposes of this study, no differentiation was made between days of continuous discharge increase and days when the river level was roughly level before or after rising, or fell slightly at the end of the day. In this instance, the difference in discharge was compared between the first and last data points and if they demonstrated a significant increase, the day was classified as a *Daily Rise*.

Daily Fall graphs demonstrate exactly the opposite patterns and classification rules to *Daily Rise-type* days, showing falling river levels throughout the 24-hour period.

Irregular days show multiple (though rarely more than two) peaks and troughs in river discharge throughout the day.

Finally, *Decreasing Diurnal* graphs show falling river levels in the morning then increasing discharge throughout the afternoon.

In the analysis of discharge pattern types (Table 7), days in the Rio Huemules showing the *Increasing diurnal* pattern can be explained by the daily contribution of glacial melt which varies with daily cycles in temperature. As the ambient temperature and energy through insolation rises throughout the day (peak typically at 16:30), glacier melt increases. Peak discharge can be observed in the middle of the night when the meltwater generated during the previous day has travelled through the glacial system and proglacial lake to reach the river channel. This is earlier than peak discharge observed between 18:00 and 20:00 in the river draining the Gangotri glacier, in the

Himalayas (Singh et al., 2005), but similar to peak discharge in Skálafellsjökull, Iceland (Young et al., 2015). These *Increasing Diurnal* pattern days are less frequent, but are still observed, in the Rio Lloncochaigua catchment which does not have any glacier cover. In this environment, the *Increasing Diurnal* days were typically associated with small day time rainfall events which added water into the river, where all the rainfall was evacuated by the river over a 24-hour period.

Daily Rise and *Daily Fall* days in the Rio Huemules occurred when the daily increases and decreases in discharge were part of a more sustained increase or decrease in discharge lasting more than 24 hours. In some instances, this was due to sustained increases in air temperature, such as the usual seasonal variations represented in Figure 13. Glacial outburst events (discussed above in section 4.3.1) and prolonged precipitation, which could be rainfall throughout the summer months, also caused larger increases in discharge, which were too big to be contained within one 24-hour period. In the de-glaciated Rio Lloncochaigua catchment, *Daily Rise* and *Daily Fall* days were typically the result of prolonged rainfall during large storms.

Irregular days, showing multiple increases and decreases in discharge within a 24-hour period, were rare in both catchments. In the glaciated catchments, they can be explained by either the daily melt cycle or a small rainfall event adding a pulse in discharge which is superimposed on top of a period of decreasing discharge. This decreasing discharge could be due to decreasing air temperatures or the aftermath of a prolonged period of precipitation such as in *Daily Fall* days. In the non-glacial river catchment, the *Irregular* days are a response to small morning rainfall events.

Decreasing diurnal days, the opposite of *Increasing Diurnal* days, were rare in both catchments throughout the year. They were typically observed linking *Daily Rise* and *Daily Fall* days to form larger scale patterns than those observed in just 24 hours.

The proportion of different types of days differs between different seasons in both catchments (Table 9). In spring in the glaciated catchment, the most common daily flow pattern is *Increasing Diurnal*, which accounted for 31% of all the days. Summer and autumn were dominated by larger cycles in discharge which were spread over multiple days, and are observed in this graph as the increase in *Daily Rise* and *Daily Fall* days (39% and 38% respectively). Winters in the Rio Huemules were characterized by a higher proportion of *Irregular* days (21%), as the larger cycles were reduced to 19% and 25% of days. *Increasing Diurnal* days also increased from 6% of days during autumn to 17% of winter days.

Daily Fall days were the most common in every season in the non-glacial Rio Lloncochaigua catchment, accounting for 58% of all the recorded days. Summer showed the highest proportions of *Daily Fall* days, at 70%. *Increasing Diurnal* days were also most common in summer, at 17%, before falling to 9% during the following spring. Proportions of *Daily Rise* days increased gradually through the seasons, from 9% during summer to 21% during the spring.

4.3 How does glacial cover affect fluxes and yields of suspended sediment?

4.3.1 How does suspended sediment concentration vary throughout the year in glacial and non-glacial rivers?

The concentration of suspended sediment in the glaciated Rio Huemules displayed in Figure 18 ranges from 0.042 g L^{-1} to 0.102 g L^{-1}, with a mean concentration of 0.081 g L^{-1} (σ: 0.0146). In the Rio Lloncochaigua in (Figure 19), turbidity ranges from 0.125 NTU to 17.2 NTU, with an annual mean turbidity of 1.12 NTU (σ: 1.99). Note that due to the differences in units used and field season dates, the axis scales on Figures 18 and 19 are different.

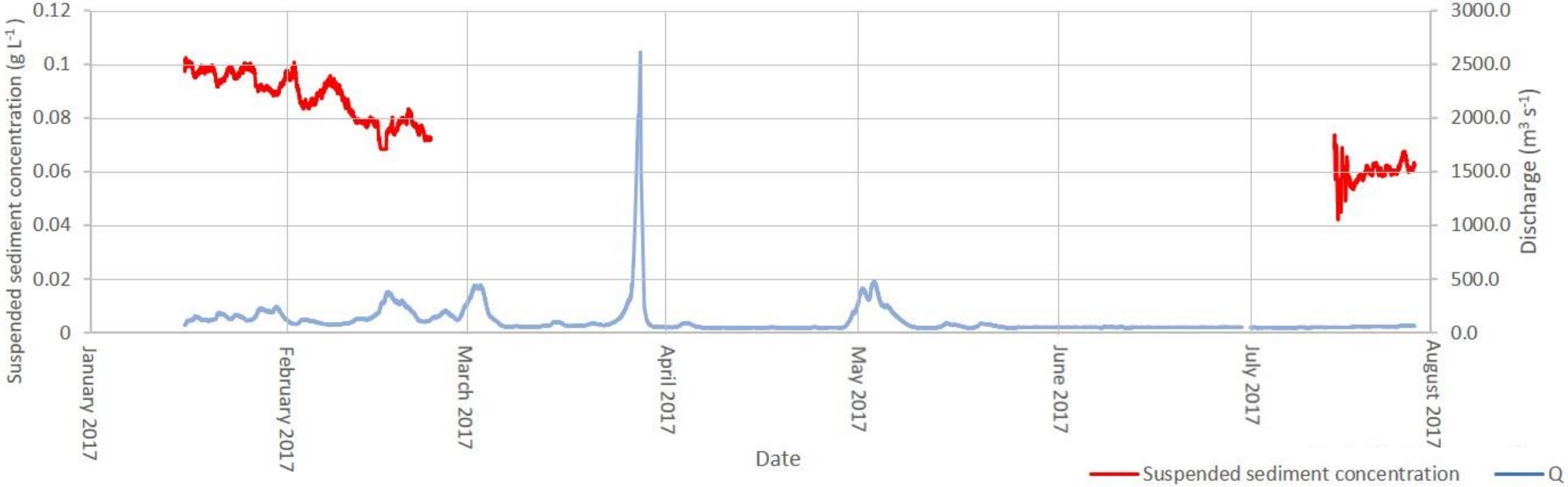

Figure 18- A time series plot showing variations in suspended sediment concentrations throughout the two field seasons in the glaciated Rio Huemules

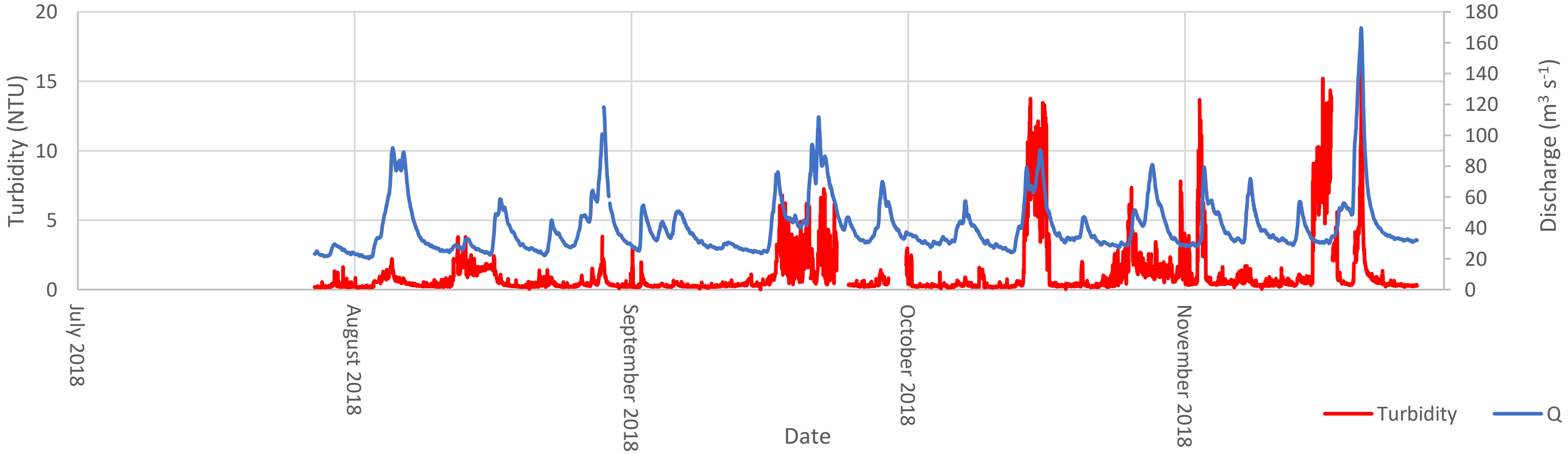

Figure 19- A time series plot showing variations in turbidity throughout the field season in the non-glaciated Rio Lloncochaigua

Table 10- A summary of suspended sediment concentration and turbidity data measured in the two catchments.

	Rio Huemules		**Rio Lloncochaigua**	
Summer (21st September-20th March)	Minimum suspended sediment concentration (g L^{-1})	0.068	Minimum turbidity (NTU)	0.143
	Maximum suspended sediment concentration (g L^{-1})	0.10	Maximum turbidity (NTU)	17.2
	Mean suspended sediment concentration (g L^{-1})	0.088	Mean turbidity (NTU)	1.50
	σ	0.00853	σ	2.53
Winter (21st March-20th September)	Minimum suspended sediment concentration (g L^{-1})	0.042	Minimum turbidity (NTU)	0.125
	Maximum suspended sediment concentration (g L^{-1})	0.074	Maximum turbidity (NTU)	6.78
	Mean suspended sediment concentration (g L^{-1})	0.060	Mean turbidity (NTU)	0.659
	σ	0.00413	σ	0.815
Whole year	Minimum suspended sediment concentration (g L^{-1})	0.042	Minimum turbidity (NTU)	0.125
	Maximum suspended sediment concentration (g L^{-1})	0.10	Maximum turbidity (NTU)	17.2
	Mean suspended sediment concentration (g L^{-1})	0.081	Mean turbidity (NTU)	1.12
	σ	0.0146	σ	1.99

While the Rio Huemules winter river discharge volume is a quarter of that recorded at the end of the summer melt period, the suspended sediment concentration observed during winter reduces by only 32% (summer mean: 0.0882 g L^{-1}, σ: 0.00853; winter mean: 0.0596 g L^{-1}, σ: 0.00413; Table 10). In the non-glacial Rio Lloncochaigua, the presence of three large storms mean that summer turbidity was double that observed in winter (1.50 NTU, σ: 2.53, as opposed to 0.659 NTU, σ: 0.815; Table 10).

4.3.2 How does glacial cover affect fluxes and yields of discharge and suspended sediment?

Table 11- Sediment flux and yield values calculated for the two catchments.

	Rio Huemules	**Rio Lloncochaigua**
Catchment area (km^2)	670	107
% glaciated	71	1.2
Total annual cumulative discharge (km^3)	3.170	0.947
Specific discharge (m)	4.73	0.885
Summer (21st September- 20th March) suspended sediment flux (tonnes)	276,591	257.3
Winter (21st March- 20th September) suspended sediment flux (tonnes)	50,017	272.8
Total annual suspended sediment flux (tonnes)	326,608	587.4
Summer (21st September- 20th March) suspended sediment yield (tonnes per km^2)	413	2.40
Winter (21st March- 20th September) suspended sediment yield (tonnes per km^2)	75	2.55
Annual suspended sediment yield (tonnes per km^2)	487	4.95

Despite being six times larger in area, the total cumulative annual river discharge is an order of magnitude higher in the glaciated Rio Huemules catchment than the Lloncochaigua (0.1905 km^3y^{-1} in the Rio Huemules; 0.0195 km^3 y^{-1} in the Rio Lloncochaigua; Table 11). This increased discharge is also reflected in the specific discharge results in the non-glaciated Rio Lloncochaigua, which is five times smaller than that measured at Rio Huemules (4.731 m in the Rio Huemules; 0.885 m in the Rio Lloncochaigua; Table 11).

Suspended sediment flux in the glaciated Rio Huemules in five times higher in summer (276,591 tonnes) than winter (50,017 tonnes). The non-glaciated Rio Lloncochaigua however has a higher suspended sediment flux in winter (272.8 tonnes), exporting only slightly more sediment than summer (257.3 tonnes). During a whole year, the Rio Huemules will export five hundred times more sediment than the Rio Lloncochaigua. This is compared to other glacial and non-glacial systems in Figure 20, which show that the Rio Huemules has a higher annual mean discharge and lower sediment flux than other glacial rivers in Chile, and the Rio Lloncochaiga has an annual mean discharge and sediment flux well within the range of other non-glacial rivers in Chile.

The masses of suspended sediment produced per km^2 of catchment area (i.e. suspended sediment yield) supports hypothesis 3, showing a strong seasonality in both catchments, particularly the glaciated Rio Huemules. Out of a total annual yield of 487 tonnes per km^2 catchment area, 84% (413 tonnes) is exported during the summer months. In the Rio Lloncochaigua catchment, the seasonality is much weaker, with 52% of sediment yield (2.55 tonnes per km^2 catchment area) exported during winter. Total annual sediment yield is over 5 orders of magnitude higher in the glaciated Rio Huemules.

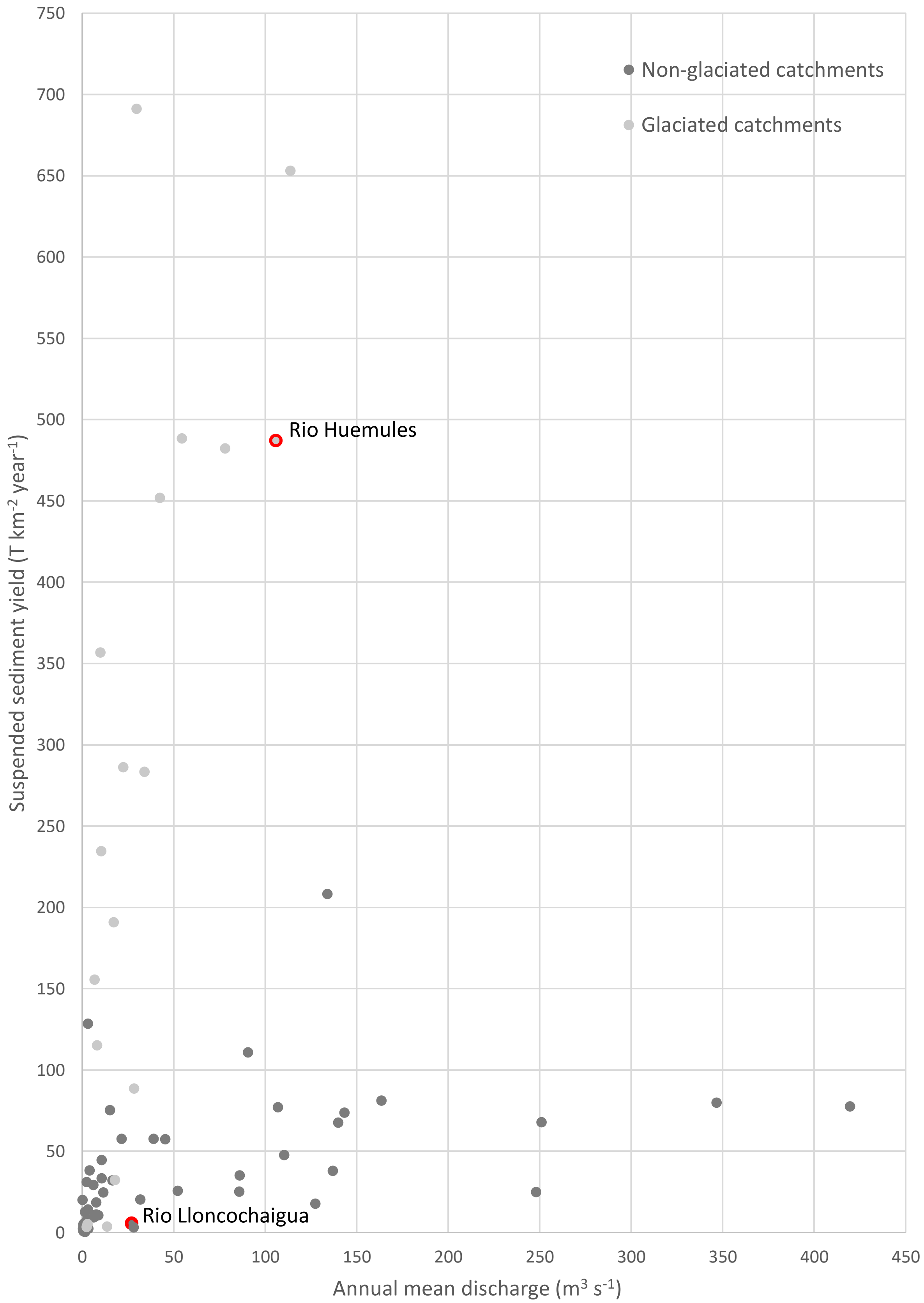

Figure 20- The relationship between sediment yields and annual mean discharge from a range of glaciated and non-glaciated catchments throughout Chile. The two field sites for this study are outlined in red. All data except for the Rio Huemules and Rio Lloncochaigua were sourced from Pepin et al., 2010.

4.3.3 Using storm hysteresis to understand catchment sediment source areas

Previous research has often analysed associations between discharge and suspended sediment concentrations in order to make inferences regarding hydrological and supply controls upon sediment transport in rivers. Figures 21- 23 display example storm hydrographs for the Rio Huemules (2^{nd}- 5^{th} February 2017) and Rio Lloncochaigua (2^{nd}- 11^{th} August 2018; 21^{st}- 24^{th} November 2018) in order to identify overriding controls upon sediment transport during melt and storm events, as discussed in research question three.

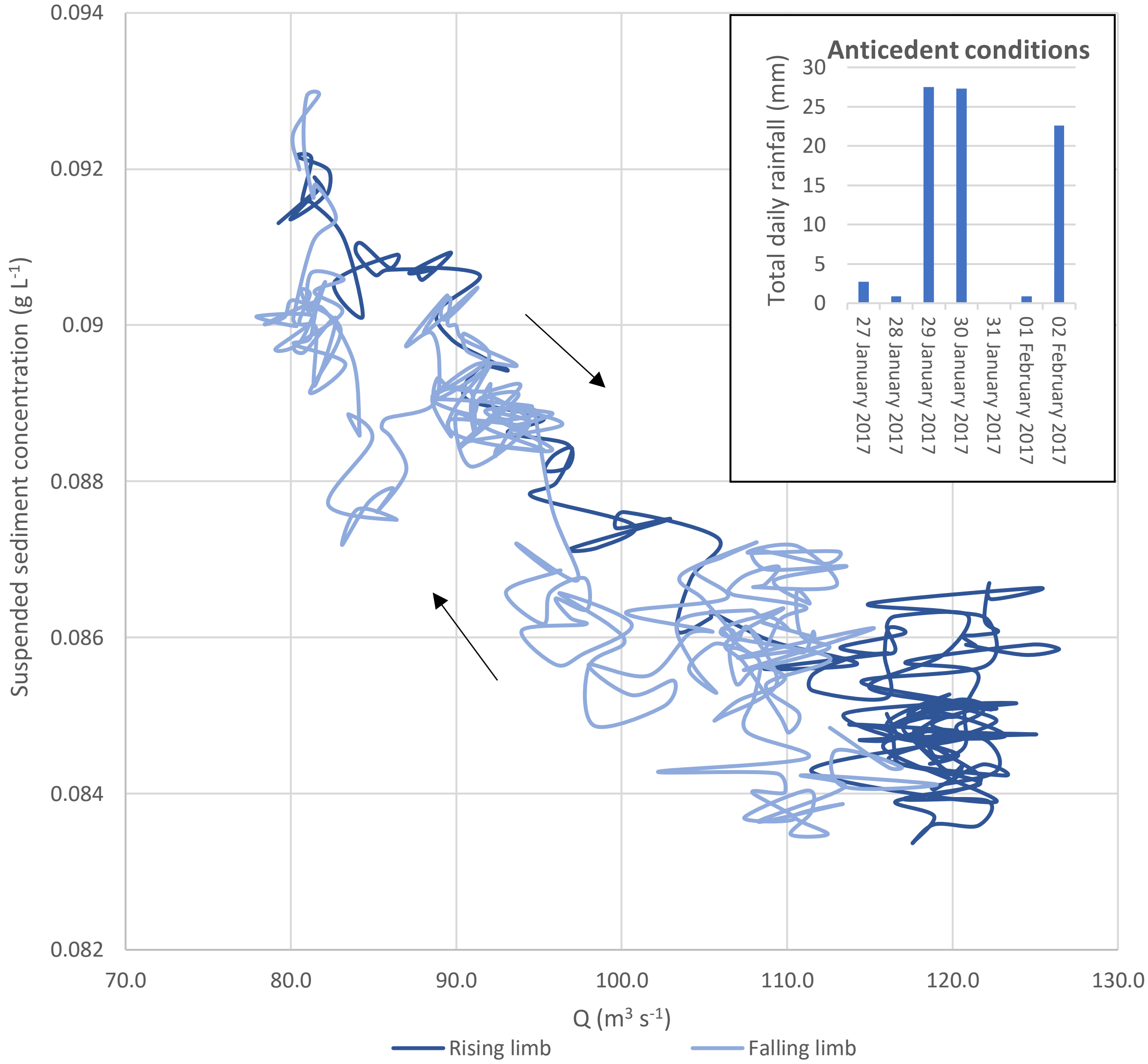

Figure 21- A storm hysteresis plot for Rio Huemules, 2nd- 5th February 2017. Arrows indicate direction of hysteresis.

Figure 21 displays a hysteresis plot for the Rio Huemules from 2nd to 5th February 2017 (austral summer). It shows that with increasing discharge (due to a rainfall event), the suspended sediment concentration falls. The plot is extremely noisy, indicating a complicated relationship between discharge and suspended sediment as the storm progresses, however on breaking it up into the two limbs, the pattern can be easier observed. The initial part of the plot shows the clearest trend, as the increased discharge is accompanied by falling suspended sediment concentrations until peak discharge (126.4 $m^3 s^{-1}$). Due to data noise at the hydrograph peak, a clear trend is difficult to establish. The suspended sediment concentration fluctuates between 0.083 g L^{-1} and 0.086 g L^{-1}, with discharge varying between 115 $m^3 s^{-1}$ and 125 $m^3 s^{-1}$. It is noted that these are very small variations.

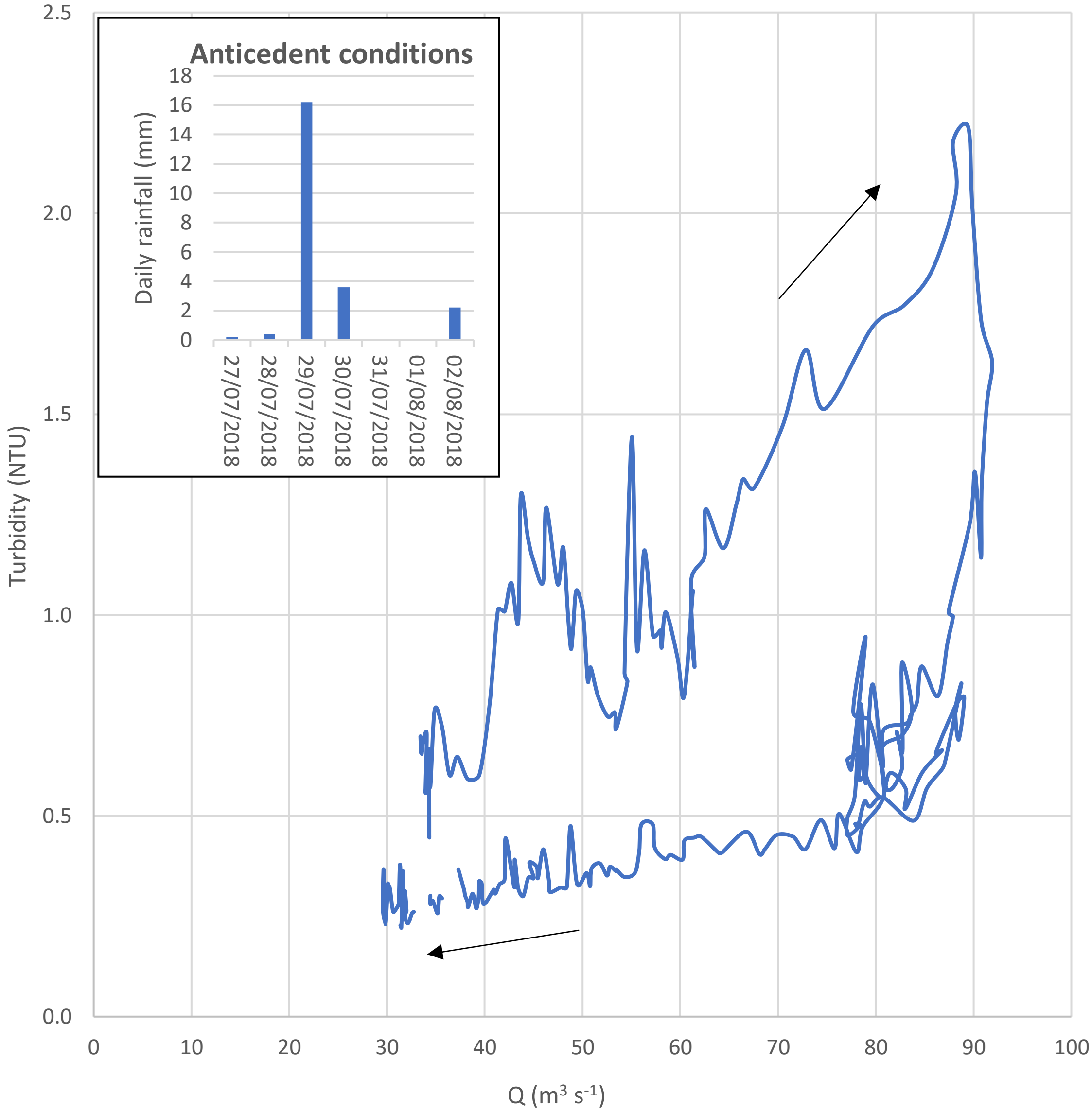

Figure 22- A storm hysteresis plot for Rio Lloncochaigua, showing a winter storm from 2nd- 11th August 2018. Arrows indicate direction of hysteresis.

Winter in the Rio Lloncochaigua was characterised by frequent small storms. Figure 22 shows the hysteresis of a typical 9-day long storm in Rio Lloncochaigua during midwinter (2nd- 11th August 2018). During this time, both discharge and turbidity increase and decrease simultaneously. The plot follows a clockwise hysteresis, originating in the lower left side of the plot- with discharge more than quadrupling from 20 m^3 s^{-1} to 92 m^3 s^{-1} leading to a rapid increase in turbidity from 0.4 NTU to 2.2 NTU. The turbidity begins to fall shortly before peak discharge, dropping sharply at first then the rate slows to a lower rate of change than observed on the upwards limb of the hydrograph.

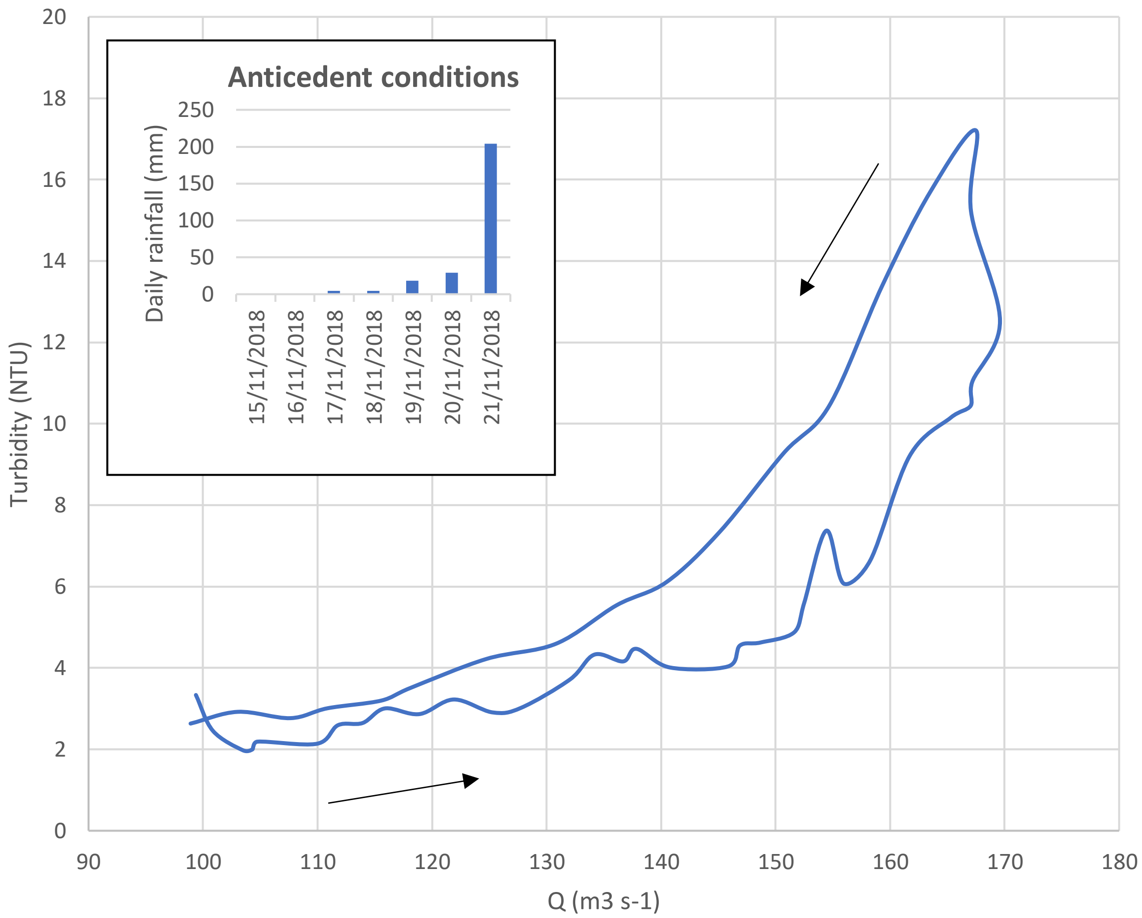

Figure 23- A hysteresis plot for a summer storm in the Rio Lloncochaigua catchment from 21st- 22nd November 2018. Arrows indicate direction of hysteresis.

Summer in the Rio Lloncochaigua saw much lower levels of river discharge (mean summer discharge: 25.06 $m^3 s^{-1}$, σ: 25.467, compared to 29.161 $m^3 s^{-1}$, σ: 22.471, during the winter months), punctuated by occasional large storms. Figure 23 shows one such storm, lasting just three days between 21st and 24th November 2018. This summer storm is much larger than the winter storms, with discharge rising to 169.59 $m^3 s^{-1}$, and the turbidity to 17.21 NTU. The relationship shown between discharge and turbidity is different during these summer storms, as demonstrated by the anti-clockwise pattern on the plot, with turbidity increasing at a relatively slower rate than discharge at the beginning of the storm.

5.0 Discussion

5.1 Assessing the seasonality of water delivery and river discharge in glaciated and non-glaciated catchments

5.1.1 Water delivery

There were expected to be fundamental differences in the delivery of water to rivers in glaciated and non-glaciated catchments, reflecting contrasts in the proportions of precipitation which reach the river (e.g. snow and ice melt in glaciated catchments, rain in non-glaciated catchments) and the contrasts in catchment characteristics (e.g. slope, forest cover, and glacier cover) (hypothesis 2).

The Rio Lloncochaigua reacts very quickly to rainfall despite being largely forested, as peat soils found within the catchment are known to encourage rapid runoff (Holden and Burt, 2002), and the small, steep-sided catchment allows water to enter the river quickly. As is evident from Figure 14, large rain storms have a considerable effect on river flows, with the river discharge increasing by 700% over 46 hours (Figure 14) during one storm on 1st May 2018, in which 120 mm of rain fell in 24 hours (Figure 11). This means that there is a much clearer association between rainfall and discharge in this catchment than in the Rio Huemules. In this non-glaciated system, the river discharge typically takes three times longer to fall after a rainfall event than it does to rise, due to water being stored in the soil on the valley sides, which takes time to be released into the river. Therefore, *Daily Fall* patterns in discharge are the most common in every season in the non-glaciated Rio Lloncochaigua catchment (Table 9).

In contrast to the Rio Lloncochigua, discharge in the Rio Huemules doesn't react quickly to precipitation events within the catchment. This may be due to a number of reasons. Firstly, in the colder winter months, this precipitation will mostly fall as snow and remain on the ground and the glacial surfaces until the atmospheric temperature warms sufficiently to allow melting and subsequent release and movement of the water. In the case of snow falling onto the upper surface of the glacier, this could be compressed and remain as ice for many decades. Secondly, in a larger (670 km^2, compared with 107 km^2 for the Rio Lloncochaigua), flatter catchment than the Rio Lloncochaigua, much of the rain falling will have further to travel through the catchment to reach the river. This, together with the slower speed due to the flatter gradient across which it is flowing, will increase the time taken for water to get to the river, and flatten the curve of the hydrograph.

Nienow et al. (1998) used rhodamine dye tracing to study evolution of subglacial discharge pathways through the melt season in Haut Glacier d'Arolla, Switzerland. The study showed that throughout the spring melt, the subglacial drainage system changed from a distributed drainage system with low flow velocities to a channelized system with higher water velocities. This made it more efficient (Hubbard and Nienow, 1997; Gordon et al., 1998; Nienow et al., 1998), and allowed both more water to be evacuated from the subglacial system, and for this water to be evacuated faster than early in the melt season (flow pathways which took 300 minutes to drain in mid-June were draining in 50 minutes by the start of July, Nienow et al., 1998). This efficient drainage system leads to shorter lag times and the discharge responds faster to variations in the air temperature (Elsberg et al., 2001; Chueca et al., 2007; Abermann et al., 2009).

5.1.2 Discharge

Discharge was expected to demonstrate higher peak flows in the glaciated Rio Huemules catchment, as the river is fed by a combination of precipitation and ice melt, whereas in the non-glaciated Rio Lloncochaigua catchment it is reliant on solely rainfall (hypothesis 2).

The higher discharge values recorded in the Rio Huemules (mean: 106.477 $m^3 s^{-1}$, σ: 156.674; Rio Lloncochaigua mean: 27.109 $m^3 s^{-1}$, σ: 23.941), reflect the contribution of glacial melt coupled with rainfall captured across a much larger catchment area (670 km^2, compared with 107 km^2 for the Rio Lloncochaigua). As anticipated, the specific discharge is also five times larger in the Rio Huemules (4.73 m in the Rio Huemules and 0.885 m in the Rio Lloncochaigua, Table 6). This is slightly above the 4.23 m mean observed in glaciated rivers worldwide (Gurnell et al., 1996). Such high specific discharges are common in glaciated catchments (Gurnell et al., 1996; Pepin et al., 2010), and reflect contributions from both precipitation and melt.

Discharge in the non-glaciated Rio Lloncochaigua catchment is reliant on rainfall, and small amounts of groundwater, therefore it has a much lower mean and specific discharge as there is only one main source of water. Higher total cumulative discharge results observed in the glaciated Rio Huemules catchment despite relatively lower rainfall being added into the system (due to regional climatic variations, as discussed in section 2.0) suggests that melting ice through the summer melt season is contributing large volumes of water to the discharge of this river, as hypothesised. The Steffen glacier is in negative mass balance (Figure 5; Rosenbluth et al., 1997; Rasmussen et al., 2007; Lopez et al., 2010; Holmlund and Fuenzalida, 1995; Rigot et al., 2003; Aniya, 2007; Rivera et al., 2007), with elevated levels of summer melt serving to increase the specific discharge. Research by Jansson et al. (2003) and Baraer et al. (2012) showed that glaciers in negative mass balance produce more run-off than those in positive mass balance by liberating extra water which had previously been stored in the ice. During glacial advances, the opposite is true.

The discharge values reported here are expected to have been dampened by the proglacial lake between the Steffen glacier and the site of the river sensors. Studies in China by Yao et al., (2010) found that glacial melt by glacial systems in negative mass balance could affect the volumes of water stored in proglacial lakes, increasing water supply by 60% in this instance which led to an 11% increase in the Chinese lake area (Yao et al., 2010).

5.1.3 Discharge seasonality

In the glaciated Rio Huemules catchment, the discharge was hypothesised to be highest during the summer months when warmer ambient temperatures lead to increased glacial melt feeding the river system, and lowest during the winter months where cooler temperatures lead to decreased glacial melt and precipitation falling as snowfall, rather than rain, and therefore being stored on the glacial surface. In the non-glaciated system however, discharge was predicted to be highest during the winter when there are higher levels of rainfall. Therefore, the seasonal patterns in discharge were expected to be inversed between the two catchments due to the relationship between discharge and the sources of water (hypothesis 3).

Seasonal variations in river discharge are a result of the fluctuations in precipitation as well as the atmospheric temperature which govern whether this precipitation falls as rain or snow throughout the year, as well as the effects of summer glacial melt. The proglacial lake is suggested to have dampened the seasonal variations reported here in the Rio Huemules.

In deglaciated basins, discharge will be higher in winter, when there is increased rainfall, and lower in summer. Rivers fed by seasonal snow will show different annual flow patterns to those fed by glaciers, peaking in late spring- early summer, as the seasonal snow melts earlier in the year than glaciers (Denner et al., 1999). In glaciated catchments however, discharge is energy driven, with glaciers acting as precipitation stores throughout the cold winter, then releasing the precipitation during melting in spring and summer when low albedo ice surfaces are exposed, leading to more melt, coupled with the opening of subglacial and englacial storage to create a highly efficient drainage system (Lang, 1987; Chen and Ohmura, 1990b; Hubbard and Nienow, 1997; Gordon et al., 1998; Denner et al., 1999; Jansson et al., 2003). With the influence of glacial melt from the Steffen Glacier, seasonal differences in discharge, suspended sediment concentration and daily discharge variation are much larger in the glaciated Rio Huemules than the non-glaciated Rio Lloncochaigua.

Rising ambient temperatures from 4.8°C (August mean temperature) to 6.4°C (September mean temperature) at the start of spring (shown in Figure 13) lead to increasing melt in the glaciated Rio Huemules catchment (La Casinière, 1974; Zuzel and Cox, 1975; Elsberg et al., 2001; Hock, 2003; Chueca et al., 2007; Abermann et al., 2009; Konya and Matsumoto, 2010;). Temperatures were typically warmest in the early afternoon, and cool overnight, which is reflected in the *Increasing Diurnal* daily flow patterns in Table 7 which peaked at 18:00 in September (Table 8). Increased ambient temperature throughout the season leads to later peaks in the daily discharge, which increase in amplitude until eventually evolving into two consecutive days showing *Daily Rise* and *Daily Fall* patterns. Research has shown that larger discharge amplitudes in glaciated environments, as observed in the Rio Huemules, suggest a more efficient subglacial drainage system (Nienow et al, 1996 and 1998; Hubbard and Nienow, 1997; Gordon et al., 1998). During the snowmelt period in early spring, the subglacial drainage system comprises of flow through inefficient flow paths (e.g. linked cavities), which leads to long lag times as the water can only travel slowly through this system (Nienow et al, 1996 and 1998; Hubbard and Nienow, 1997; Gordon et al., 1998).

In the non-glaciated Rio Lloncochaigua catchment, spring shows the highest proportion of days showing a *Daily Rise* pattern throughout the year (followed by winter, then autumn and finally summer). This reflects patterns in the rainfall data, in which spring is the season with the highest volume of rainfall and the largest storms. Studies of other non-glacial systems in European rivers by Abrahamsson and Håkanson (1998) also observed the highest seasonal variability during spring.

The summer melt in the Rio Huemules creates a steady base flow over this period. Mean summer air temperatures in the proglacial zone of Steffen Glacier (30m asl elevation) are 10.8°C (σ: 1.181; Table 5). Applying the environmental lapse rate (ELR) to this air temperature data (collected at 10 m asl elevation), suggests that a temperature of zero degrees, and precipitation falling as snow, will likely not occur until elevations above 2,200 m, which are only present on the sides of the highest peak in the catchment, accounting for approximately 2% of the catchment area. To add to this, water storage in the pro-glacial lake causes the river to have a less storm responsive hydrograph than that observed at the de-glaciated Rio Lloncochaigua.

Although more variable than the Rio Huemules, less prolonged rainfall events in the Rio Lloncochaigua during the summer months coupled with the gradual release of small amounts of water from storage on the valley sides creates a lower daily discharge regime during summer in this catchment (25.1 $m^3 s^{-1}$ in summer compared with 29.2 $m^3 s^{-1}$ in winter).

As summer comes to an end in the glaciated Rio Huemules, the mean river discharge is reduced by 25% (from 143 $m^3 s^{-1}$, σ: 83.9, to 88.9 $m^3 s^{-1}$, σ: 179.0). This is due to a reduction in melt, as air temperatures cool and precipitation starts to fall as snow on approximately 60% of the catchment. The snow is stored on the glacier surfaces until the warmer summer melt period. Studies of glacial discharge in the Alps show that glacial elevation (Abermann et al., 2009), air temperature (Elsberg et al., 2001; Chueca et al., 2007; Abermann et al., 2009), albedo (Paul et al., 2005; Abermann et al., 2009), topography of the glacier and surrounding valley (Chueca et al., 2007; Furbish and Andrews, 1984; Abermann et al., 2009), and glacial area (Elsberg et al., 2001; Abermann et al., 2009) will all affect melt rates. As demonstrated in Figures 14 and 15, the amplitude of discharge variation changes through the year in both river catchments. Amplitude was highest in May (autumn) in both catchments. May was a particularly stormy month during the study period in the Rio Lloncochaigua catchment (mean daily rainfall was 13.5 mm, σ: 16.2), and this extra input of water caused the large fluctuations in the river discharge as there was no storage of water in lakes or snowfall during this month. To add to this, the soils on the valley sides were dry following the drier summer months meaning that the water was unable to percolate and flows over the surface which leads to much more efficient transfer of water into the channel. The first flood hydrograph at the start of May shows an increase in discharge from a base flow of 10 $m^3 s^{-1}$ on 1st May 2018 to a peak at 74 $m^3 s^{-1}$ on 2nd May 2018 (see Figure 14), a sevenfold increase in discharge over the 46-hour period. The rainfall required to generate this peak discharge would be 74 m^3 divided by the 107,000,000 m^2 catchment area, which results in a required precipitation rate of 0.415 mm rainfall per minute. Given that the storm on 26th April peaked at 0.36 mm rainfall per minute on two occasions only three hours apart (total rainfall for the whole day was 120 mm; see Figure 11), the rainfall required for an amplitude of this magnitude seems plausible.

Winter in the Rio Huemules experienced cooler ambient temperatures (winter mean: 5.4°C, σ: 1.77; summer mean: 10.8°C, σ: 1.18), leading to reduced melt. This also lowered the hypothetical altitude at which snow would fall from 2,200 m (during summer) to 550 m leading to an estimated 60% of the precipitation falling as snow, as this is the proportion of the catchment area above 550m asl, which was stored throughout winter on the valley sides and surface of the glacier. These factors combine to reduce discharge from a mean of 142.91 $m^3 s^{-1}$ (σ: 83.854) during summer to 88.88 $m^3 s^{-1}$ (σ: 179.036) during winter. This is also reflected in the proportions of different daily flow patterns in the seasonal pie charts in Table 9: proportions of *Daily Rise* and *Daily Fall* days have decreased to 19% and 25% respectively whereas the *Increasing Diurnal, Decreasing Diurnal* and *Irregular* have all increased to 17%, 10% and 21%. Although there is still water movement in the subglacial environment, this may have been reduced by the partial closure of subglacial and englacial water pathways which are typically shut by freezing or englacial deformation (Hock and Hooke, 1993).

Through the middle and late winter, the Rio Lloncochaigua responses to increased precipitation become dampened (Figure 14). Figure 16 shows that despite mean daily rainfall varying year-round by a factor of 10, (2 - 22 mm per day), the discharge doesn't reflect this: only varying by a factor of 3 (varying between 23 and 62 $m^3 s^{-1}$). As shown in Figure 16, the same volume of precipitation falling in summer leads to an increased discharge 10 $m^3 s^{-1}$ larger than the same amount of rainfall falling in the catchment in winter. As the river discharge isn't rising relative to the increased winter precipitation, this suggests that water is being stored somewhere within the catchment. Snowfall observed within the higher reaches of the catchment during the field seasons would suggest that the precipitation is stored on the mountainsides until the start of the spring melt (see Figure 24) though there was unfortunately no way of quantifying this storage.

Figure 24: The Rio Lloncochaigua catchment in winter.

5.2 Investigating variations in the delivery of suspended sediment between glaciated and de-glaciated catchments in summer and winter, and the extent to which this is governed by discharge

5.2.1 Volumes of suspended sediment

The different flow pathways delivering water to rivers in glaciated and non-glaciated catchments were predicted to have an impact on sediment mobilisation and transport, which was expected to differ in glacial and de-glacial catchments, with much higher levels of suspended sediment expected to be discharged by the glaciated River Huemules (hypothesis 3). This difference between the catchments was hypothesised to be due to the relationships between discharge and sediment availability. In the Rio Huemules, the suspended sediment concentration was expected to be high and relatively invariable throughout the year, and the sediment flux was expected to vary proportionally to the discharge (hypothesis 3). Suspended sediment concentrations were expected to be lower in this catchment than other glaciated catchments due to the presence of the proglacial lake, which was anticipated to absorb the heaviest fraction of sediment as the water loses energy (hypothesis 3).

As well as higher cumulative and specific discharge, the data presented above additionally supports the hypothesis that glacial environments also have significantly higher yields of suspended sediment (hypothesis 3), with 487 T km^{-2} y^{-1} calculated to be generated in the Rio Huemules catchment as opposed to 4.95 T km^{-2} y^{-1} in the Rio Lloncochaigua catchment (Table 11, section 4.3.2). The suspended sediment concentrations observed in the Rio Huemules catchments in Table 10, section 4.4.1 (annual mean suspended sediment concentration: 0.081 g L^{-1}, σ: 0.0146) suggest that glaciated Patagonian catchments have high rates of physical erosion in comparison to local non-glaciated catchments, such as the Rio Lloncochaigua. However, it must be noted that relative to other glacial catchments worldwide, the suspended sediment concentrations observed in the Rio Huemules are low, due to the pro-glacial lake.

This further supports common glaciological knowledge that glaciers generate significant amounts of sediment (Gastaldi, 1873; Bonney, 1893; Russell, 1898; Denner et al, 1999, Filippelli, 2002; Riihimaki et al., 2005; Lydersen et al., 2014). This is because the erosive power of the glacier in summer due to increased flow (Perutz, 1947; Collins, 1990) is much larger than the power of rainfall and bank erosion in the Rio Lloncochaigua even in winter. The fine suspended sediment particles observed in the glaciated Rio Huemules leads to its characteristic turbid appearance, and can originate from transport of material in glacier-free areas of the drainage basin (Denner et al., 1999), proglacial, or subglacial sources (the "most important source", according to Warburton, (1990)). Recently-deglaciated systems still have proglacial sediment sources, however drainage basins which have been deglaciated for thousands of years, such as the Rio Lloncochaigua, will show more developed soil structures which are less easily washed into rivers. This is because organic matter deposited into the soil by the woodlands acts as a binding agent (Oades and Waters, 1991), and drying of the soil by plants absorbing water has been shown to increase soil stability (Horn and Dexter, 1989). To add to this, root growth compacts soil (Bui Hui Tri, 1968) as well as linking pore spaces (Beven and Germann, 1982; Angers and Caron, 1998) which increases permeability by creating flow paths through which the water can easily drain into the river.

The suspended sediment yield calculated for the glaciated Rio Huemules in this study is just over half of the yield calculated for the Gornera Glacial river in the European Alps by Collins, (1990) (1,271 tonnes km^2 $year^{-1}$, compared to 617 tonnes km^2 $year^{-1}$ which was observed in the Rio Huemules). This can be explained by the presence of the large (5 km x 1.6 km) proglacial lake at the snout of Steffen glacier (see Figure 3). As the water flushes sediment out of the subglacial environment, it loses speed and therefore energy upon entering the lake and thus is unable to continue to support a high suspended sediment load. Glacial retreat in Norway also lead to the development of proglacial lakes, which were studied by Bogen et al. (2015). The three glaciers in this study: Nigardsbreen, Engabreen and Tunsbergdalsbreen, developed lakes 1.8km, 1.9km and 0.3km long respectively, in which 80%, 84% and 36% of the sediment flux from the glaciers was deposited before entering the rivers (Bogen et al., 2015). This deposition of the courser, heavier fraction of subglacial sediments (Karlen, 1981; Sugden et al., 2009), leads to an artificially low suspended sediment concentration recorded in the suite of sensors downstream. This loss of sediment was anticipated in hypothesis 3, and for this reason suspended sediment fluxes and yields reported in the literature are commonly smaller than for similar glacial catchments in other locations e.g. the Alps (Collins, 1990) which do not have pro-glacial lakes. However, Stevens et al. (2016) noted that subglacial drainage varies laterally along the ice front, therefore the proglacial lake may in fact aid studies of sediment inputs into the Steffen river by averaging out the signal. Despite the proglacial lake, much of the fine fraction continues to be borne by the river to the sensors and sampling site - causing the distinctive 'milky' colouration of the Rio Huemules. The concentrations of suspended sediment observed in the Rio Huemules catchment supports previous research from other glaciated regions (Collins, 1979; Gurnell, 1982; Hodson and Ferguson, 1999; Stevens et al., 2016; Wan et al., 2019) who have noted that glacially modified waters were "more turbid than waters found near the mouth of the fjord" (in Greenland: Stevens et al., 2016).

Comparison of suspended sediment yields reported in this study to the yields calculated in Gurnell et al. (1996), from an average of 90 glaciated rivers worldwide, shows this catchment to generate a slightly below average quantity of sediment: 617 tonnes km^2 year^{-1} compared to 714 tonnes km^2 year^{-1} as a worldwide mean. However, as this result from the Rio Huemules is suggested to be an underestimation, due to loss of sediment in the proglacial lake as discussed above, this similarity to Gurnell et al. (1996) allows conclusions from this study to be drawn upon and used by other studies all over the globe. Figure 20 compares the yields of suspended sediments with the annual mean discharge values for a variety of glaciated and non-glaciated catchments across Chile.

5.2.2 Seasonality of suspended sediment

Suspended sediment concentrations were expected to be high and regular throughout the year in the glaciated Rio Huemules catchment, and the sediment flux was expected to vary as a function of discharge (hypothesis 3). In the other, non-glaciated Rio Lloncochaigua catchment, the relationship between suspended sediment and discharge was expected to be more complicated, as the flux was hypothesised to be dependent on sediment availability as well as discharge. Therefore, in this catchment, the suspended sediment concentration- and subsequently also the flux- was expected to be more variable throughout the year, and significantly lower than the glaciated catchment (hypothesis 3).

During summer, the suspended sediment concentrations observed in the glaciated Rio Huemules fall from 0.1 g L^{-1} (16^{th} January 2017, daily mean, σ: 0.00708) to 0.07 g L^{-1} (22^{nd} February 2017, daily mean, σ: 0.00181) (Figure 18). Although small, this decreasing concentration indicates an exhaustion of the sediment supply as it's not accompanied by falling discharge, however due to the inter-dependent nature of sediment production and transport (Fenn, 1987), the hydrology during this period is important. There are two possible causes of this summer seasonal exhaustion. Firstly, it may suggest that erosion of subglacial material continues throughout the winter months, when the lower levels of discharge (observed in Figure 15) didn't have sufficient energy to transport all of the sediment generated, leading to a build-up until the discharge increased the following summer. This would suggest that in winter, the discharge energy is the limiting factor controlling the suspended sediment concentration, however in summer, the opposite is true and the suspended sediment concentrations are limited by the generation of sediment by sub-glacial erosion (Ostrem, 1975; Hammer and Smith, 1983; Riihimaki et al., 2005). A second factor affecting the exhaustion of suspended sediments is the subglacial hydrological system, which is known to affect both the generation of suspended sediment and the water available to transport it (Hooke, 1989; Riihimaki et al., 2005; Delaney et al., 2018). There are two main types of subglacial drainage systems: distributed (where the water is spread out in multiple small channels), and channelised (where the water is confined to one larger sub-glacial channel, which may be eroded into either the subglacial bedrock or the ice, or a combination), and most subglacial systems have a mixture of the two. The proportions of these found in the subglacial system has a profound impact on both the generation of suspended sediment, and its removal from the system (Fowler 1987; Harbor 1992; Riihimaki et al., 2005; Delaney et al., 2018). When a higher proportion of the drainage system is distributed, the water covers a larger area and therefore has access to greater amounts of sediment. However, as the water is divided into multiple small channels, the velocity is reduced, meaning that it has less energy to transport this sediment. A higher proportion of subglacial water in a channelised draining system however will increase these water velocities, although as the water is contained within fewer channels, it has access to less sediment to erode and transport (Collins, 1979), and also reduces glacial sliding and therefore erosion (Iverson, 1990; 1991; Riihimaki et al., 2005). Research by Rothlisberger and Lang (1987) and Willis et al (1996) suggested that the changing of subglacial hydrological systems from distributed to channelised over the course of the summer may result in the exhaustion of sediment over the course of a summer.

In tandem with a 75% decrease in river discharge at the end of the summer melt period at Steffen Glacier, the suspended sediment concentration in Rio Huemules is also reduced (winter mean suspended sediment concentration: 0.060 g L^{-1}, σ: 0.00413; summer mean suspended sediment concentration: 0.0882 g L^{-1}, σ: 0.00853; Table 10). This suggests that although reduced, the glacier drainage system is still active over winter, sustained by continued melt on the low elevation glacier tongue and rainfall inputs. An active subglacial drainage system suggests that the glacier may still be moving, and thus eroding the subglacial bedrock, which is then exported in the discharge. It also is likely that in both seasons, the lake stores some suspended sediments. Although the glacier continues to move, suggesting that erosion is occurring, and that there are connected subglacial pathways by which the material can be flushed out (as demonstrated in Figure 18), the sediment flux calculations presented in Table 11 emphasise that the erosion and evacuation of sediment from the Rio Huemules in winter is minimal.

5.2.3 Using hysteresis to explore the delivery of suspended sediment

Hysteresis analysis involves plotting the suspended sediment concentration (typically on the Y axis) against the discharge (typically on the X axis) measured within a river for a set period (for example during a storm, or during a daily melt cycle) whilst both discharge and suspended sediment concentration are above baseline values. The graphs display loops, as the discharge and suspended sediment concentration rise and fall relative to one another, which can be clockwise or anticlockwise in direction. Clockwise hysteresis plots mean that the suspended sediment concentration is peaking before the discharge, which suggests a sediment source near the sensor and therefore a very small transport distance. Anticlockwise hysteresis plots, on the other hand, mean that the discharge is peaking before the suspended sediment concentration. This suggests that the source of sediment is far from the sensor, and that the sediment has travelled a greater distance.

The sources of increased river discharge and suspended sediment concentration required to study hysteresis were hypothesised to be different in each river (hypothesis 3). In the glaciated Rio Huemules, hysteresis patterns were expected to be clearer in summer, and follow the daily melt patterns which were predicted to exert a stronger influence on river discharge levels than the storms. In the non-glaciated Rio Lloncochaigua however, hysteresis was expected to be clearer in the winter months when the valley is exposed to large storms (hypothesis 3).

In the glaciated Rio Huemules, the hysteresis was expected to show that the discharge energy was the limiting factor in removing eroded material from the sub-glacial environment, with very tight loops showing that the suspended sediment concentration was the same on rising and falling limbs of the hydrograph (hypothesis 3). This means that a 45˚ angle of the hysteresis plot was expected, as the suspended sediment concentration and discharge were predicted to rise and fall in tandem. In the non-glaciated Rio Lloncochaigua, the quantity of eroded material available for the river to transport was expected to be the factor affecting the suspended sediment concentration observed following storms and thus this was expected to be different on the rising and falling limbs of the hydrograph resulting in open hysteresis plots. Sediment was also hypothesised to be moved from the valley sides into the river channel, and therefore a lag in increasing suspended sediment concentrations was predicted.

Mean lag time between peak rainfall and peak turbidity was 128 hours in the Rio Lloncochaigua (Figure 19), suggesting there was not rapid mobilization of sediment sources near to the river. This is due to the valley sides being covered with vegetation (grass in the valley bottoms and forested slopes), which have been reported to prevent erosion of the underlying soil (Prosser et al., 1995) by decelerating and breaking up the size of the raindrops, therefore reducing their erosive potential (Moss, 1989), as well as binding the soil together with their roots (Coppus and Imeson, 2002). This mirrors early research in similar catchments studying the movement of sediment from the valley sides into the river channel (Macklin and Lewin, 1989; Church and Ryder, 1972; Knox, 1983; Carling, 1986; Harvey, 1986), which concludes that bank erosion typically advances episodically as it relies on rainfall events to provide the water, and therefore the energy, to move the sediment. Episodic removal of sediment from the catchment continues once the sediment is in the river, and research by Church (1983) shows that the most common way eroded material is removed from the catchment is by erosion of the riverbed then deposition of this material in channel bars which are subsequently eroded, and the material is transported and re-deposited further downstream (Church, 1983). Wood (1977) found that small storms without enough energy to exhaust the sediment supply formed hysteresis plots in the form of single lines, as the relationship between suspended sediment concentration and discharge didn't change throughout the storm hydrograph and thus were the same on the rising and falling limbs. That the hysteresis plots formed in the Rio Lloncochaigua show different relationships between discharge and turbidity on the rising and falling limbs of the storm suggests an exhaustion of sediment supplies, as discussed in Mao et al. (2016) and Kelly et al. (2018). However, sediment exhaustion does not seem to occur over multiple storm events in this catchment. Larger storms will generate higher levels of river discharge, and therefore higher erosive energy, for longer periods of time than smaller storms. This leads to greater exhaustion of sediment resources within the catchment, as the increased energy is sufficient to wash out more, or all, of the available sediment. This is presented as more open hysteresis plot forms (Wood, 1977) as discharge values on the falling limb of the hydrograph have much lower suspended sediment concentrations than the equivalent discharge values on the rising limb.

Suspended sediment variations in glacial rivers have been linked to variations in both hydrological regimes and sediment supply (Collins, 1979; Denner et al., 1999; Riihimaki et al., 2005; Mao et al., 2016; Delaney et al., 2018; Kelly et al., 2018). Seasonal differences in the reactions of discharge to precipitation were observed to affect instream suspended sediment concentrations (Denner et al., 1999; Delaney et al., 2018), as the movement of available sediment appeared to be meltwater driven. In the Rio Huemules catchment, the generation of sediment is also closely linked to the movement of the Steffen glacier, which changes according to the atmospheric temperature via its impact on melt generation. This means that the concentration of suspended sediment is closer linked to the temperatures and therefore generation of meltwater and movement of the glacier than to the precipitation.

During a storm at the beginning of February (Figure 21), the rising discharge levels recorded in the Rio Huemules were accompanied by decreasing concentrations of suspended sediment. This dilution caused by the increasing discharge indicates that the water added to the river during this storm was transporting less sediment than already present in the river. This contradicts research by Bezinge et al. (1989), who found high levels of suspended sediment in glacial rivers following winter storms in Val d'Herons, Switzerland, however, it mirrors research in the meltwaters draining temperate Norwegian glaciers by Bogen and Bonsnes (2003), who found that there was rarely a correlation between sediment concentration and water discharge, and that the variations in suspended sediment concentration were in fact closer linked to glacial erosive processes.

Interestingly, in many other glaciated catchments, the literature suggests that it is more common for the discharge to be the factor controlling suspended sediment concentration, as the discharge usually mirrors water velocity, the main factor causing mechanical shear stress and affecting the transport of sediment, and therefore the discharge and suspended sediment concentration will rise and fall simultaneously. This synchronised rise in discharge and suspended sediment concentration suggests that the energy of the water was the limiting factor in removing eroded material from the subglacial environment (Bogen and Bonsnes, 2003; Riihimaki et al., 2005; Delaney et al., 2018), with the largest storms having the greatest energy potential for carrying large volumes of suspended sediment (Warburton, 1990; Bogen and Bosnes, 2003; Kelly et al., 2018). The limited studies of suspended yield in the Andean catchments tend to focus on the northern non-glaciated catchments (for example Guyot, 1993; Aalto et al., 2006; Restrepo et al., 2006a; Molina et al., 2007, 2008; Laraque et al., 2009; Armijos et al., 2013), with the exception of Pépin et al., 2010; whose study of 66 catchments in the Chilean Andes from the far north to the south of Patagonia found that even despite varying levels of glaciation, suspended sediment yield was closely linked to the degree of slope and discharge found within each individual catchment.

The storm hysteresis plot from the Rio Huemules presented in Figure 21 is extremely noisy, which demonstrates the variety in potential suspended sediment source areas as concentrations rise on the falling limb of the hydrograph. The falling limb of the hydrograph shows three pulses of sediment (from discharge values 110 $m^3 s^{-1}$ – 100 $m^3 s^{-1}$, 95 $m^3 s^{-1}$ – 85 $m^3 s^{-1}$ and 85 $m^3 s^{-1}$ - 80 $m^3 s^{-1}$), as the suspended sediment concentrations return to previous concentrations. The discharge falling limb doesn't mirror these pulses, suggesting that the pulses in sediment concentration increase are due to variations in sediment supply. The first pulse likely originates from the nearest source of sediment, as has taken the least amount of time to reach the sensors. In this case, the local valley sides are the closest sediment sources as they are covered with proglacial debris, for example moraines and rock flour, which is very easily transported by overland flow of rainwater and contributes minor amounts of sediment (Warburton, 1990). The second pulse in sediment probably originates from an adjacent valley to the glacier, which is transported to the Rio Huemules by a small tributary. Following this, the final peak in sediment represents the material which has been transported the greatest distance from the furthest reaches of the catchment. There may also be minor amounts of sediment contributed by subglacial material and material from the proglacial lake, which is deposited in the lake due to loss of energy in low flow conditions cannot be mobilised until higher energy conditions are reached, for example after prolonged rainfall events. As the water has had to travel through the glacier from the surface to reach the subglacial environment, before traveling through the subglacial environment and the lake to reach the sensors, this would be part of the last pulse recorded in this hysteresis plot. Stormwater in glaciers can transport sediment englacially (within crevasses, englacial pockets and the englacial drainage network) or subglacially moving material in subglacial cavities, the subglacial drainage network, and in subglacial aquifers in the till of the glacier bed (Jansson et al., 2003; Riihimaki et al., 2005; Delaney et al., 2018). Studies of sediment transport during storm events in Findelengletscher, in the Swiss Alps, by Barrett and Collins (1997) observed turbidity in subglacial water through a borehole. The study discovered that pressure built up as the flow pathway became blocked, leading to a loss in energy and deposition of sediment. However, when the water pressure was sufficient to break the dam holding it back, there would be a sudden increase in water velocity and subsequent remobilization of the sediment. These opening and closing of water pathways can also help to explain pulses of sediment, however in the Rio Huemules these would be unlikely to be observed due to the proglacial lake leading to a drop in energy and therefore sediment deposition before it reaches the sensor.

Low mean summer discharge in the Rio Lloncochaigua (25.06 m^3 s^{-1} in summer, σ: 25.467, compared with 29.16 m^3 s^{-1} in winter, σ: 22.471) is accompanied by higher mean turbidity (1.50 NTU, σ: 2.53, as opposed to 0.659, σ: 0.815, in winter), due to the summer precipitation in this catchment taking the form of short (lasting only a few days), but intense storms. This is very different to the persistent drizzle observed during winter, and results in anti-clockwise hysteresis plots (ie the river discharge peaks before the concentration of suspended sediment), as seen in Figure 23. This suggests that the sediment is travelling a great distance to the river, probably from the higher reaches of the catchment. As seen in Figure 23, this storm deposited a far greater amount of water in the catchment than the accompanying winter storm in Figure 22 (204 mm rain fell in a day, in comparison to 16 mm during the winter storm). In addition to this, the rain was falling on already saturated ground (19/11/2018 total daily rainfall: 18.6 mm; 20/11/2018 total daily rainfall: 29.4mm; 21/11/2018 total daily rainfall: 204 mm). This leads to increased runoff and thus rainfall reaching the river channel faster than had there been dry antecedent conditions (Penna et al., 2011). The steeper angle in this summer plot can be explained by the multiple tributaries in the upper reaches of the river catchment. Rain falling on the valley sides will be transported to the river via this network of tributaries. This movement takes time, however the water from multiple tributaries will all reach the main river at the same time, leading to a rapid increase in discharge at the sensor site.

The river gets nine times more turbid in the summer storm (turbidity increases from 2.5 NTU at the beginning of the storm to 17.5 NTU at the peak of the hysteresis plot, Figure 23), due to the increased discharge having more energy to mobilise greater sources of sediment (summer max turbidity: 17.2 NTU; winter max turbidity: 6.78 NTU). As discharge increased, turbidity experienced a much longer lag time than can be seen during winter storms, only reaching a peak after the discharge has stated to fall. This anticlockwise nature of the hysteresis plot suggests that the saturated soil may result in overland flow dominating flow pathways mobilising sediments from further afield than during the winter storms. Research by Klein (1984) showed that anticlockwise hysteresis plots in a small non-glacial catchment in Yorkshire, England were found when the water and material were travelling a greater distance, whereas clockwise hysteresis plots were observed when the river channel was the only source of sediment.

At the beginning of winter in the non-glaciated Rio Lloncochaigua catchment, June and April have the second and third highest total monthly rainfall in the year. Increased numbers and sizes of rainfall events over these months (see Table 4 and section 4.2) lead to a higher river discharge, and increased daily variations in discharge. The clockwise direction of the hysteresis plot shown in Figure 22, demonstrated by every winter storm in the Rio Lloncochaigua (5 storms identified and analysed), shows the build-up of sediment during the antecedent period and removal of sediment during the August storm. This supports work by Mao et al. (2016) and Kelly et al. (2018) that sediment builds up in river basins during periods of low discharge, then is subsequently exhausted in periods of higher discharge and therefore higher energy. After the end of the previous storm, sediment continued to be transported into the river by smaller rainfall events, delayed runoff, and erosion of banks weakened by saturation. This sediment built up in the river in areas of lower flow, and therefore lower energy, until the rainfall event shown above increased the discharge and therefore the energy levels in the river to a sufficient level at which sediment could be flushed downstream past the sensors. After peak discharge, the energy levels fell in the river, however the sediment source which the river had energy to transport on the rising limb of the hydrograph had been exhausted by the time the river was falling, leading to a lower concentration of suspended sediment on the falling limb of the hydrograph. As discussed in Wood (1977), multiple storms in quick succession will lead to exhaustion of the sediment source, therefore the antecedent conditions to each storm are important to consider.

5.3 Future implications of deglaciation on water and sediment delivery in southern Patagonia

These two catchments were chosen for study due to their contrasting levels of glaciation. The results presented in this thesis are hoped to enable a better understanding of the effects of deglaciation on both water and sediment delivery to the vulnerable Patagonia Fjord ecosystems. Deglaciation is expected to lead to a transition from conditions observed in the currently glaciated Rio Huemules to those seen in the non-glaciated Rio Lloncochaigua, with water delivery expected to become more rapid as precipitation enters the river faster due to a reduction in glacial storage. This will lead to a much flashier hydrological regime. In addition to this, sediment delivery to the rivers is expected to be greatly reduced following the disappearance of the highly erosive glacier.

5.3.1 How will deglaciation affect river discharge?

As was hypothesised (hypothesis 4), and later discussed in the literature review and first chapter, glacial cover within a river catchment affects the hydrological regime of that river in two main ways: firstly, via the proportion of annual precipitation which reaches the river and secondly the seasonal patterns in discharge.

Despite higher levels of precipitation in winter in both catchments, the glaciated Rio Huemules showed lower levels of discharge in this season (Tables 4 and 6), as an estimated 60% of the precipitation fell as snow, and therefore didn't immediately add water to the river as it was stored on the surface of the glacier, supporting research by Jansson et al., 2003; Lawson 1993 and Denner et al., 1999. Retreat of the Steffen glacier can be expected to lead to a reduction in storage of precipitation, and therefore a clearer relationship between precipitation and river discharge, as observed in the non-glaciated Rio Lloncochaigua.

Changes in the storage of precipitation on and within glaciers will lead to changes in seasonal patterns of discharge, as suggested by Tables 6-9. River systems draining glacial catchments typically demonstrate high flow conditions in summer, as presented in the Rio Huemules catchment in Table 7. Intermediate rivers draining areas of seasonal snowpacks were not included in this study, however research by Denner et al. (1999) suggests that peak discharge occurs during spring. Rivers draining non-glaciated catchments, such as the Rio Lloncochaigua, typically experience their highest flow conditions in winter, as shown in Table 8. With the retreat of Steffen glacier as part of Patagonian Icefield shrinkage, the specific discharge of the Rio Huemules will first increase, as a reduction in seasonal snow exposes darker areas of ice whose lower albedo encourages enhanced melt. However, this is unsustainable, and will be followed by a period of decreasing specific discharge in tandem with increased mass loss. Research by Milner et al. (2017) has also suggested that as glaciers retreat, the rivers they feed will become more strongly influenced by precipitation events. This is important because the local ecosystem has evolved to cope with annual cycles in the influxes of water, and the associated decrease in salinity, and therefore upsetting this balance will affect the timings of ecosystem processes.

This study has shown that annual mean discharge and specific discharge are higher in the glaciated Rio Huemules (Figure 15 and Table 8) than the non-glaciated Lloncochaigua, matching other Chilean rivers which are summarized in Figure 17 (Pepin et al, 2010). The Steffen glacier is an important source of water for the Rio Huemules due to melting of the glacier, which releases precipitation stored from previous winters. Research has shown that during glacial retreat, the specific discharge will first increase in response to the increased melting, then decrease as the glacier shrinks and is unable to sustain previously observed mass-loss (Jansson et al., 2003; Milner et al., 2017). This is important because deglaciation will reduce this source of extra water as the glacier disappears. Masiokas et al. (2008) and Pasquini et al. (2008) showed other glaciated river systems in Patagonia to be on the rising curve of water availability. Unfortunately, this study was too short to test this theory in the Rio Huemules, and it would be an interesting area for further research.

5.3.2 How will deglaciation affect suspended sediment concentrations and fluxes?

As was hypothesised, this study agreed with previous research (Embleton and King, 1975; Jansson, 1988; Ferguson, 1984; Warburton, 1990; Harbor and Warburton 1992 and Riihimaki et al., 2005), finding higher concentrations of suspended sediment in the glaciated Rio Huemules (Figures 18 and 19, Table 10) than the Rio Lloncochaigua. This is due to the presence of the Steffen glacier within the catchment, which is a highly active erosional environment. The high concentrations of suspended sediment in the Rio Huemules affect the local ecosystem by transporting nutrients (Kumar et al., 1995), and also by blocking out the light available to benthic marine organisms as well as the deposition covering organisms which live on horizontal surfaces (Lemaire et al., 2002; Loucaide et al., 2008). Therefore, the retreat of this glacier will lead to a reduction of suspended sediment concentrations as is observed in the currently non-glaciated Rio Lloncochaigua. This may also be compounded by the growth of its proglacial lake which traps sediment. This transition from a glaciated to a non-glaciated river catchment has been studied in Iceland by Gilbert et al. (2017). The study found that during periods where a glacier is present in the river catchment, such as the Steffen glacier in the Rio Huemules catchment, sediment was found to be supplied by the glacier. During deglaciation, the sediment supply switches from fresh sediment from the glacier to a re-working of old glacial deposits. This creates a meandering braided river system, and later incision as the river erodes into the landscape to form a single-channel system with exhaustion of the glacial sediment, as observed in the Rio Lloncochaigua catchment today.

As discussed above, deglaciation will also affect the storage of precipitation, leading to a clearer relationship between precipitation and river discharge. This will mean that suspended sediment delivery will be much closer linked to the seasonal patterns in rainfall, rather than temperature.

6.0 Conclusions

Two rivers were studied to enable a comparison between a glaciated and non-glaciated river catchment, and therefore a prediction of how the Rio Huemules and the associated fjord ecosystems may change in the upcoming century as glaciers recede. The data presented in this thesis expands on current research, and widens the study area into the southern hemisphere.

This study aimed to answer four main research questions:

1. **How and why does the quantities and seasonality of precipitation vary between the glaciated and de-glaciated catchments?**

Section 4.1 demonstrated that rainfall patterns are different in the two sites in northern and central Patagonia, concluding that this affected the rivers differently in glaciated and non-glaciated catchments.

Mean rainfall was shown to be higher in the Rio Lloncochaigua catchment, with a greater range, frequently reaching over 50 mm per day (mean: 11.5 mm, σ: 0.158, max: 203.8 mm). In the Rio Huemules, rainfall rarely reached over 40mm per day (mean: 7.0 mm, σ: 10.685, max: 62.2 mm). Despite rain falling on a higher percentage of days in the Rio Huemules catchment (78% of annual days, as opposed to 69% of days in the Lloncochaigua catchment), it was shown that the higher mean rainfall resulted in a far greater input of precipitation into the catchment (total annual rainfall in the Lloncochaigua catchment: 4788 mm; total annual rainfall in the Rio Huemules catchment: 2469 mm). The seasonality of precipitation was also demonstrated, with 55.9% of precipitation in the Rio Huemules catchment falling in winter, and 58.8% of precipitation in the Rio Lloncochaigua catchment.

In keeping with other research in the area (Pickard 1971; Castilla et al., 1993; Forsterra et al., 2005; Aravena et al., 2009), these variations were concluded to be due to the Southern Annular Mode (SAM) causing pressure differences between 40 ˚S and 65 ˚S which leads to zonal winds and thus latitudinal variations in the quantity and seasonality of precipitation.

2. **How and why does the relationship between the differing sources of water feeding into the rivers and their discharge vary seasonally in glaciated and non-glaciated catchments, and how are these seasonal variations comparable between the two study sites?**

Section 5.1 of this thesis examined the relationship between different sources of water feeding into the two rivers and their discharge, comparing variations of this relationship between different seasons in the same catchment, and the same season in both catchments.

The data presented showed that the Rio Lloncochaigua reacts faster to rainfall that the Rio Huemules. This was concluded to be due to the steep valley sides and peaty soil, compared to the Rio Huemules catchment which is much flatter and largely glaciated. This means that there is a much clearer association between rainfall and discharge in the Rio Lloncochaigua catchment than in the Rio Huemules, and that large rain storms observed in the Rio Lloncochaigua catchment have a considerable effect on river flows, with the river discharge increasing by 700% over 46 hours (Figure 14) during one storm on 1st May 2018, in which 120 mm of rain fell in 24 hours (Figure 11). The different specific discharge values were also explored, concluding that this is higher in the Rio Huemules (4.73 m) because the water is sourced from glacial melt and precipitation, whereas in the Rio Lloncochaigua (0.885 m) it is reliant on rainfall and small amounts of groundwater.

Seasonal differences in discharge and the daily flow patterns were examined in both catchments. The same six daily flow patterns were observed in both catchments, the proportions of which varied between seasons and could be used to quantify the activity of each river. In the Rio Huemules catchment, high numbers of *Increasing Diurnal* daily flow patterns in spring represented the onset of the spring melt, whereas in the Rio Lloncochaigua catchment this high proportion of *Increasing Diurnal* were attributed to large numbers of small storms. At the end of summer, the *Daily Fall* pattern was most common in the glaciated catchment, whereas in the Rio Lloncochaigua the most common was

Daily Rise, suggesting the transition into rainy winter weather. Therefore, the seasonal patterns in discharge were concluded to be a result of seasonal patterns in precipitation (in the Rio Lloncochaigua) and ambient temperature (in the Rio Huemules, as it is an energy-driven system).

3. **How does the delivery of suspended sediment vary between glaciated and de-glaciated catchments in summer and winter, and to what extent is this governed by discharge?**

Section 4.3 presented data regarding suspended sediment concentrations and fluxes for the two rivers. The study found that the glaciated Rio Huemules had a higher mean annual suspended sediment concentration (annual mean 0.0811 g L^{-1}, σ: 0.0146; in comparison to 0.00062 g L^{-1}, σ: 0.00037 in the Rio Lloncochaigua). This was concluded to be due to the erosive power of the glacier, particularly during the increased flow conditions in summer (Perutz, 1947; Collins, 1990) which is much larger than the power of rainfall and bank erosion in the Rio Lloncochaigua even in winter. These higher suspended sediment concentrations were shown to lead to significantly higher yields of suspended sediment, with 487 T km^{-2} y^{-1} calculated to be generated in the Rio Huemules catchment as opposed to 5.49 T km^{-2} y^{-1} in the Rio Lloncochaigua catchment (Table 11, section 4.3.2).

The seasonality of suspended sediment concentration was also explored, and showed to be strongly influenced by the seasonality of discharge, with opposing patterns observed in the two catchments. In the Rio Huemules, 75% higher levels of discharge in summer mirrored the increase in suspended sediment concentrations (summer mean suspended sediment concentration: 0.0882 g L^{-1}, σ: 0.00853; winter mean suspended sediment concentration: 0.060 g L^{-1}, σ: 0.00413; Table 10). In the Rio Lloncochaigua however, discharge was higher in winter due to increased precipitation. This was accompanied by a halving in mean turbidity from 1.50 NTU during summer (σ: 2.53) to 0.659 NTU during winter (σ: 0.815) (Table 10), which was attributed to differences in precipitation regimes, with the more persistent winter precipitation causing the river to behave in a much more stable manner than during the summer storms, as demonstrated by the smaller standard deviation values.

Hysteresis analysis was presented to examine the effects of storms in the glaciated Rio Huemules (3 storms) and non-glaciated Rio Lloncochaigua (7 storms). The hysteresis plots from both catchments formed open loops, which was concluded to show an exhaustion of sediment supply. In the Rio Huemules, the stormwater was found to dilute the river, causing a temporary reduction in the suspended sediment concentration, however this was a very noisy relationship, concluded to be a result of the complex nature of sediment movement within this catchment. This was the opposite of the effect in the Rio Lloncochaigua, where both suspended sediment concentration and discharge rose smoothly in response to the rainfall. In the Rio Lloncochaigua catchment, the hysteresis patterns were examined in both summer and winter, revealing that the plots take on different directions and magnitudes in summer (anticlockwise direction, increase in turbidity of 15 NTU, Figure 23) and winter (clockwise direction, increase in turbidity of 1.8 NTU, Figure 22). This was concluded to be due to a difference in storm types, with summer storms being short (lasting only a few days) but very intense, as opposed to winter storms which typically lasted longer but the precipitation was less intense. These differences in precipitation were concluded to enable different sediment mobilization, with the summer storms having sufficient energy to transport sediment a greater distance- probably from the upper reaches of the catchment, whereas in winter, the majority of sediment was sourced from the river channel.

4. What are the implications of these differences in water and sediment delivery in a deglaciating Patagonia?

The implications of differences in water and sediment delivery in a deglaciating Patagonia were discussed in section 5.4.

Despite precipitation levels in both catchments being higher in winter than summer (55.9% of annual precipitation in the Rio Huemules catchment and 58.8% of annual precipitation in the Rio Lloncochaigua catchment fell in winter, as demonstrated in section 4.1), this study has shown the winter river discharge in the Rio Huemules to be lower than summer. Section 5.1 concluded that these lower levels of discharge are due to the winter precipitation falling as snow, which is stored on the surface of the glacier. However, as the glacier has been shown to be retreating, the resultant increased glacial melt is supporting precipitation to create a higher specific discharge (4.73 m) than could be expected without the influence of glacial melt. This study was contextualized with other research to conclude that this specific discharge can be expected to increase in parallel with increasing glacial melt, until this melting becomes unsustainable, at which point it will fall to the levels observed in the Rio Lloncochaigua (0.885 m). Alongside this, the changing of winter precipitation from mainly snowfall to mainly rainfall is concluded to cause a transition in annual flow patterns, as the river discharge moves from an energy driven system, following annual cycles in ambient temperature, to a system closer following the annual precipitation patterns as shown in the Rio Lloncochaigua.

Alongside this, this study concluded that the changes in river discharge patterns can be expected to be accompanied by changes in the volume, concentration, and seasonal variability of suspended sediment export. Section 5.2 concluded that in the present Rio Huemules system, erosion by the Steffen glacier generates a higher volume of suspended sediment than was recorded in the non-glacial Rio Lloncochaigua (Rio Huemules annual sediment flux: 326,608 T y^{-1}, Rio Lloncochaigua annual sediment flux: 587.4 T y^{-1}). The study then concluded that a reduction of the glaciated part of the catchment would result in less glacial erosion and therefore greater influence from hillslope processes resulting in a fall in suspended sediment concentration from current levels (Rio Huemules annual mean suspended sediment concentration: 0.081 g L^{-1}, σ:0.0146) to the levels observed in the Rio Lloncochaigua (annual mean suspended sediment concentration: 0.00062 g L^{-1}, σ: 0.00037). Furthermore, the seasonal variations in suspended sediment concentrations were expected to align much closer with the seasonal patterns in rainfall, rather than temperature, as was observed in the Rio Lloncochaigua (Rio Lloncochaigua summer suspended sediment flux: 257.3 T, winter suspended sediment flux: 272.8 T; Rio Huemules summer suspended sediment flux: 276,591 T, winter suspended sediment flux: 50,017 T).

This study adds an important insight into how glacially-fed rivers may be impacted in the upcoming years due to the predicted reduction in precipitation (Vera et al., 2006) and retreat of many glaciers in Chilean Patagonia (Rivera et al 2002; Rivera 2004; Bown, 2004; Masiokas et al, 2008). The conclusions are of vital importance to local fishermen and ecologists, in order to better prepare for the expected changes. This type of study, comparing glaciated and non-glaciated rivers, is rare, especially in Patagonia. However, the conclusions drawn can be applied to other catchments worldwide.

7.0 Limitations

In this section, the errors associated with the collection and preparation of each dataset will be discussed. It is important to remember that on top of the specifics discussed below, this data was collected during multiple field seasons by multiple team members (as detailed in section 9.1). Whilst the use of one key team member to train all other team members in the methodology attempted to reduce the effects of different teams adhering to slightly different standards, it must be acknowledged that different teams may have used slightly different methodology.

7.1 Rainfall data

A rain gauge must be installed and kept level. If the opening to the funnel is at angle, then that will affect the relative area into which the rain can fall, which will vary with wind direction; and therefore the data (Strangeways, 1996). The area into which rain is collected can also be affected by dents or manufacturing errors in the circumference of the gauge, which must remain highly accurate. Strangeways (1996) calculated that a dent or manufacturing error reducing the area of a 200cm^2 funnel by 0.5mm^2 will reduce the area by 1.25%, with subsequent errors in the rainfall data. Once installed, rain gauges require regular maintenance (Stow and Dirks, 1998) and calibration checks (Strangeways, 1996) however these were reported to rarely have been done especially if the rain gauge is situated in a remote area. None of the rain gauges used in this study were installed by anyone affiliated with the study, and although the gauges in the Rio Lloncochaigua catchment were inspected by the author, the installation and current condition of the gauge used for the Rio Huemules data is unknown. However, the gauges in the Rio Lloncochaigua catchment were found to be in good condition, and as a nationally-managed facility, this is expected to also be the case for the gauges in the Rio Huemules catchment. To add to this, the automated nature of both rain gauges eliminated any possibility of human error in the collection of this dataset post-installation.

Further research (Kurtyka, 1953; Rodda, 1967a; Strangeways, 1996) has also questioned the accuracy of rain gauges, especially under windy conditions, due to the gauge interfering with the flow of air, causing turbulence above the gauge which entrains some of the rain which should have fallen. Studies by Kurtyka in particular demonstrated that increasing wind speed with height resulted in a decrease in rain capture by 5% and 15%, at 30cm and 6m height respectively. To add to this, 20mm over 100 rainfall events is expected to be lost to post-rainfall evaporation.

A study by Stow and Dirks (1998) creating a network of rain gauges found great variability over a $33km^2$ island, concluding that reliance on one rain gauge could underestimate precipitation within a drainage basin by 55%. However, island locations may have more inconstant weather than the sheltered fjords used in this study. The study concluded that “even crude indices of the rainfall climatology are seriously biased if they depend on individual point measurements”. A 1996 study by Strangeways concluded similarly, claiming that “rainfall data from around the world cannot be reliably inter-compared because every design of rain gauge has its own mix and degrees of error.”.

7.2 Discharge

As mentioned above, absorption of rhodamine into suspended sediment, stream bed gravel alluvium sediment and organic matter is a known issue in conditions with high rhodamine concentrations (Sabatini and Austin, 1991; Vasudevan, 2001; Tazioli, 2011). However, this was mitigated in this study by visually estimating the river discharge before calculating a sensible volume of rhodamine to use in order to avoid this issue. Repeat tests were not possible in these catchments, however repeat tests by Tazioli (2011) used the same method as was used within this study to produce results with 5% error.

The rating curves produced in this study examine the relationship between pressure and discharge, then assumes a linear relationship between the two. However, despite this linear relationship being a very good fit with the data (r^2: 0.998, Figure 9), this is an over-simplification of the situation as the banks of the rivers are irregular in their slope angles. This issue was particularly exemplified during one large storm in the Rio Lloncochaigua, when the river flooded over the top of the bank making a journey upstream to inject the rhodamine dye impossibly dangerous and requiring an extrapolation of the ratings curve for those few days to calculate the approximate discharge. The conveyance-slope method of extrapolation (Rantz, 1982) was discounted, as it requires a uniform increase in slope throughout the upper reaches of the river, and this was not the case in the Rio Lloncochaigua. The areal comparison method of calculating peak run-off rates (Rantz, 1982) was also discounted as it requires a comparison with other gauging stations within the catchment, which were not available in this study. The step-backwater method (Rantz, 1982) was deemed to be a possible solution to this issue, converting the water pressure recorded by the CTD to a measurement of above-sensor water height, then modelling the surface area of the surrounding valley which lay below that height and subsequent volume of water which would fill this area to the recorded height. However, the GIS and modelling skills required for these calculations were beyond the scope of this project and thus it was decided not to use this method of extrapolation and instead to simply extend the linear relationship observed in the lower flow part of the ratings curve. However, with an increase in pressure caused by a rise in river levels of only approximately 40cm, the water flooded the whole of the valley floor, and this huge increase in channel width meant that the actual volume of water discharged by the river was disproportionately larger than was estimated using the ratings curve. Had a stage measurement been able to have been taken, this breaching of the flow from the main channel and flowing over the banks in the base of the valley was expected to put a bend in the ratings curve, however, as there was no data to guide the angle at which this high-discharge section of the ratings curve should lie, the amount by which the ratings curve under-estimates discharge is unknown.

7.3 Suspended sediment data

During the installation of the turbidity sensor, an assumption was made that the point of installation would represent a mean turbidity of the whole river. However, the need to mount the sensor onto a metal pole (with holes drilled in the side allowing a throughflow of water, but nevertheless still interfering with the current and thus the energy and ability of the water to carry sediments in suspension) on the end of a fallen tree meant that the sensor was installed in an area of below-average flow and therefore an area of below-average turbidity. To add to this, a sensor without an automatic biofilm removing wiper was installed due to financial restraints, meaning that the sensor had to be removed and wiped clean periodically. This means that the effect of biofilm on the sensor irregularly affects the data collected.

Samples were collected from the river in 5L containers, again assuming that the sampling point represented a mean concentration of suspended sediment, and that it was a regular concentration across the channel. In the lab, the 5L container was shaken to ensure that all of the sediment was in suspension and equally-concentrated before pouring it into the filter stack, however it is inevitable that some sediment remained in the containers (and also the top part of the filter stack) and therefore was not included in the filter weight.

In order to calculate the suspended sediment flux and yield values for the Rio Lloncochaigua catchment, 7 samples from an earlier field season (from 28th January 2018 until 16th February 2018) were added to the 5 remaining suspended sediment samples from the July 2018- April 2019 field season (collected between 4th December 2018 and 28th February 2019). This more than doubles the data available, giving more strength to the resultant mean value calculated, and the collection of the sediment samples over consecutive years reduces the chance of unusual hydrological conditions affecting the data. The suspended sediment samples were collected during a range of hydrological conditions from 17.4- 55.4 m^3 s^{-1}. Although the peaks of the largest storms, probably carrying the largest concentrations of suspended sediment, do lie outside this range, Figure 14 shows that the majority of the river discharge does lie within these boundaries year-round. To add to this, the mean river discharge from the times at which the suspended sediment concentration was measured was similar to the total annual mean discharge (mean discharge during times of suspended sediment sample collection: 39.1 m^3 s^{-1}, σ: 11.1; annual mean discharge: 27.1 m^3 s^{-1}, σ: 23.9) and therefore it was assumed that although the data for this mean suspended sediment concentration was collected solely during the summer, it could also be applied in winter.

8.0 References

1 Aalto, R., Dunne, T., and Guyot, J. L.: Geomorphic controls on Andean denudation rates, J. Geol., 114, 85–99, doi:10.1086/498101, 2006.

2 Abermann, J., Lambrecht, A., Fischer, A. and Kuhn, M., 2009. Quantifying changes and trends in glacier area and volume in the Austrian Ötztal Alps (1969-1997-2006). *The Cryosphere*, *3*(2), pp.205-215.

3 Abrahamsson, O. and Håkanson, L., 1998. Modelling seasonal flow variability of European rivers. Ecological Modelling, 114(1), pp.49-58.

4 Andermann, C., Longuevergne, L., Bonnet, S., Crave, A., Davy, P. and Gloaguen, R., 2012. Impact of transient groundwater storage on the discharge of Himalayan rivers. Nature Geoscience, 5(2), p.127.

5 Anderson, S.P., 2005. Glaciers show direct linkage between erosion rate and chemical weathering fluxes. Geomorphology, 67(1-2), pp.147-157.

6 Anderson, S.P., Drever, J.I and Humphrey, N.F. 1997. Chemical weathering in glacial environments. Geology, v. 25, p. 399-402 doi:10.1130/00917613(1997)025<0399:CWIGE>2.3.CO;2

7 Angers, D.A. and Caron, J., 1998. Plant-induced changes in soil structure: processes and feedbacks. Biogeochemistry, 42(1-2), pp.55-72.

8 Aniya, M. 2007. Glacier variations of Hielo Patagonico Norte, Chile, for 1944/45-2004/05. Bull. Glaciol. Res., 24, 59–70.

9 Antezana, T. 1999. Hydrographic features of Magellan and Fuegian inland passages and adjacent Subantarctic waters. Sci. Mar., 63(Suppl. 1):23-34.

10 Apollonio, S., 1973. Glaciers and nutrients in Arctic seas. Science, 180(4085), pp.491-493.

11 Aravena, J.C. and Luckman, B.H., 2009. Spatio-temporal rainfall patterns in southern South America. International Journal of Climatology: A Journal of the Royal Meteorological Society, 29(14), pp.2106-2120.

12 Armijos, E., Crave, A., Vauchel, P., Fraizy, P., Santini, W., Moquet, J., Arevalo, N., Carranza, J., and Guyot, J. L.: Suspended sediment dynamics in the Amazon River of Peru, J. S. Am. Earth Sci., 44, 75–84, doi:10.1016/j.jsames.2012.09.002, 2013.

13 Ayes Rivera, I., Callau Poduje, A.C., Molina-Carpio, J., Ayala, J.M., Armijos Cardenas, E., Espinoza-Villar, R., Espinoza, J.C., Gutierrez-Cori, O. and Filizola, N., 2019. On the Relationship between Suspended Sediment Concentration, Rainfall Variability and Groundwater: An Empirical and Probabilistic Analysis for the Andean Beni River, Bolivia (2003–2016). Water, 11(12), p.2497.

14 Baraer, M., Mark, B.G., McKENZIE, J.M., Condom, T., Bury, J., Huh, K.I., Portocarrero, C., Gómez, J. and Rathay, S., 2012. Glacier recession and water resources in Peru's Cordillera Blanca. *Journal of Glaciology*, *58*(207), pp.134-150.

15 Barrett, A.P. and Collins, D.N., 1997. Interaction between water pressure in the basal drainage system and discharge from an Alpine glacier before and during a rainfall-induced subglacial hydrological event. Annals of Glaciology, 24, pp.288-292.

16 Bartholomew, I., Nienow, P., Mair, D., Hubbard, A., King, M.A. and Sole, A., 2010. Seasonal evolution of subglacial drainage and acceleration in a Greenland outlet glacier. Nature Geoscience, 3(6), p.408.

17 Behrens, H., Lo¨schhorn, U., Ambach, W., Moser, O., 1976. Studie zum Schmelzwasserabfluss aus dem Akkumulationsgebiet eines Alpengletschers (Hintereisferner, tztaler Alpen). II. Mitteilung. Z. Gletscherkd. Glazialgeol. 12 (1), 69–74.

18 Behrens, H., Oerter, H., Reinwarth, O., 1982. Results from tracer experiments with fluorescent dyes on Vernagtferner (Oetztal Alps, Austria) from 1974 to 1982. Z. Gletscherkd. Glazialgeol. 12 (1), 219–228.

19 Beven, K. and Germann, P., 1982. Macropores and water flow in soils. Water resources research, 18(5), pp.1311-1325.

20 Bezinge, A., Clark, M.J., Gurnell, A.M. and Warburton, J., 1989. The management of sediment transported by glacial melt-water streams and its significance for the estimation of sediment yield. Annals of Glaciology, 13, pp.1-5.

21 Bjerklie, D.M., Birkett, C.M., Jones, J.W., Carabajal, C., Rover, J.A., Fulton, J.W. and Garambois, P.A., 2018. Satellite remote sensing estimation of river discharge: Application to the Yukon River Alaska. Journal of Hydrology, 561, pp.1000-1018.

22 Bogen, J. 1995: Sediment transport and deposition in mountain rivers. In I. D. L. Foster et al. (eds.): Sediment and water quality in river catchments. Pp. 437–451. New York: Wiley & Sons.

23 Bogen, J. 1996: Erosion and sediment yield in Norwegian rivers. In D. E. Walling & B. W. Webb (eds.): Erosion and sediment yield: global and regional perspectives. IAHS Publ. 236. Pp 73–84. Wallingford, UK: International Association of Hydrological Sciences.

24 Bogen, J. and Bønsnes, T.E., 2003. Erosion and sediment transport in High Arctic rivers, Svalbard. *Polar Research*, *22*(2), pp.175-189.

25 Bogen, J., Xu, M. and Kennie, P., 2015. The impact of pro-glacial lakes on downstream sediment delivery in Norway. *Earth Surface Processes and Landforms*, *40*(7), pp.942-952.

26 Bonney, T.G., 1893. Do glaciers excavate?. The Geographical Journal, 1(6), pp.481-499.

27 Bown, F., 2004. Cambios climáticos en la Región de Los Lagos y respuestas recientes del Glaciar Casa Pangue (41°08’S). MSc Thesis, Universidad de Chile, Santiago, pp. 131.

28 Brattström H, Johanssen A (1983) Ecological and regional zoogeography of the marine benthic fauna of Chile. Sarsia 68:289–339

29 Brooks, C.F., 1923. The Ice Sheet of Central Greenland: A Review of the Work of the Swiss Greenland Expedition.

30 Bull, L.J., 1997. Magnitude and variation in the contribution of bank erosion to the suspended sediment load of the River Severn, UK. Earth Surface Processes and Landforms: the Journal of the British Geomorphological Group, 22(12), pp.1109-1123.

31 Calvete, C., and M. Sobarzo. 2011. Quantification of the surface brackish water layer and frontal zones in southern Chilean fjords between Boca del Guafo (43◦ 30 S) and Estero Elefantes (46◦ 30S). Continental Shelf Research. 31: 162–171.

32 Camus PA (2001) Marine biogeography of continental Chile. Rev Chil Hist Nat 74:587–617

33 Cape, M.R., Straneo, F., Beaird, N., Bundy, R.M. and Charette, M.A., 2019. Nutrient release to oceans from buoyancy-driven upwelling at Greenland tidewater glaciers. Nature Geoscience, 12(1), p.34.

34 Carling, P. A. 1986. 'The Noon Hill flash floods; July 17th 1983. Hydrological and geomorphological aspects of a major formative event in an upland landscape', Transactions, Institute of British Geographers, 11, 105-118.

35 Carrasco, J., G. Casassa, and A. Rivera, 2002: Meteorological and climatological aspects of the Southern Patagonia Ice Cap. The Patagonian Icefields: A Unique Natural Laboratory for Environmental and Climate Change Studies, G. Casassa, F. V. Sepu´lveda, and R. M. Sinclair, Eds., Kluwer Academic, 29–41.

36 Castilla JC, Navarrete SA, Lubchenco J (1993) Southeastern Pacific coastal environments: main features, large-scale perturbations, and global climate change. In: Mooney HA, Fuentes ER, Kronberg BI (eds) Earth System Responses to Global Change: Contrasts between North and South America. Academic Press, pp 167-188

37 Castillo, M.I., O. Pizarro, U. Cifuentes, N. Ramirez, and L. Djurfeldt. 2012. Subtidal dynamics in a deep fjord of southern Chile. Continental Shelf Research. 49: 73–89.

38 Chauche, N., Hubbard, A., Gascard, J.-C., Box, J.E, Bates, R., Koppes, M., Sole, A., Christoffersen, P., and Pattern, H. 2014. "Ice-ocean interaction and calving front morphology at two west Greenland tidewater outlet glaciers" The Cryosphere, 8, 1457-1478

39 Chen, J., Ohmura, A., 1990. Estimation of Alpine glacier water resources and their change since the 1870s. In: Hydrology in Mountainous areas. I. Hydrological Measurements; The Water Cycle. Proceedings of the two Lausanne Symposia, August 1990. IAHS Publ. 193, pp. 127–135.

40 Chen, J., Ohmura, A., 1990. On the influence of Alpine glaciers on runoff. In: Hydrology in Mountainous areas. I. Hydrological Measurements; The Water Cycle. Proceedings of the two Lausanne Symposia, August 1990. IAHS Publ. 193, pp. 117–125.

41 Chueca, J., Julián, A. and López-Moreno, J.I., 2007. Recent evolution (1981–2005) of the Maladeta glaciers, Pyrenees, Spain: extent and volume losses and their relation with climatic and topographic factors. *Journal of glaciology*, *53*(183), pp.547-557.

42 Church, M and Ryder, J.M., 1972. 'Paraglacial sedimentation: a consideration of fluvial processes conditioned by glaciation'. Bulletin geological society of America, 83**,** 3059- 3072.

43 Church, M. 1983. 'Patterns of instability in a wandering gravel bed channel', in Collinson, J. D. and Lewin, J. (Eds), Modern and Ancient Fluvial Systems. International Association of Sedimentologists Special publication, 6, 169-180.

44 Clark, O.R., 1940. Interception of rainfall by prairie grasses, weeds, and certain crop plants. Ecological monographs, 10(2), pp.243-277.

45 Colgan, W., Rajaram, H., Anderson, R., Steffen, K., Phillips, T., Joughin, I., Zwally, H.J. and Abdalati, W., 2011. The annual glaciohydrology cycle in the ablation zone of the Greenland ice sheet: Part 1. Hydrology model. Journal of Glaciology, 57(204), pp.697-709.

46 Collins, D.N., 1979. Sediment concentration in melt waters as an indicator of erosion processes beneath an Alpine glacier. Journal of Glaciology, 23(89), pp.247-257.

47 Collins, D.N., 1989. 'Seasonal development of subglacial drainage and suspended sediment delivery to melt waters beneath an Alpine glacier', *Ann. Glaciol.,* **13**, 45- 50.

48 Collins, D.N., 1990. Seasonal and annual variations of suspended sediment transport in meltwaters draining from an Alpine glacier. *IAHS Publ*, *193*, pp.439-446.

49 Conley, D. J. 1997. Riverine contribution of biogenic silica to the oceanic silica budget. Limnol. Oceanogr. 42: 774–777.

50 Conley, D. J. 2002. Terrestrial ecosystems and the global biogeochemical silica cycle. Glob. Biogeochem. Cycles 16: 1121, doi:10.1029/2002GB001894

51 Coppus, R. and Imeson, A.C., 2002. Extreme events controlling erosion and sediment transport in a semi-arid sub-Andean valley. Earth Surface Processes and Landforms: The Journal of the British Geomorphological Research Group, 27(13), pp.1365-1375.

52 D´avila, P.M., D. Figueroa, and E. M¨uller. 2002. Freshwater input into the coastal ocean and its relation with the salinity distribution off austral Chile (35–55◦S). Continental Shelf Research. 22: 521–534.

53 Dai, S.B., Yang, S.L. and Li, M., 2009. The sharp decrease in suspended sediment supply from China's rivers to the sea: anthropogenic and natural causes. *Hydrological Sciences Journal*, *54*(1), pp.135-146.

54 Dasilva, J. L., 1995. "Seismic facies investigation and late quaternary glacial history of the Chilean shelf and fjords and Antarctic shelf and fjords" MA thesis, Rice University, Houston, Texas.

55 Delaney, I., Bauder, A., Werder, M.A. and Farinotti, D., 2018. Regional and annual variability in subglacial sediment transport by water for two glaciers in the Swiss Alps. *Frontiers in Earth Science*, *6*, p.175.

56 Denner, J.C., Lawson, D.E., Larson, G.J., Evenson, E.B., Alley, R.B., Strasser, J.C. and Kopczynski, S., 1999. Seasonal variability in hydrologic-system response to intense rain events, Matanuska Glacier, Alaska, USA. Annals of Glaciology, 28, pp.267-271.

57 Derry, L. A., Kurtz, A. C., Ziegler, K., and Chadwick, O. A. 2005. Biological control of terrestrial silica cycling and export fluxes to watersheds. Nature 433: 728–731.

58 Dincer, T. (1967). Application of radiotracer methods in streamflow measurements. International Atomic Energy Agency (IAEA): IAEA.

59 Dove, P. M., AND S. F. ELSTON. 1992. Dissolution kinetics of quartz in sodium-chloride solutions—analysis of existing data and a rate model for 25uC. Geochim. Cosmochim. Acta 56: 4147–4156.

60 Dove, P.M., and Crerar, D. A. 1990. Kinetics of quartz dissolution in electrolyte solutions using a hydrothermal mixed flow reactor. Geochim. Cosmochim. Acta 54: 955–969.

61 Dunbar, M.J., 1973. Glaciers and nutrients in Arctic fiords. Science, 182(4110), pp.398-398.

62 Dussaillant, A., Benito, G., Buytaert, W., Carling, P., Meier, C. and Espinoza, F., 2010. Repeated glacial-lake outburst floods in Patagonia: an increasing hazard?. Natural hazards, 54(2), pp.469-481.

63 Eads, J.B., 1878. Improvement of the St John's river (Florida). Van Nostrand's Eclectic Engineering Magazine (1869-1879), 114(18), p.489.

64 Ellis, W.R., 1967. A review of radioisotope methods of stream gauging.

65 Elsberg, D. H., Harrison, W. D., Echelmeyer, K. A., and Krimmel, R. M.: Quantifying the effects of climate and surface change on glacier mass balance, J. Glaciol., 47, 649–658, 2001.

66 Embleton, C. and King, C.A.M., 1975. Glacial and periglacial geomorphology.

67 Escher-Vetter, H., Reinwarth, O., 1994. Two decades of runoff measurements (1974 to 1993) at the pegestation Vernagtbach/ Oetztal Alps. Z. Gletscherkd. Glazialgeol. 30, 53–98.

68 Fenn, C.R., 1987. 'Sediment transfer processes in Alpine glacier basins' in Gurnell, A.M., and Clarke, M.J., (Eds), *Glacio-fluvial sediment transfer: an alpine perspective.* Wiley, Chichester. Pp. 59-85.

69 Ferguson, R.I., 1984. Sediment load of the Hunza River. The International Karakoram Project, 2, pp.581-598.

70 Fernández, M., Jaramillo, E., Marquet, P.A., Moreno, C.A., Navarrete, S.A., Ojeda, F.P., Valdovinos, C.R. and Vasquez, J.A., 2000. Diversity, dynamics and biogeography of Chilean benthic nearshore ecosystems: an overview and guidelines for conservation.

71 Fernandez, R. A., J. B. Anderson, J. S. Wellner, and B. Hallet (2011), Timescale dependence of glacial erosion rates: A case study of Marinelli Glacier, Cordillera Darwin, southern Patagonia, J. Geophys. Res., 116, F01020, doi:10.1029/2010JF001685.

72 Filippelli, G.M., 2002. The global phosphorus cycle. *Reviews in mineralogy and geochemistry*, *48*(1), pp.391-425.

73 Florkowski, T., Davis, T.G., Wallander, B. and Prabhakar, D.R.L., 1969. The measurement of high discharges in turbulent rivers using tritium tracer. Journal of Hydrology, 8(3), pp.249-264.

74 Försterra, G., Beuck, L., Häussermann, V. and Freiwald, A., 2005. Shallow-water Desmophyllum dianthus (Scleractinia) from Chile: characteristics of the biocoenoses, the bioeroding community, heterotrophic interactions and (paleo)-bathymetric implications. In Cold-water corals and ecosystems (pp. 937-977). Springer, Berlin, Heidelberg.

75 Fountain, A.G., 1989. The storage of water in, and hydraulic characteristics of, the firn of South Cascade Glacier, Washington State, USA. Ann. Glaciol. 13, 69–75.

76 Fountain, A.G., Tangborn, W.V., 1985. The effect of glaciers on streamflow variations. Water Res. Res. 21 (4), 579–586.

77 Fowler, A.C., 1987. 'Sliding with cavity formation.' *J. Glaciol.,* **33**, 255- 267.

78 Furbish, D.J. and Andrews, J.T., 1984. The use of hypsometry to indicate long-term stability and response of valley glaciers to changes in mass transfer. *Journal of glaciology*, *30*(105), pp.199-211.

79 Garreaud, R., Lopez, P., Minvielle, M. and Rojas, M., 2013. Large-scale control on the Patagonian climate. Journal of Climate, 26(1), pp.215-230.

80 Gastaldi, S.B., 1873. On the effects of glacier-erosion in Alpine valleys. Quarterly Journal of the Geological Society, 29(1-2), pp.396-401.

81 Ghose, D.K. and Samantaray, S., 2019. Sedimentation Process and Its Assessment Through Integrated Sensor Networks and Machine Learning Process. In Computational Intelligence in Sensor Networks (pp. 473-488). Springer, Berlin, Heidelberg.

82 Gillett, N.P. and Thompson, D.W., 2003. Simulation of recent Southern Hemisphere climate change. Science, 302(5643), pp.273-275.

83 Gonz´alez, H.E., L. Castro, G. Daneri, J.L. Iriarte, N. Silva, C.A. Vargas, R. Giesecke, and N. S´anchez. 2011. Seasonal plankton variability in Chilean Patagonia fjords: Carbon flow through the pelagic food web of Aysen Fjord and plankton dynamics in the Moraleda Channel basin. Continental Shelf Research. 31: 225– 243.

84 Gordon, S., Sharp, M., Hubbard, B., Smart, C., Ketterling, B. and Willis, I., 1998. Seasonal reorganization of subglacial drainage inferred from measurements in boreholes. *Hydrological Processes*, *12*(1), pp.105-133.

85 Gurnell, A., Hannah, D. and Lawler, D., 1996. Suspended sediment yield from glacier basins. IAHS Publications-Series of Proceedings and Reports-Intern Assoc Hydrological Sciences, 236, pp.97-104.

86 Gurnell, A.M., 1982. The dynamics of suspended sediment concentration in an Alpine pro-glacial stream network. Hydrological Aspects of Alpine and High Mountain Areas, 138, pp.319-330.

87 Guyot, J. L.: Hydrogéochimie des fleuves de l'Amazonie bolivienne, ORSTOM, Paris, France, 261 pp., 1993.

88 Guzm´an, D., and N. Silva. 2002. Physical and chemical characterization and water masses of the southern channels of Chile between Boca del Guafo and Golfo Elefantes (Cimar Fiordo 4 Cruise). Ciencia y Tecnolog´ıa del Mar. 25(2): 45–76.

89 Hammer, K.M., and Smith, N.D., 1983. 'Sediment production and transport in a proglacial stream: Hilda Glacier, Alberta, Canada', *Boreas,* **12**, 91-106.

90 Harbor, J.M., 1992. 'Application of a general sliding law to simulate flow in a glacier cross-section', *J. Glaciol.,* **38**, 182- 190.

91 Harbor, J.O.N. and Warburton, J., 1992. Glaciation and denudation rates. Nature, 356(6372), pp.751-751.

92 Harrison, S., Glasser, N., Winchester, V., Haresign, E., Warren, C. and Jansson, K., 2006. A glacial lake outburst flood associated with recent mountain glacier retreat, Patagonian Andes. The Holocene, 16(4), pp.611-620.

93 Hart, J.K., 1995. Subglacial erosion, deposition and deformation associated with deformable beds. Progress in Physical Geography, 19(2), pp.173-191.

94 Harvey, A. M. 1986. 'Geomorphic effects of a 100 year storm in the Howgill Fells, Northwest England', Zeitschrijl fur Geomorphologie, 30, 71-91

95 Hasnain, S.I. and Chauhan, D.S., 1993. Sediment transfer in the glaciofluvial environment—a Himalayan perspective. Environmental Geology, 22(3), pp.205-211.

96 Hasnain, S.I., 1996. Factors controlling suspended sediment transport in Himalayan glacier meltwaters. Journal of hydrology, 181(1-4), pp.49-62.

97 Häussermann, V. and Försterra, G., 2005. Distribution patterns of Chilean shallow-water sea anemones (Cnidaria: Anthozoa: Actiniaria, Corallimorpharia); with a discussion of the taxonomic and zoogeographic relationships between the actinofauna of the South East Pacific, the South West Atlantic and the Antarctic. Scientia Marina, 69(S2), pp.91-102.

98 Häussermann, V. and Försterra, G., 2007. Extraordinary abundance of hydrocorals (Cnidaria, Hydrozoa, Stylasteridae) in shallow water of the Patagonian fjord region. Polar Biology, 30(4), pp.487-492.

99 Häussermann, V., 2006. Biodiversity of Chilean sea anemones (Cnidaria: Anthozoa): distribution patterns and zoogeographic implications, including new records for the fjord region. Latin American Journal of Aquatic Research, 34(2), pp.23-35.

100 Hawkings, J.R., Wadham, J.L., Tranter, M., Lawson, E., Sole, A., Cowton, T., Tedstone, A.J., Bartholomew, I., Nienow, P., Chandler, D. and Telling, J., 2015. The effect of warming climate on nutrient and solute export from the Greenland Ice Sheet. Geochem. Perspect. Lett, 1, pp.94-104.

101 Haylock, M.R., Peterson, T.C., Alves, L.M., Ambrizzi, T., Anunciação, Y.M.T., Baez, J., Barros, V.R., Berlato, M.A., Bidegain, M., Coronel, G. and Corradi, V., 2006. Trends in total and extreme South American rainfall in 1960–2000 and links with sea surface temperature. Journal of climate, 19(8), pp.1490-1512.

102 Hicks, D.M., Gomez, B. and Trustrum, N.A., 2000. Erosion thresholds and suspended sediment yields, Waipaoa River basin, New Zealand. *Water Resources Research*, *36*(4), pp.1129-1142.

103 Hindshaw, R.S., Rickli, J., Leuthold, J., Wadham, J., Bourdon, B. 2014. Identifying weathering sources and processes in an outlet glacier of the Greenland Ice Sheet using Ca and Sr isotope ratios. Geochimica et Cosmochimica Acta 145 50-71

104 Hock, R. 2003. Temperature index modelling in mountain areas, J. Hydrol., 282, 104 – 115.

105 Hock, R. and R.LeB. Hooke. 1993. Evolution of the internal drainage system in the lower part of the ablation area of Storglacia¨ren, Sweden. Geol. Soc. Am. Bull., 105(4), 537–546.

106 Hodson, A.J. and Ferguson, R.I., 1999. Fluvial suspended sediment transport from cold and warm-based glaciers in Svalbard. Earth Surface Processes and Landforms, 24(11), pp.957-974.

107 Hodson, A.J., Mumford, P.N., Kohler, J. and Wynn, P.M., 2005. The High Arctic glacial ecosystem: new insights from nutrient budgets. Biogeochemistry, 72(2), pp.233-256.

108 Holden, J. and Burt, T.P., 2002. Infiltration, runoff and sediment production in blanket peat catchments: implications of field rainfall simulation experiments. *Hydrological Processes*, *16*(13), pp.2537-2557.

109 Holmlund, P., and H. Fuenzalida, 1995: Anomalous glacier responses to 20th century climatic changes in the Darwin Cordillera, southern Chile. J. Glaciol., 41, 465–473.

110 Hood, E., Fellman, J., Spencer, R.G., Hernes, P.J., Edwards, R., D'Amore, D. and Scott, D., 2009. Glaciers as a source of ancient and labile organic matter to the marine environment. Nature, 462(7276), p.1044.

111 Hooke, R. Le B. 1989. 'Englacial and subglacial hydrology: a qualitative review' *Arctic Alpine Res*., **21,** 221-233.

112 Hopkinson, C., Young, G.J., 1998. The effect of glacier wastage on the flow of the Bow River at Banff, Alberta, 1951–1993. Hydrol. Proc. 12 (10/11), 1745–1762.

113 Horn, R. and Dexter, A.R., 1989. Dynamics of soil aggregation in an irrigated desert loess. Soil and Tillage Research, 13(3), pp.253-266.

114 Horowitz, A.J., 2003. An evaluation of sediment rating curves for estimating suspended sediment concentrations for subsequent flux calculations. Hydrological processes, 17(17), pp.3387-3409.

115 Hubbard, B. and Nienow, P., 1997. Alpine subglacial hydrology. *Quaternary Science Reviews*, *16*(9), pp.939-955.

116 Hurd, D.C., 1977. The effect of glacial weathering on the silica budget of Antarctic waters. Geochimica et Cosmochimica Acta, 41(9), pp.1213-1222.

117 IPCC (Intergovernmental Panel on Climate Change) (2001): The Scientific Basis. Contribution to the Working Group I to the Third Assessment Report of the Intergovernmental Panel on Climate Change, Cambridge University Press, Cambridge, UK

118 IPCC (Intergovernmental Panel on Climate Change) (2014): The Scientific Basis. Contribution to the Working Group I to the fifth Assessment Report of the Intergovernmental Panel on Climate Change, Cambridge University Press, Cambridge, UK

119 Iriarte, J.L., González, H.E. and Nahuelhual, L., 2010. Patagonian fjord ecosystems in southern Chile as a highly vulnerable region: problems and needs. Ambio, 39(7), pp.463-466.

120 Iverson, N.R., 1990. 'Laboratory simulations of glacial abrasion: comparisons with theory', *J. Glaciol.* **36**, 304- 314.

121 Iverson, N.R., 1991. 'Potential effects of sub-glacial water-pressure fluctuations on quarrying', *J. Glaciol.,* **37** 27-36.

122 Jansson, M.B., 1988. A global survey of sediment yield. Geografiska Annaler: Series A, Physical Geography, 70(1-2), pp.81-98.

123 Jansson, P., Hock, R. and Schneider, T., 2003. The concept of glacier storage: a review. Journal of Hydrology, 282(1-4), pp.116-129.Masiokas, M.H., Villalba, R., Luckman, B.H., Lascano, M.E., Delgado, S., Stepanek, P. (2008) "20th century glacier recession and regional hydroclimatic changes in north western Patagonia" Global and planetary change 60 85-100.

124 Karlén, W., 1981. Lacustrine sediment studies: a technique to obtain a continous record of Holocene glacier variations. Geografiska Annaler: Series A, Physical Geography, 63(3-4), pp.273-281.

125 Kasser, P., 1973. Influence of changes in the glacierized area on summer run-off in the Porte du Scex drainage basin of the Rhne. In: Symposium on the Hydrology of Glaciers. Cambridge, 7–13 September 1969. IAHS Publ. No. 95, pp. 221–225.

126 Kelly, P.T., Vanni, M.J. and Renwick, W.H., 2018. Assessing uncertainty in annual nitrogen, phosphorus, and suspended sediment load estimates in three agricultural streams using a 21-year dataset. Environmental monitoring and assessment, 190(2), p.91.

127 Kitchener, B.G., Wainwright, J. and Parsons, A.J., 2017. A review of the principles of turbidity measurement. *Progress in Physical Geography*, *41*(5), pp.620-642.

128 Klein, M., 1984. Anti clockwise hysteresis in suspended sediment concentration during individual storms: Holbeck Catchment; Yorkshire, England. *Catena*, *11*(2-3), pp.251-257.

129 Knox, J. C. 1983. 'Responses of river systems to Holocene climates', in Wright, H. E. Jr. (Ed.), Late Quaternary Environments of the United States, University of Minnesota Press, Minneapolis, 2M1.

130 Kohler, J., 1995. Determining the extent of pressurized flow beneath Storglacia¨ren, Sweden, using results of tracer experiments and measurements of input and output discharge. J. Glaciol. 41 (138), 217–231.

131 Konya, K. and Matsumoto, T., 2010. Influence of weather conditions and spatial variability on glacier surface melt in Chilean Patagonia. Theoretical and applied climatology, 102(1-2), pp.139-149.

132 Kumar, N., Anderson, R.F., Mortlock, R.A., Froelich, P.N., Kubik, P., Dittrich-Hannen, B. and Suter, M., 1995. Increased biological productivity and export production in the glacial Southern Ocean. Nature, 378(6558), p.675.

133 Kushner, P.J., Held, I.M. and Delworth, T.L., 2001. Southern Hemisphere atmospheric circulation response to global warming. Journal of Climate, 14(10), pp.2238-2249.

134 La Casinie`re de, A. C. (1974), Heat exchange over a melting snow surface, J. Glaciol., 13(67), 55 – 72.

135 Lancellotti DA, Vásquez JA (1999) Biogeographical patterns of benthic macroinvertebrates in the south-eastern Pacific littoral. J Biogeogr 26:1001–1006

136 Lang, H., 1987. Forecasting meltwater runoff from snow-covered areas and from glacier basins. In: Kraijenhoff, D.A., Moll, J.R. (Eds.), River Flow Modelling and Forecasting, Reidel, Dordrecht, pp. 99–127.

137 Lang, H., Scha¨dler, B., Davidson, G., 1977. Hydroglaciological investigations on the Ewigschneefeld. Gr. Aletschgletscher. Z. Gletscherkd. Glazialg. 12 (2), 119–124.

138 Laraque, A., Bernal, C., Bourrel, L., Darrozes, J., Christophoul, F., Armijos, E., Fraizy, P., Pombosa, R., and Guyot, J. L.: Sediment budget of the Napo River, Amazon basin, Ecuador and Peru, Hydrol. Process., 23, 3509–3524, doi:10.1002/hyp.7463, 2009.

139 Lawson, D.E. (1993) Glaciohydrologic and glaciohydraulic effects on runoff and sediment yield in glacierized basins. CRREL Monogr. 93-02

140 Lefrançois, J., Grimaldi, C., Gascuel-Odoux, C. and Gilliet, N., 2007. Suspended sediment and discharge relationships to identify bank degradation as a main sediment source on small agricultural catchments. Hydrological Processes: An International Journal, 21(21), pp.2923-2933.

141 Lemaire, E., Abril, G., De Wit, R., and Etcheber, H. (2002). Distribution of phytoplankton pigments in nine European estuaries and implications for an estuarine typology. Biogeochemistry 59: 5–23.

142 Lliboutry, L., 1998. Glaciers of Chile and Argentina. In: Williams, R.S., Ferrigno, J.G. (Eds.), Satellite Image Atlas of Glaciers of the World: South America. USGS Professional Paper 1386-I, Online version 1.02.

143 Lopez, P., P. Chevallier, V. Favier, B. Pouyaud, F. Ordenes, and J. Oerlemans, 2010: A regional view of fluctuations in glacier length in southern South America. Global Planet. Change, 71, 85–108.

144 Loriaux, T. and Casassa, G., 2013. Evolution of glacial lakes from the Northern Patagonia Icefield and terrestrial water storage in a sea-level rise context. Global and Planetary Change, 102, pp.33-40.

145 Loucaides, S., Cappelle, P.V. and Behrends, T., 2008. Dissolution of biogenic silica from land to ocean: role of salinity and pH. Limnology and Oceanography, 53(4), pp.1614-1621.

146 Lydersen, C., Assmy, P., Falk-Petersen, S., Kohler, J., Kovacs, K.M., Reigstad, M., Steen, H., Strøm, H., Sundfjord, A., Varpe, Ø. and Walczowski, W., 2014. The importance of tidewater glaciers for marine mammals and seabirds in Svalbard, Norway. *Journal of Marine Systems*, *129*, pp.452-471.

147 Macaya, E.C. and Zuccarello, G.C., 2010. Genetic structure of the giant kelp Macrocystis pyrifera along the southeastern Pacific. Marine Ecology Progress Series, 420, pp.103-112.

148 Macklin, M.G. and Lewin, J., 1989. Sediment transfer and transformation of an alluvial valley floor: the River South Tyne, Northumbria, UK. Earth surface processes and landforms, 14(3), pp.233-246.

149 Mao, L., Comiti, F., Carrillo, R. and Penna, D., 2019. Sediment transport in proglacial rivers. In Geomorphology of proglacial systems (pp. 199-217). Springer, Cham.

150 Mao, L., Dell'Agnese, A., Huincache, C., Penna, D., Engel, M., Niedrist, G. and Comiti, F., 2014. Bedload hysteresis in a glacier-fed mountain river. Earth Surface Processes and Landforms, 39(7), pp.964-976.

151 Masiokas, M.H., Villalba, R., Luckman, B.H., Lascano, M.E., Delgado, S. and Stepanek, P., 2008. 20th-century glacier recession and regional hydroclimatic changes in northwestern Patagonia. Global and Planetary Change, 60(1-2), pp.85-100.

152 Masiokas, M.H., Villalba, R., Luckman, B.H., Lascano, M.E., Delgado, S., Stepanek, P. 2008. 20th century glacier recession and regional hydroclimatic changes in north western Patagonia. Global and planetary change 60 85-100

153 McMillan, H., Krueger, T. and Freer, J., 2012. Benchmarking observational uncertainties for hydrology: rainfall, river discharge and water quality. Hydrological Processes, 26(26), pp.4078-4111.

154 Meade, R.H., Yuzyk, T.R., Day, T.J., 1990. Movement and storage of sediment in rivers of the United States and Canada, in surface water hydrology. The Geology of North America, 255–280.

155 Milner, A.M., Khamis, K., Battin, T.J., Brittain, J.E., Barrand, N.E., Füreder, L., Cauvy-Fraunié, S., Gíslason, G.M., Jacobsen, D., Hannah, D.M. and Hodson, A.J., 2017. Glacier shrinkage driving

global changes in downstream systems. Proceedings of the National Academy of Sciences, 114(37), pp.9770-9778.

156 Misset, C., Recking, A., Legout, C., Poirel, A., Cazilhac, M., Esteves, M. and Bertrand, M., 2019. An attempt to link suspended load hysteresis patterns and sediment sources configuration in alpine catchments. Journal of Hydrology, 576, pp.72-84.

157 Mitchell, A.C., Lafreniere, M.J., Skidmore, M.L. and Boyd, E.S. 2013. Influence of bedrock mineral composition on microbial diversity in a subglacial environment. Geology, v. 41, no.8, p. 855-858

158 Molina, A., Govers, G., Poesen, J., Van Hemelryck, H., De Bievre, B., and Vanacker, V.: Environmental factors controlling spatial variation in sediment yield in central america mountain area, Geomorphology, 98, 176–186, 2008.

159 Molina, A., Govers, G., Vanacker, V., Poesen, J., Zeelmaekers, E., and Cisneros, F.: Runoff generation in a degraded Andean ecosystem: interaction of vegetation cover and land use, Catena, 71, 357–370, 2007.

160 Montecino, V., Rutllant, J. and Salinas, S., 2005. Coastal ocean circulation off western South America. The Global Coastal Ocean-Regional Studies and Syntheses, 11, p.273.

161 Montross, S.N., Skidmore, M., Tranter, M., Kivimaki, A.L and Parkes, J.R. 2013. A microbial driver of chemical weathering in glaciated systems. Geology; vol 41, no. 2, p. 215-218, doi: 10.1130/G33572

162 Morera, S., Condom, T., Vauchel, P., Guyot, J.L., Galvez, C. and Crave, A., 2013. Pertinent spatio-temporal scale of observation to understand suspended sediment yield control factors in the Andean region: the case of the Santa River (Peru).

163 Moss, A.J., 1989. Impact droplets and the protection of soils by plant covers. Soil Research, 27(1), pp.1-16.

164 Müller, G. and Förstner, U., 1968. General relationship between suspended sediment concentration and water discharge in the Alpenrhein and some other rivers. Nature, 217(5125), pp.244-245.

165 Nienow, P., Sharp, M. and Willis, I., 1998. Seasonal changes in the morphology of the subglacial drainage system, Haut Glacier d'Arolla, Switzerland. Earth Surface Processes and Landforms: The Journal of the British Geomorphological Group, 23(9), pp.825-843.

166 Nienow, P.W., Sharp, M., Willis, I., 1996. Velocity-discharge relationships derived from dye trace experiments in glacial meltwaters: Implications for subglacial flow conditions. Hydrol. Proc. 10 (10), 1411–1426.

167 Oades, J.M. and Waters, A.G., 1991. Aggregate hierarchy in soils. Soil Research, 29(6), pp.815-828.

168 Oerter, H., Baker, D., Moser, H., Reinwarth, O., 1982. Glaciohydrological investigations on the Vernagtferner glacier as a basis for a discharge model. Nord. Hydrol. 12 (4/5), 335–348.

169 Oerter, H., Moser, H., 1982. Water storage and drainage within the firn of a temperate glacier (Vernagtferner, Oetztal Alps, Austria). In: Glen, J.W., (Ed.), Hydrological Aspects of Alpine and High Mountain Areas, Proceedings of the Exeter symposium, July 1982. IAHS Publ. 138, pp. 71–81.

170 Østrem, G., 1973. Runoff forecasts for highly glacierized basins, The Role of Snow and Ice in Hydrology. Proceedings of the Banff Symposium, September 1972. IAHS Publ. 107, pp. 1111–1129.

171 Ostrem, G., 1975. ‘Sediment transport in glacial meltwater streams’ in Jopling, A.V., and McDonald, B.C., (Eds), *Glaciofluvial and glaciolacustrine sedimentation. Soc. Econ. Palaeontol, Mineral. Spec. Publ.,* **23**. Pp. 101-122.

172 Pantoja, S., Iriarte, J.L. and Daneri, G., 2011. Oceanography of the Chilean Patagonia. Continental shelf research, 31(3-4), pp.149-153.

173 Pasquini, A.I., Lecomte, K.L. and Depetris, P.J., 2008. Climate change and recent water level variability in Patagonian proglacial lakes, Argentina. Global and Planetary Change, 63(4), pp.290-298.

174 Paul, F., Machguth, H., and Ka¨ab, A.: On the impact of glacier ¨ albedo under conditions of extreme glacier melt: the summer of 2003 in the Alps, EARSeL Workshop on Remote Sensing of Land Ice and Snow, Berne, 21–23.2.2005. EARSeL eProceedings, 4, 139–149, CD-ROM, 2005.

175 Pedrozo, F., Chillrud, S., Temporetti, P. and Diaz, M., 1993. Chemical composition and nutrient limitation in rivers and lakes of northern Patagonian Andes (39.5-42 S; 71 W)(Rep. Argentina). Internationale Vereinigung für theoretische und angewandte Limnologie: Verhandlungen, 25(1), pp.207-214.

176 Peña Torrealba, H. and Escobar Cáceres, F., 1983. Análisis de una crecida por vaciamiento de una represa glacial.

177 Penna, D., Tromp-van Meerveld, H.J., Gobbi, A., Borga, M. and Dalla Fontana, G., 2011. The influence of soil moisture on threshold runoff generation processes in an alpine headwater catchment. *Hydrology and Earth System Sciences*, *15*(3), pp.689-702.

178 Pepin, E., Carretier, S., Guyot, J.L. and Escobar, F., 2010. Specific suspended sediment yields of the Andean rivers of Chile and their relationship to climate, slope and vegetation. Hydrological Sciences Journal–Journal des Sciences Hydrologiques, 55(7), pp.1190-1205.

179 Perutz, M.F., 1947. Report on problems relating to the flow of glaciers. Journal of Glaciology, 1(2), pp.47-51.

180 Petrovich, R., 1981, Kinetics of dissolution of mechanically comminuted rock-forming oxides and silicates—I. Deformation and dissolution of quartz under laboratory conditions: Geochimica et Cosmochimica Acta, v. 45, p. 1665–1674.

181 Pickard, G.L. 1971. Some physical oceanographic features of inlets of Chile. Journal of the Fisheries Research Board of Canada. 28: 1077–1106.

182 Pickard, G.L. 1973. Water structure in Chilean fjords. In: Oceanography of the south Pacific, pp 95-104. New Zealand National commission for UNESCO, Wellington.

183 Pizarro, G., J.L. Iriarte, V. Montecino, J.L. Blanco, and L. Guzm´an. 2000. Distribution of phytoplankton biomass and maximum primary productivity of southern fjords and channels (47–50◦S) in October 1996. Ciencia y Tecnolog´ıa del Mar. 28: 25–48.

184 Pizarro, G., V. Montecino, L. Guzm´a, V. Mu˜noz, V. Chac´on, H. Pacheco, M. Frang´opulos, L. Retamal, and C. Alarc´on. 2005. Recurrent local patterns of phytoplankton in austral Chilean fjords and channels (43–56◦S) in spring and summer. Ciencia y Tecnolog´ıa del Mar. 28(2): 63–83.

185 Prado-Fiedler, R. 2009. Winter and summer distribution of dissolved oxygen, pH and nutrients at the heads of fjords in Chilean Patagonia with possible phosphorus limitation. Revista de Biolog´ıa Marina y Oceanograf´ıa. 44(3): 783–789.

186 Prado-Fiedler, R., and J. Salcedo-Castro. 2008. Fluvial and rain contributions of nitrogen and phosphorus to Aysen Fjord and JacafVentisquero-Puyuhuapi channels. Ciencia y Tecnolog´ıa del Mar. 31(2): 75–95.

187 Prosser, I.P., Dietrich, W.E. and Stevenson, J., 1995. Flow resistance and sediment transport by concentrated overland flow in a grassland valley. Geomorphology, 13(1-4), pp.71-86.

188 Ptacnik R, Solimini A, Andersen T, Tamminen T, Brettum P, Lepisto L, Willen E, Rekolainen S. Diversity predicts stability and resource use efficiency in natural phytoplankton communities. Proceedings of the National Academy of Sciences USA. 2008;105:5134–5138. doi: 10.1073/pnas.0708328105.

189 Rantz, S.E., and others, 1982, Measurement and computation of streamflow: Volume 1. Measurement of stage and discharge: U.S. Geological Survey Water-Supply Paper 2175, 284 p.

190 Rasmussen, L., H. Conway, and C. Raymond, 2007: Influence of upper air conditions on the Patagonia icefields. Global Planet. Change, 59, 203–216.

191 Rebolledo L, Lange CB, Figueroa D, Pantoja S, Muñoz P, Castro R. 20th century fluctuations in the abundance of siliceous microorganisms preserved in the sediments of the Puyuhuapi channel (44°S), Chile. Revista chilena de Historia Natural. 2005;78:469–488. doi: 10.4067/S0716-078X2005000300009.

192 Restrepo, J. D., Kjerfve, B., Hermelin, M., and Restrepo, J. C.: Factors controlling sediment yield in a major South American drainage basin: the Magdalena River, Colombia, J. Hydrol., 316, 213–232, 2006a.

193 Rignot, E., A. Rivera, and G. Casassa, 2003: Contribution of the Patagonia icefields of South America to sea level rise. Science, 302, 434–437.

194 Riihimaki, C.A., MacGregor, K.R., Anderson, R.S., Anderson, S.P. and Loso, M.G., 2005. Sediment evacuation and glacial erosion rates at a small alpine glacier. *Journal of Geophysical Research: Earth Surface*, *110*(F3).

195 Rivera, A., 2004. Mass balance investigations at Glacier Chico, Southern Patagonia Icefield, Chile. PhD thesis, University of Bristol, UK

196 Rivera, A., Acuña, C., Casassa, G., Bown, F., 2002. Use of remote sensing and field data to estimate the contribution of Chilean glaciers to the sea level rise. Annals of Glaciology 34, 367–372.

197 Rivera, A., Benham, T., Casassa, G., Bamber, J. and Dowdeswell, J.A., 2007. Ice elevation and areal changes of glaciers from the Northern Patagonia Icefield, Chile. Global and Planetary Change, 59(1-4), pp.126-137.

198 Ro¨thlisberger, H., Lang, H., 1987. Glacial hydrology. In: Gurnell, A.M., Clark, M.J. (Eds.), Glacio-fluvial Sediment Transfer, Wiley, New York, pp. 207–284.

199 Roberts, M.C. and Klingeman, P.C., 1970. The influence of landform and precipitation parameters on flood hydrographs. Journal of Hydrology, 11(4), pp.393-411.

200 Rosenblu¨th, B., H. Fuenzalida, and P. Aceituno, 1997: Recent temperature variations in southern South America. Int. J. Climatol., 17, 67–85.

201 Rothlisberger, H., and Lang, H., 1987. 'Glacial hydrology' in Gurnell, A.M., and Clarke, M.J., (Eds), *Glacio-fluvial sediment transfer: an alpine perspective.* Wiley, Chichester. Pp. 207- 284.

202 Russell, I.C., 1898. Glaciers of Mount Rainier. US Government Printing Office.

203 Salcedo-Castro, J., Montiel, A., Jara, B. and Vásquez, O., 2015. Influence of a glacier melting cycle on the seasonal hydrographic conditions and sediment flux in a subantarctic glacial fjord. Estuaries and coasts, 38(1), pp.24-34.

204 Santiago, S., Thomas, R.L., Larbaigt, G., Corvi, C., Rossel, D., Tarradellas, J., Gregor, D.J., McCarthy, L. and Vernet, J.P., 1994. Nutrient, heavy metal and organic pollutant composition of suspended and bed sediments in the Rhone River. Aquatic Sciences, 56(3), pp.220-242.

205 Schneider, T., 1999. Water movement in the firn of Storglacia¨ren, Sweden. J. Glaciol. 45 (150), 286–294.

206 Schommer, P., 1977. Wasserspiegelmessungen im Firn des Ewigschneefeldes (Schweizer Alpen) 1976. Z. Gletscherkd. Glazialgeol. 12 (2), 125–141.

207 Seaberg, S.Z., Seaberg, J.Z., Hooke, R.LeB., Wiberg, D.W. 1988. Character of the englacial and subglacial drainage system in the lower part of the ablation area of Storglacia¨ren, Sweden, as revealed by dye-trace studies. J. Glaciol. 34 (117), 217–227.

208 Sepulveda J, Pantoja S, Hughen K, Lange C, Gonzalez F, Muñoz P, Rebolledo L, Castro R, Contreras S, Avila A, Rossel P, Lorca G, Salamanca M, Silva N. Fluctuations in export productivity over the last century from sediments of a southern Chilean fjord (44°S) Estuarine, Coastal and Shelf Science. 2005;65:587–600. doi: 10.1016/j.ecss.2005.07.005.

209 Sharp, R.P., 1951. Meltwater behaviour in the Upper Seward Glacier, St Elias Mountains, Canada, General Assembly of Brussels. IAHS Publ. 32, pp. 246–253.

210 Sievers, H.A. 2008. Temperature and salinity in the austral Chilean channels and fjords. In Progress in the oceanographic knowledge of Chilean interior waters, from Puerto Montt to Cape Horn, Comit´e Oceanogr´afico Nacional - Pontificia Universidad Cat´olica de Valpara´ıso, eds. Silva, N., and S. Palma, 31–36.

211 Silva, N., V. De Vidts, and J.I. Sep´ulveda. 2001. Organic matter, C and N, their distribution and stoiquiometry, in surface sediments of the Chilean fjords and channels: Central zone (Cimar-Fiordo 2 Cruise). Ciencia y Tecnolog´ıa del Mar. 24: 23–40.

212 Silvestri, G.E. and Vera, C.S., 2003. Antarctic Oscillation signal on precipitation anomalies over southeastern South America. Geophysical Research Letters, 30(21).

213 Singh, P., Haritashya, U.K., Ramasastri, K.S. and Kumar, N., 2005. Diurnal variations in discharge and suspended sediment concentration, including runoff-delaying characteristics, of the Gangotri Glacier in the Garhwal Himalayas. Hydrological Processes: An International Journal, 19(7), pp.1445-1457.

214 Skliris, N., Marsh, R., Josey, S.A., Good, S.A., Liu, C. and Allan, R.P., 2014. Salinity changes in the World Ocean since 1950 in relation to changing surface freshwater fluxes. Climate dynamics, 43(3-4), pp.709-736.

215 Smith, R. B., and J. P. Evans, 2007: Orographic precipitation and water vapour fractionation over the southern Andes. J. Hydrometeor., 8, 3–19.

216 Stammerjohn, S.E., Martinson, D.G., Smith, R.C., Yuan, X. and Rind, D., 2008. Trends in Antarctic annual sea ice retreat and advance and their relation to El Niño–Southern Oscillation and Southern Annular Mode variability. Journal of Geophysical Research: Oceans, 113(C3).

217 Stevens, L.A., Straneo, F., Das, S. B., Pluedemann, A. J., Kukulya, A. L., and Morlighem, M. 2016. Linking glacially modified waters to catchment-scale subglacial discharge using autonomous underwater vehicle observations. The Cryosphere, 10, 417-432

218 Stow, C.D. and Dirks, K.N. 1998. High-resolution studies of rainfall on Norfolk Island: Part 1: The spatial variability of rainfall. Journal of hydrology, 208(3-4), pp. 163-186.

219 Strangeways, I.C., 1996. Back to basics: The 'met. enclosure': Part 2 (b)—Rain gauges, their errors. Weather, 51(9), pp.298-303.

220 Strub, P.T., Mesias, J.M., Montecino, V., Rutllant, J. and Salinas, S. 1998. Coastal ocean circulation off western South America. In: A.R Robinson and H.K. Brink (eds.), The sea, pp. 273-313. John Wiley and Sons.

221 Sugden, D.E., McCulloch, R.D., Bory, A.J.M. and Hein, A.S., 2009. Influence of Patagonian glaciers on Antarctic dust deposition during the last glacial period. Nature Geoscience, 2(4), p.281.

222 Tanaka, K., 1980. Geographical Contribution to a Periglacial Study of the Hielo Patagónicao Norte with Special Reference to the Glacial Outburst Originated from Glacier-dammed Lago Arco, Chilean Patagonia. Centre Co Ltd, Tokyo 97

223 Tazioli, A., 2011. Experimental methods for river discharge measurements: comparison among tracers and current meter. Hydrological sciences journal, 56(7), pp.1314-1324.

224 Thatje, S., and Mutschke, E. 1999. Distribution of abundance, biomass, production and productivity of macrozoobenthos in the sub-Antarctic Magellan Province (South America). Polar biology. 22: 31-37

225 Thompson, D.W. and Solomon, S., 2002. Interpretation of recent Southern Hemisphere climate change. Science, 296(5569), pp.895-899.

226 Tri, B.H., 1968. Dynamique de la granulation du sol sous prairie (Doctoral dissertation, Faculté des sciences de Paris)

227 Valdovinos, C., Navarrete, S.A., and Marquet, P.A. 2003. Mollusk species diversity in the south-eastern Pacific: why are there more species towards the pole? Ecography, 26:139-144

228 Valle-Levinson, A., M. C´aceres, H.H. Sep´ulveda, and K. Holderied. 2002. Flow patterns in the channels associated to the mouth of Ays´en Sound. Ciencia y Tecnolog´ıa del Mar. 25(2): 5–16.

229 Valle-Levinson, A., N. Sarkar, R. Sanay, D. Soto, and J. Le´on. 2007. Spatial structure of hydrography and flow in a Chilean fjord, Estuario Reloncav´ı. Estuaries and Coasts. 30(1): 113–126.

230 van den Broeke, M., Bamber, J., Ettema, J., Rignot, E., Schrama, E., van de Berg, W.J., van Meijgaard, E., Velicogna, I. and Wouters, B., 2009. Partitioning recent Greenland mass loss. science, 326(5955), pp.984-986.

231 Vera, C., Silvestri, G., Liebmann, B. and González, P., 2006. Climate change scenarios for seasonal precipitation in South America from IPCC-AR4 models. Geophysical research letters, 33(13).

232 Vidal R, Meneses I, Smith M. 2008. Phylogeography of the genus Spongites (Corallinales, Rhodophyta) from Chile. J Phycol 44:173–18

233 Villanueva, V.D., Navarro, M.B. and Albariño, R., 2016. Seasonal patterns of organic matter stoichiometry along a mountain catchment. Hydrobiologia, 771(1), pp.227-238.

234 Wan, D., Li, F.H., Yu, W., Chen, C. and Gao, Y., 2019. Sediment delivery of partially-unfrozen loam soil rill by snow/glacier meltwater flow. Scientific reports, 9(1), pp.1-7.

235 Warburton, J., 1990. An alpine proglacial fluvial sediment budget. Geografiska Annaler: Series A, Physical Geography, 72(3-4), pp.261-272.

236 Ward, T.J., Vanderklift, M.A., Nicholls, A.O., Kenchington, R.A. 1999. Selecting marine reserves using habitats and species assemblages as surrogates for biological diversity Ecol. Appl., 9:691-698.

237 Warren, C.R. and D.E. Sugden. 1993. The Patagonian Icefields: A Glaciological Review. Arctic and Alpine Research. 25(4): p. 316-331.

238 Weis, A. and Melzer, R. R. 2012. How did sea spiders recolonize the Chilean fjords after glaciation? DNA barcoding of Pycnogonida, with remarks on phylogeography of Achelia assimilis (Haswell, 1885). Systematics an Biodiversity, Volume 10, Issue 3

239 Willis, I.C., 1995. 'Intra-annual variations in glacier motion: a review', *Progr. Phys. Geogr.,* **19**, 61-106.

240 Willis, I.C., Richards, K.S. and Sharp, M.J., 1996. Links between proglacial stream suspended sediment dynamics, glacier hydrology and glacier motion at Midtdalsbreen, Norway. *Hydrological Processes*, *10*(4), pp.629-648.

241 Wood, P.A., 1977. Controls of variation in suspended sediment concentration in the River Rother, West Sussex, England. Sedimentology, 24(3), pp.437-445.

242 Yang, S.L., Zhang, J., Zhu, J., Smith, J.P., Dai, S.B., Gao, A. and Li, P. (2005). Impact of dams on Yangtze River sediment supply to the sea and delta intertidal wetland response. *J. Geogr. Res.* **110**, FO3006, doi:10.1029/2004JF000271.

243 Yao, T., Li, Z., Yang, W., Guo, X., Zhu, L., Kang, S., Wu, Y. and Yu, W., 2010. Glacial distribution and mass balance in the Yarlung Zangbo River and its influence on lakes. Chinese Science Bulletin, 55(20), pp.2072-2078.

244 Young, D.S., Hart, J.K. and Martinez, K., 2015. Image analysis techniques to estimate river discharge using time-lapse cameras in remote locations. Computers & Geosciences, 76, pp.1-10.

245 Young, G.J., Hewitt, K., 1993. Glaciohydrological features of the Karakoram Himalaya: measurement possibilities and constraints. In: Young, G.J., (Ed.), Snow and Glacier Hydrology, Proceedings of the Kathmandu Symposium 1992. IAHS Publ. 218, pp. 273–283.

246 Zhang, W., Wei, X., Jinhai, Z., Yuliang, Z. and Zhang, Y., 2012. Estimating suspended sediment loads in the Pearl River Delta region using sediment rating curves. Continental Shelf Research, 38, pp.35-46.

247 Zuzel, J. F., and L. M. Cox (1975), Relative importance of meteorological variables in snowmelt, Water Resour. Res., 11(1), 174 – 176.

9.0 Appendix

9.1 Sample collections used in this thesis

This thesis presents a large dataset collected over a timespan too great for collection solely within the time constraints of a masters. The contribution of a few colleagues is gratefully accepted, and presented below.

	Rio Lloncochaigua (non-glaciated)	Rio Huemules (glaciated)
Meteorological data	• Collected by two meteorological stations situated in the Huinay valley, funded by both the Huinay Scientific Field Station and IFOP. The data is freely available online for download. • Huinay station: https://www.hobolink.com/p/bc04eec9360b61e12bc920b7f4623829 • IFOP station: https://www.hobolink.com/p/baa69a935234dc9d71febde8a42aa5a7	• Collected by a meteorological station funded and maintained by the Direccion General de Aguas (DGA). This data is freely available online for download: https://snia.mop.gob.cl/BNAConsultas/reportes (n.b. Caleta Tortel station was used, as the nearest to the study site)

Discharge data	• A HOBO pressure sensor was installed in the river by Professor Wadham and Dr Hawkins on 9th January 2017. It was retrieved by Anna Covey and Professor Wadham on 12th February 2018. • A CTD sensor was installed by Anna Covey, Dr Hawkins and Professor Dussaillant on 28th January 2018. The protective plastic tubing, also responsible for maintaining the sensor's depth in the water column, was washed away during a large storm event on 8th July 2018, and the sensor was re-installed once the water level had fallen and it was safe to do so by Anna Covey on 1st August 2018. This storm event has been removed from the records presented in this thesis. The sensor was retrieved by Anna Covey on 31st March 2019.	• A CTD sensor was installed on 28th August 2016, and retrieved on 28th July 2017. • The sensor installation and dye tracing was undertaken by Dr Jon Hawkins, Dr Mathew Marshall, Dr Alejandra Urra-Gallardo, Miss Helena Pryer, Miss Sarah Tingy and Mr Rory Burford. The ratings curve was compiled by Dr Jon Hawkins and the data presented in discharge format for use in this thesis.

	• Dye tracing was conducted by Anna Covey, Dr Jon Hawkins and Professor Jemma Wadham, and the ratings curve compiled by Anna Covey.	
Suspended sediment data	• A Turner Cyclops-7 turbidity sensor was installed on 28th January 2018 by Dr Hawkins and Anna Covey, and retrieved on 16th February 2018 by Professor Wadham and Anna Covey. • An RBR Tu turbidity sensor was installed by Anna Covey on 1st August 2018 and removed on 31st March 2019. However, the on 27th November 2018 it suffered a technical glitch and all data after this point was discounted. • All suspended sediment samples were collected, filtered, and weighed by Anna Covey. The conversion of the Tu data to a suspended sediment flux was carried out by Anna Covey.	• A Turner Cyclops-7 turbidity sensor was installed on 15th January 2017, and retrieved on 23rd February 2017 by Dr Jon Hawkins, Dr Mathew Marshall, Dr Alejandra Urra-Gallardo and Mr Rory Burford. • The sensor was returned from 15th July 2017 to 28th July by Dr Jon Hawkins and Miss Sarah Tingey. • Suspended sediment samples were taken by all of the above, and weighed and analysed by Dr Hawkins. The turbidity- suspended sediment calibration was undertaken by Dr Hawkins, and the data presented in this format for use in this thesis.